STATISTICAL CHARACTERISATION OF ENDOCARDIAL BREAKTHROUGHS IN ATRIAL FIBRILLATION

By

Jay Nguyen
MESCB

Thesis
Submitted to Flinders University
for the degree of

Master of Engineering Science

College of Science and Engineering
06.06.2022

DECLARATION

I certify that this thesis:

1. does not incorporate without acknowledgment any material previously submitted for a degree or diploma in any university
2. and the research within will not be submitted for any other future degree or diploma without the permission of Flinders University; and
3. to the best of my knowledge and belief, does not contain any material previously published or written by another person except where due reference is made in the text.

Signature of student.....

Print name of student.....Jay Nguyen.....

Date.....16/06/2022.....

I certify that I have read this thesis. In my opinion it is/is not (please circle) fully adequate, in scope and in quality, as a thesis for the degree of Master of Engineering Science (Biomedical) Furthermore, I confirm that I have provided feedback on this thesis and the student has implemented it minimally/partially/fully (please circle).

Signature of Principal Supervisor.....

Print name of Principal Supervisor.....Kenneth Pope

Date.....16/6/2022

ACKNOWLEDGEMENTS

I would like to thank the people who have provided me with support and guidance throughout my research project. Firstly, I would like to thank my supervisor A/Prof. for his direction and support to my research journey in the biomedical engineering field. He has been giving me a lot of inspiration by his wonderful expertise and unique ideas in the study of cardiac fibrillation. Then I would like to thank my co-supervisor Dr Dhani Dharmaprani for her sincere support and motivation in developing my research project and writing my thesis. Her experience in the field and various skills helped me a lot in finalising and delivering my research project. I would also like to thank my engineering co-supervisor A/Prof. Kenneth Pope for his continuous support and guidance in implementing my research project, especially in computational algorithm and statistical analyses. His expertise and experience in the field helped me a lot in the engineering aspects of my research project.

I would also like to thank other people in Flinders Heart Rhythm Research Group who have provided me with support and motivation. I would like to thank Dr Alvin Quah for providing me with electrical mapping data of atrial fibrillation patients and the basic foundation on atrial fibrillation. Then I would like to thank Evan Jenkins for his suggestions and ideas in implementing my research project. Finally, I would like to thank Choo Nguyen, who is my research partner and also my beloved wife, for her wonderful inspiration, motivation and support in both my research project and my journey in the field.

EXECUTIVE SUMMARY

Atrial fibrillation (AF) is the most common sustained cardiac arrhythmia in humans. During AF, phenomena known as endocardial breakthroughs have been observed, which have been proposed as the mechanism for maintaining AF. An important question that is not fully understood is whether endocardial breakthroughs occur randomly, or if they perhaps represent ‘drivers’ of AF. In this study, the statistical properties of endocardial breakthroughs were analysed by applying the Renewal theory. It was recently proposed as a quantitative framework for phase singularities, a stochastic electrical activity during atrial fibrillation.

This study was based on the HD-grid catheter data from AF patients. Pre-processing of the signal and phase mapping were provided by Flinders Heart Rhythm Research Group. Then novel custom image algorithm was developed to detect endocardial breakthroughs and calculate the inter-formation times. Subsequently, statistical analyses were performed to test the statistical distribution of inter-formation times and the impact of different factors on the formation of endocardial breakthroughs during AF.

This study found that the inter-formation times of endocardial breakthroughs were statistically independent and has an exponential distribution in AF patient's hearts. It means that endocardial breakthrough is a stochastic process with no underlying constant driver and does not constantly drive AF. It also means that Renewal theory is applicable to understand endocardial breakthroughs. The exponential probability distribution of inter-formation times and means that the formation rate of endocardial breakthroughs is measurable. The measurable rate allows the characterisation of endocardial breakthroughs during the maintenance of AF. Another finding was that clinical types of AF have a significant impact on the formation of endocardial breakthroughs. It is consistent with previous studies on the role of endocardial breakthroughs in AF progression. Its incidence was found to relate to the damage of sustained AF. Its propagation contributes to the complexity of electrical patterns sustaining AF.

TABLE OF CONTENTS

LIST OF FIGURES

LIST OF TABLES

INTRODUCTION

1.1 Overview of the research

Atrial fibrillation (AF), the most common sustained cardiac arrhythmia in humans, is characterised by aperiodic and turbulent electrical activation of the atrial myocardium. Despite more than a century of research, the mechanisms sustaining this arrhythmia remain unresolved, with several potential mechanisms suggested to be involved with the maintenance of AF. Historically, the dominant classical theories of AF have been the multiple wavelet and rotor theories (Waks and Josephson, 2014). But recently, it has been accepted that several mechanisms may be responsible for triggering and sustaining AF (Hansen et al., 2016).

Recent research on AF suggested that endocardial breakthrough is an important factor contributing to the maintenance of AF (Verheule et al., 2014). Endocardial breakthrough is the result of excessive electrical dissociation between the endocardium and the epicardium of the heart. There is no clear description of endocardial breakthroughs on text. It can only be observed through cardiac mapping. Mapping has been a common method to uncover the activity of endocardial breakthroughs. However, mapping alone cannot fully characterise the mechanisms of endocardial breakthroughs in AF (Aronis and Trayanova, 2020). An important question that is not fully understood is whether endocardial breakthroughs occur randomly, or if they perhaps represent ‘drivers’ of AF. This relates to the long-standing debate about whether any particular mechanism is responsible for sustaining AF (Cheniti et al., 2018), as this would allow the driving mechanism to be targeted in order to terminate the arrythmia.

Although it has been postulated that rotors and wavelets may be such drivers, recently the Flinders Heart Rhythm Research Group found that these rotors and wavelets occur randomly in time, as characterised by a renewal process (Dharmaprani et al., 2019). In this study, it was therefore hypothesized that this theory could be extended to demonstrate that endocardial breakthroughs also randomly occur in time, and hence support an underlying renewal process of AF rather than the presence of singular drivers.

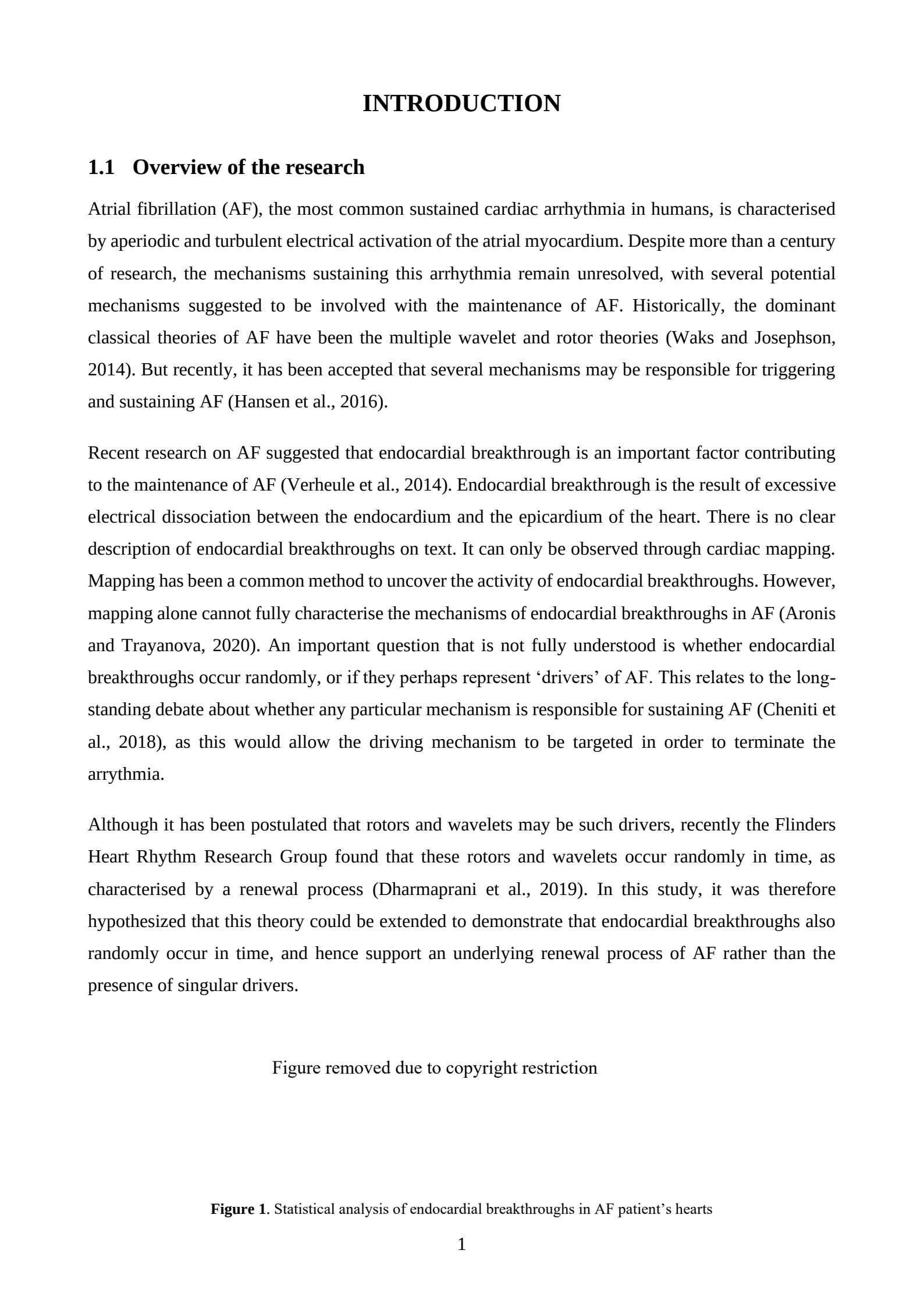

Figure 1. Statistical analysis of endocardial breakthroughs in AF patient’s hearts

1.2 Aims of the research

This research aims to apply Renewal theory to understand the statistical properties of endocardial breakthroughs and determine their role in the maintenance of AF. In summary, this was explored by:

- Understanding the probability distribution of inter-formation event times. The probability distribution that is generated by a process can give valuable insights about the underlying generative mechanisms. Here, it was hypothesised that the occurrence of endocardial breakthroughs in the heart could be modelled as a stochastic ('random') process, giving rise to the following implications:
    - If the timing between new endocardial breakthroughs, referred to as inter-formation times, are random they will give rise to an exponential probability distribution. This means that the average formation rate of these endocardial breakthroughs will be measurable.
    - If inter-event times of endocardial breakthroughs are random, it means that endocardial breakthroughs are statistically independent and do not act as the singular driving mechanism of AF.

- Investigating the impacts of different clinical factors on the formation of endocardial breakthroughs. Although it is well known in literature that certain clinical factors (gender, anatomy, lifestyle) can increase the likelihood of developing AF, it is not well known how or if these factors are associated with a higher incidence of endocardial breakthrough events. Here, it was evaluated whether:
    - A higher prevalence of endocardial breakthroughs is associated with particular anatomical regions. If so, this is consistent with the fact that the structural organisation and thickness of the atrial walls (i.e., differences in anatomy) plays a part in promoting dissociation between electrical activity between the epicardium and endocardium, hence promoting the likelihood endocardial breakthroughs.
    - If gender is found to have an influence, it is consistent with literature suggesting that variances in the structural and electrophysiological properties of the atria are present between genders, which is closely associated with the sustenance of AF.
    - If differences in clinical risk factors attributed to lifestyle are found to have any influence, it is consistent with the literature that unhealthy hobbies such as smoking and drinking alcohol negatively affect cardiac function and increases the risk of having AF.
    - If different clinical sub-types of AF are found to influence the prevalence of endocardial breakthroughs, it provides evidence for the hypothesis that the presence of AF results in structural and electrophysiological remodelling of the atria. Progressive remodelling of

the endo-epi trabecular network is thought to be the main cause of endocardial breakthroughs during AF.

The main hypotheses in this research are therefore as follows:

1. Inter-formation times of endocardial breakthroughs will be statistically independent, and therefore suggest that endocardial breakthroughs occur randomly and do not act as the singular driving mechanism of AF.
2. Different factors as such anatomical regions, genders, lifestyles and clinical types of AF could influence the statistical distribution of endocardial breakthroughs.

1.3 Structure of the thesis

Introduction provides an overview, the aims and objectives, and the meaning of the study.

Literature review provides the current background and previous studies on atrial fibrillation and endocardial breakthroughs, as well as the research gaps.

Methodology details the methods for data acquisition, pre-processing, phase mapping, detection and validation of endocardial breakthroughs, and statistical analyses.

Results presents the key findings on the statistical distribution of endocardial breakthroughs and the impact of different factors the formation of on endocardial breakthroughs.

Discussion interprets the meaning of key findings in the study by referring to current literature on endocardial breakthroughs during atrial fibrillation, as well as addressing the limitations of the study and providing suggestions for future studies.

Conclusions provides the summary of the key findings in the study and the meaning of those findings, as well as the contributions to the field, the current limitations, and the suggestions for future work.

2 LITERATURE REVIEW

2.1 Current knowledge on mechanisms of AF

2.1.1 Normal cardiac electrophysiology

Sinus rhythm is a term to define the electrophysiological activity of a normal heart. A normal heart rhythm begins with action potentials initiated at the sinoatrial (SA) node, which is a group of pacemaker cells located in the upper posterior wall of the right atrium (Kashou et al., 2021). Electrical impulses are then generated and pass to the atrioventricular (AV) node, which is another group of pacemaker cells located in the posterior region of the interatrial septum providing electrical connection between the atria and the ventricles of the heart (Meijler and Janse, 1988). Electrical impulses from the AV node are then relayed by the His-Purkinje System (HPS), which is a group of electrically excitable cells located in the inner ventricular walls (Vigmond and Stuyvers, 2016). As a result, electrical impulses are distributed throughout the ventricles to electrically activate ventricular muscles and coordinate the ventricles to contract synchronously with the atria (Klabunde, 2017). Figure 1 shows the pathway of electrical impulses along electrically excitable regions in a normal heart.

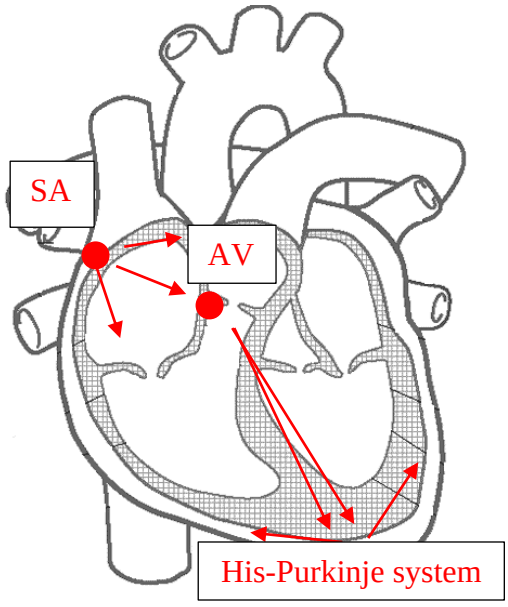

Figure 2. Schematic of normal cardiac electrophysiology

Sinus rhythm has specific components of the electrocardiogram (ECG) (Figure 3). The first component is the P wave, which represents atrial depolarization (Platonov, 2012). This wave has a positive deflection but a smaller amplitude than other waves because the atrial muscle mass is small compared with the ventricles. The next component is the QRS complex, which is generally the largest in voltage amplitude representing ventricular depolarization. Finally, the last component is the T wave, which is generated by ventricular repolarization (Yan et al., 2003).

Figure removed due to copyright restriction

Figure 3. ECG component waves of normal cardiac rhythm

2.1.2 Cardiac electrophysiology during AF

During AF, the normal sinus rhythm is disturbed by abnormal electrical behaviour within the atria (Nattel, 2002). Instead of action potentials only at the SA node, electrical activation initiates at several regions of the atria generating electrical impulses propagating in several directions. Consequently, the chaotic movements of electrical impulses produce distinct electrical waveforms, causing the atria to contract irregularly and asynchronously. Also, as electrical impulses chaotically propagating within the atria, it is impossible to achieve the proper electrical conduction between the atria and the ventricles at the AV node (Danilov et al., 2016). It causes the uncoordinated contraction between the atria and the ventricles.

AF can be identified by observing ECG recordings (Figure 4). Since the atrial contraction is very fast, the amplitude of action potentials is low. Hence, there is no P wave component on the ECG from patients suffering AF (Censi et al., 2016). In this case, the atrial depolarization may be observed as fibrillatory waves. Another difference between the ECG from a normal heart and the ECG from a heart with AF is on the QRS complex. Because of the chaotic electrical activity in the atria, the AV node cannot allow all the electrical impulses passing through to the ventricles. Hence, the ECG from patients with AF has an irregular pattern of QRS complexes, which is normally described as RR intervals (Petrutiu et al., 2006).

Figure removed due to copyright restriction

Figure 4. ECG from normal heart vs ECG from heart with AF

2.2 Study approaches to mechanisms of AF

There are many existing theories for the initiation and maintenance of AF due to the fact that the condition is a complicated and chaotic phenomenon. Consequently, it has to date been almost impossible to completely elucidate the underlying mechanisms that trigger and sustain AF. The first challenge has been to discover the mechanism responsible for the initiation of AF, while the second to uncover the mechanisms responsible for its maintenance. This section outlines some of the most notable theories proposed for the initiation and maintenance of AF in current literature.

Figure removed due to copyright restriction

Figure 5. Mechanisms of AF (Roney et al., 2019)

2.2.1 Ectopic triggers

It has been long reported that the mechanism for triggering AF in the heart are ectopic foci. This term describes a phenomenon in which action potentials initiate at irregular excitable regions other than the SA node when the heart begins its contraction. The regions that were first found to have ectopic activities initiating AF are the pulmonary veins (PVs) (Haissaguerre et al., 1998). Subsequently, several studies also found that ectopic beats at PVs are responsible for triggering AF (Chen et al., 1999, WU et al., 2001, Mahida et al., 2015). However, there were ectopic sources outside the PVs that were found to be related to the initiation of AF. Lin et al. (2003) reported the initiation of AF by ectopic beats from non-PV areas, which was found on 28% of the patients studied, including left atrial posterior wall, superior vena cava and interatrial septum. Previously, superior vena cava were found to be the source of ectopic tachycardia, which is a condition that makes rapid heartbeat (Shah et al., 2002, Dong et al., 2002). In light of these studies, treatment approaches have been developed to stop these ectopic foci in order to terminate or control AF.

2.2.2 Rotors

Compared to the initiation of AF, there have been more heated debates on the underlying drivers of its complexity and maintenance. Reentrant circuits and multiple wavelets are the classical theorised mechanisms that sustaining AF. There are two types of reentrant circuits, which is functional reentry and anatomical reentry. The simplest form of functional reentry can be demonstrated by the leading circle concept (Allessie et al., 1977). It is a circus movement of electrical waves in which the wavefront continuously encroaches the wavetail to form a functional barrier and sustain itself by the constant centripetal activation of the central tissue. A Rotor is a specific form of functional reentry. In a rotor, the curved wavefront meets the wavetail at the core of the rotor, which is widely known as phase singularity (PS). Rotors were typically found to be responsible for the sustenance of AF (Winfree, 1994, Jalife et al., 2002, Weiss et al., 2005). Anatomical reentry, or localised reentry, is initiated and sustained by the slow conduction of local functional block. Early evidence of localised reentry maintaining AF was found by Schuessler et al. (1993). Subsequently, the role of localised reentry in the maintenance of AF was reported in several studies (Haïssaguerre et al., 2006, Hocini et al., 2011).

2.2.3 Wavelets

Multiple wavelet hypothesis was first proposed by Moe et al. (1964) (Moe et al., 1964). The model of this study demonstrated that the continuous interaction of several wavefronts results in random wavebreaks and thus the formation of other waveforms. This phenomenon continuously occurs from one generation to another, driving the maintenance of AF. The proposed model of multiple wavelet dynamics were evaluated and considered by subsequent studies (Allessie, 1985, Lee et al., 2020).

2.2.4 Endocardial epicardial dissociation and breakthrough

Endocardial epicardial dissociation (EED) is a difference in electrical activation between the endocardium and the epicardium. This concept was first mentioned by Schuessler et al. (1993), in the study to challenge the dominant assumption that the atria have the electrophysiological properties of a two-dimensional surface. In this study, electrical activation in the endocardium and the epicardium was found to be discordant. The discordance is dependent on anatomical regions of the atria and anatomical architecture of the atrial tissue. In healthy atria, the differences in activation time between the endocardium and the epicardium are small, so the fibrillation waves propagate on the surface of the atrial walls. The maintenance and progression of AF is thought to increase the duration of EED between the atrial walls, which results in the appearance of breakthrough locations (Eckstein et al., 2011, Eckstein et al., 2013), also referred to as ‘endocardial breakthroughs’.

2.3 Structural remodelling of atria during sustained AF

The chaotic and rapid electrical activity of sustained AF alters the structural organisation between atrial tissue. This has importantly been shown to further promote the presence of AF, by creating electrophysiological and structural changes that make it easier for the heart to sustain AF (Wijffels et al., 1995). The most important structural remodelling that is related to AF is atrial fibrosis. This is the development of fibrous connective tissue in response to damages of sustained AF to cardiac cells (Everett IV and Olgin, 2007). There are broadly two patterns of fibrosis, which is reparative fibrosis and reactive fibrosis (Burstein and Nattel, 2008). Reparative fibrosis is the replacement of death cardiac cells while reactive fibrosis is the interstitial expansion between cardiac cell bundles. The structural alteration of fibrosis on the endocardial epicardial trabecular network increases EED between the two walls (Verheule et al., 2013, Hansen et al., 2015). The development of connective tissue increases the separation between existing cardiac muscle cells. This separation disrupts the electrical connection between the trabecular bundles of the two atrial walls.

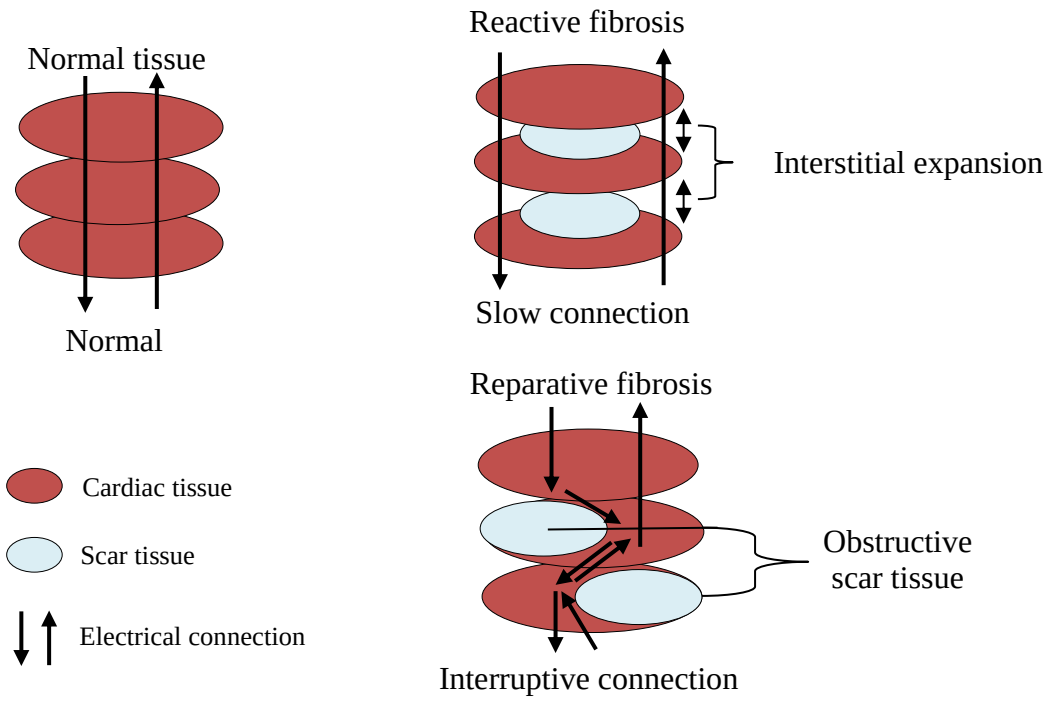

Figure 6. Structural remodelling and electrical connection of atria during sustained AF

2.4 Breakthrough waves

Breakthrough waves are the result of excessive electrical dissociation between the endocardium and the epicardium of the heart (Gharaviri et al., 2020). It is indicated by the increased incident of breakthroughs waves between the endocardium and the epicardium, as the result of propagation between the two atrial walls. It has been observed through the simultaneous mapping of the epicardial surface and the endocardial surface. In the study to justify the source of breakthrough waves in AF, Eckstein et al. (2013) demonstrated breakthrough events by analysing vivo mapping data. Figure 7 visualises the incident of a breakthrough event through the mapping of the activation time and direction of propagation on the epicardial surface to the endocardial surface.

Figure 7. Visualisation of endocardial breakthroughs (Eckstein et al., 2013)

In addition to the mapping of activation time, optical mapping was another study methods. Hansen et al. (2015) obtained simultaneously the 3-dimensional optical mapping of the endocardial surface and the epicardial surface of the atria in human diseased hearts using three high resolution Complementary Metal Oxide Semiconductor (CMOS) cameras. The study visualised breakthrough wave patterns by coupling high resolution 3-dimensional structural imaging with the optical mapping data.

Another method to study breakthrough waves is wave mapping technique, which was introduced by Allessie et al. (2010). This technique was performed by de Groot et al. (2010) in the study of the detection and spatial distribution of breakthrough waves. The study also developed an algorithm to distinguish breakthrough site from sources of other fibrillation waves.

Recently, Parameswaran et al. (2020) performed the phase mapping to study breakthrough events in AF patients. In this study, mapping was performed using 2 high-density grid catheters on AF patients undergoing cardiac surgery.

2.5 Renewal theory for quantitative analysis of electrical patterns during AF

2.5.1 Renewal process

Figure 8. Poisson renewal process (Quah et al., 2021)

Renewal theory is a branch of mathematics used to model events that occur randomly in time. Statistically speaking, these events are referred to as 'independent' (Smith, 1958). For example, one can model calls received by a customer service line using a renewal process, as the timing between individual calls are not related and are hence independent. In such a process, the timings between events (in this case new calls) are referred to as 'inter-event times'. Mathematically, such a process can therefore be modelled as a renewal process when the inter-event times are mutually independent and possess the same probability distribution (Doob, 1948).

There are several types of renewal processes, with the Poisson renewal process being the simplest form due to possessing a first-order or exponential distribution of inter-event times (Granek and Cates, 1992). Higher order renewal processes can also exist wherein the process fits to higher-order distributions such as the gamma or Weibull (Mainardi et al., 2007).

In the case of Poisson renewal process, the fact that events are independent of one another (i.e. the occurrence of one event has no effect on the probability of another event occurring) results in a constant instantaneous probability of events, as the likelihood of observing a new event after 1 second versus 1 minute is the same (Granek and Cates, 1992). This means that mathematically, there is a constant average rate of events that can be measured (Daley and Vere-Jones, 2003). This is given by the exponential rate parameter, λ, which summarises the average rate of events per unit time. Renewal processes have been found useful in other disciplines outside of cardiology as they provide a quantitative framework to model, characterise and predict statistically independent processes by estimating this constant underlying rate parameter λ.

There are several statistically independent processes in nature that can be modelled as renewal processes. Radioactive decay is a common type of natural systems that has stochastic time intervals between decaying events. Renewal theory enables the study of radioactive substances by modelling their decaying events as a Poisson renewal process. A Poisson renewal process determines the constant decay rate of individual radioisotopes within substances. Early application of Poisson renewal process in radioactive was mentioned by Mylon and McBeth (1983). The study undertook measurements with ^{99m}Tc and ^{116m}In to confirm the adaptation of Poisson renewal process in obtaining half-life values of radioactive decay. Subsequently, Campbell and Duarte (2008) found that the decay events in a bulk source of ^{137}Cs, which was earlier observed as a statistically independent process, can be modelled as a Poisson renewal process.

Another natural process that can be modelled as a Poisson renewal process is the spontaneous activity in afferent neurons. Lee and Wang (2003) analysed the spontaneous generation of action potentials in afferent neurons by fitting the data recorded from zebrafish to a Poisson renewal process model. The model provided the evidence that spontaneous activity is dependent on the physiological properties of different systems.

2.5.2 Renewal process models of phase singularities during AF

Figure removed due to copyright restriction

Figure 9. Renewal process models of phase singularities in mammalian cardiac fibrillation (Dharmaprani et al., 2019)

Similar to radioactive decay, the sustenance of AF involves several chaotic electrical patterns (rotors, wavelets, endocardial breakthroughs) that occur in the heart. It is challenging to examine the impact of different mechanisms on the maintenance due to the complexity of AF. However, similar to the

decay of radioisotopes, the formation and destruction of notable electrical patterns such as rotors and wavelets has been shown to be statistically independent. This is insightful for understanding the underlying AF mechanism, as it suggests that: i) rotors and wavelets occur randomly in time; and ii) rotors and wavelets occur at a constant average rate, λ. This importantly suggests that singular rotors and wavelets are therefore likely not 'driving' AF as there is a continual process of random formation and annihilation (Dharmaprani et al., 2019).

Specifically, this was shown by Dharmaprani et al. (2019) who were the first to model phase singularities, which are common to rotors and wavelets, as Poisson renewal processes. The study was performed to quantify and characterise the formation and the destruction of phase singularities in mammalian cardiac fibrillation. The results showed that all phase singularities identified in human, sheep and rat can be modelled as Poisson renewal processes. The results were consistent in both atrial fibrillation and ventricular fibrillation.

From the quantitative models, the constant rate of formation and destruction of phase singularities were determined to characterise the fibrillation processes. Subsequently to the success of the Poisson renewal theory-based quantitative framework in in vivo data, Quah et al. (2020) employed it to design a pilot study investigate the correlation between the association of formation rates and destruction rates with the characteristics of different AF clinical and structural risk factors such as age, BMI, atrial size and the incidence of stroke, which have been shown to associate with more adverse AF outcomes. The pilot study was expected to expand the use of formation rates and destruction rates determined by the proposed quantitative framework in clinical practice, and showed that the rate constants calculated using the renewal theory framework was able to differentiate patients with more severe clinical outcomes, and higher likelihood of AF recurrence (Quah et al., 2021).

Recently, Jenkins et al. (2022) further demonstrated that the formation and destruction of fibrillatory dynamics can be predicted by renewal theory approach. The study aimed to explain the origin of the renewal theory in studying the spatiotemporal pattern of cardiac fibrillation. Two classical systems were mentioned to evidence that the stochastic nature of chaotic systems is statistically predictable, which was demonstrated by the logistic map and the baker's transformation. Then the utility of the previously developed Renewal theory approach to statistically predict the spatiotemporal pattern of those classical chaotic systems was demonstrated. This importantly emphasises the conceptual significance of the Poisson renewal theory-based quantitative framework in clinical and mechanistic research.

2.6 Research gaps

Currently, there is no article studying EED and breakthroughs in various anatomical regions within the atria of a human heart. Early evidence of EED was found in the isolated canine right atrium (Schuessler et al., 1993). Another animal model used in previous studies was the atrial free walls of goats (Eckstein et al., 2013, Verheule et al., 2013). To study on human atria, there are typically two methods of data acquisition. One is to perform on diseased hearts explanted from cardiac patients (Hansen et al., 2015). The other is to perform on the heart of patients undergoing cardiac surgery (de Groot et al., 2010, Parameswaran et al., 2020). Current intraoperative studies were performed on the whole area of atrial walls but had no focus on individual regions within the atria. In this study, 16 atrial regions were studied to investigate the impact of anatomical difference on the incidence of breakthroughs.

In terms of study methods, this study was the first to use computational methods for the detection of breakthrough waves and the calculation of inter-event times. In previous studies, a common technique to detect breakthrough sites has two steps. The first step is to locate the activation site of breakthroughs. There are two different methods for the location of breakthrough sites, based on the protocol of mapping. If only one surface of the atrial walls was mapped, a breakthrough site has to be activated earlier than the surrounding sites (de Groot et al., 2010). If the simultaneous mapping of both surface of the atrial walls was performed, a breakthrough site is located based on the difference in activation time between the endocardial surface and the epicardial surface (Eckstein et al., 2013). Based on the difference in activation time, the activation site of breakthrough is located. The second step is to check the detected site with the border of the mapping array. The detected site is an activation site of breakthrough if it is located within the mapping array. This study developed and implemented a computational algorithm to automatically detect breakthrough sites on the phase mapping of the endocardial surface of different atrial regions, as well as estimating the inter-event times on long segments of human AF.

In this study, the power of computational methods facilitated the very first use of Renewal theory for statistical analysis of breakthroughs in AF patient's hearts. Previous studies focused mainly on the incidence and spatial distribution of breakthroughs (de Groot et al., 2010, Eckstein et al., 2013, Verheule et al., 2013). However, spatial characteristics of breakthrough cannot fully uncover the role of breakthroughs in the sustenance and progression of AF. Renewal theory is a new approach to revolutionise the study of AF. It showed the power in modelling and characterising rotors and wavelets in AF (Dharmaprani et al., 2019). It therefore has the potential to be expanded to other electrical patterns in AF (Quah et al., 2021, Jenkins et al., 2022). Hence, this study employed renewal theory as an approach to understand the statistical distribution of endocardial breakthroughs in AF.

3 METHODOLOGY

3.1 Overview of the study method

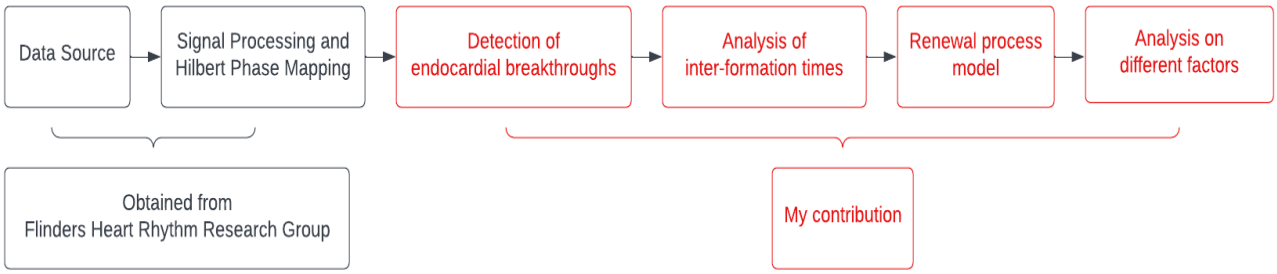

Figure 10. Overview of the methodology and the contributions of the study

Patient data was obtained from the database of Flinders Heart Rhythm Research Group (summarised briefly below). MATLAB code in this research was adapted by the code provided by the research group. The provided code was developed in previous studies on computational approaches for analysing phase singularities and rotors in AF, which automatically:

1. Imports patient data
2. Performs pre-processing of input signals
3. Performs phase mapping and data interpolation
4. Performs phase singularity and rotor detection
5. Creates look-up tables to determine lifetimes and inter-formation times
6. Performs statistical analyses on lifetimes and inter-formation times

In the current study, this was built upon to investigate endocardial breakthroughs from clinical human AF patient recordings. The key phases of this project are summarised briefly below (further detailed in section 3.2 – 3.7):

1. Develop an algorithm to detect endocardial breakthroughs
2. Modify the phase singularity detection algorithm of the provided code
3. Assemble the new detection algorithm into the provided code
4. Test and refine the code on multiple data sets
5. Perform statistical analyses on inter-formation times to examine if endocardial breakthroughs could be modelled as a renewal process
6. Investigate the impacts of different factors on the formation of endocardial breakthroughs.

All the works were based on signal processing toolbox and image processing toolbox on MATLAB.

3.2 Data source

In this study, clinical human AF data was used to investigate endocardial breakthroughs. The data was obtained as part of a prospective multi-centre study called the 'RENEWAL-AF' study, which aimed to assess how Renewal theory can be used to identify clinical, electrical and structural markers of AF (Quah et al., 2020). Data was taken from patients prior to catheter ablation, an invasive treatment that burns pathological regions in the heart to terminate AF.

Two sub-types of AF assessed in this study: 1) paroxysmal AF, which usually lasts less than 7 days and will spontaneously terminate without the need for medication or intervention; and 2) persistent AF, which continuously lasts more than 7-days. Consenting patients had to provide written informed consent to be enrolled. All consent forms and personal information were stored and retrieved with confidentiality. Subsequently, clinical assessment of the patient's clinical characteristics (i.e., gender, age, BMI, lifestyle factors), as well as cardiac structural assessment to evaluate the patient's atrial anatomy (i.e., atrial size, ejection fraction) was assessed using echocardiography. This was performed on patients prior to an electrophysiology study, which is routine procedure performed for AF patients undergoing catheter ablation.

During the electrophysiology study, a HD-grid mapping catheter was used to obtain intracardiac (from within the heart) electrical data from patient's during AF. A cardiac mapping catheter is a long apparatus which typically possesses electrodes at the tip to record electrical voltages from the heart. Specifically, the HD-grid catheter is 3-3-3-mm and has a paddle shape. It has 4 four splines ('arms') with 4 electrodes on each spline, giving a total of 16 electrodes (Figure 11. In this study, a unipolar electrode configuration was used, which resulted in 16 channels of intracardiac voltages (referred to as 'electrograms'). Simultaneously with HD-grid catheter mapping, 12-lead surface ECG data was also recoded. HD-grid catheter data was recorded for 1 minutes on each of the pre-specified 16 anatomical regions throughout the left atrium, right atrium and pulmonary veins. All anatomical regions involved in this study are listed in Table 1.

Figure 11. Abbott Advisor HD-grid mapping catheter

Heart	Anatomical Region	Abbreviation
Left	Anterior	LA_ANT
	High posterior	LA_HI_POST
	Lateral surface	LA_LAT
	Low Posterior	LA_LOW_POST
	Septum	LA_SEPT
	Left atrial appendage	LAA
Left pulmonary vein	Interior	LIPV
	Superior	LSPV
Right	Cavo-tricuspid isthmus	RA_CTI
	Lateral	RA_LAT
	Posterior	RA_POST
	Septum	RA_SEPT
	Right atrial appendage	RAA
Right pulmonary vein	Inferior	RIPV
	Superior	RSPV

Table 1. Anatomical regions involved in this study

3.3 Pre-processing of input signals

The automatic process of cleaning, filtering and signal processing was performed using existing code provided by the Flinders Rhythm Heart Research group, as previously published were as described below (Dharmaprani et al., 2019).

3.3.1 Importing data

Unipolar electrograms and surface ECG data were exported from the cardiac 'Precision Mapping System' (Abbott, IL). Raw unipolar electrogram and ECG data was in Excel.csv and .xlsx format. The procedure to import the raw data from Excel files into MATLAB was as published previously (Dharmaprani et al., 2019). Specifically, the code was written to extract the voltage values for each electrogram and convert it into a numeric array in MATLAB. A built-in function is used to extract only the channels of interest, while discarding the others.

3.3.2 QRS subtraction

As this study aims to evaluate the electrical activity within the atria, the ventricular component of signal needs to be removed. This is because the ventricular walls are much more muscular, and hence

create much larger electrical potentials in comparison to the atrial walls, obscuring atrial activity. This typically occurs when the ventricles are contracting, as electrical impulses are generated to tell the cardiac cells to depolarize and hence contract. This ventricular component is associated with the characteristic QRS complex on the ECG, however, is much harder to annotate within the electrogram. Therefore, standard methods of ventricular component removal use the QRS complex on the ECG to find the corresponding timing of ventricular activity in the electrogram, hence the term 'QRS subtraction'.

The procedure to perform QRS subtraction was as to previously published (Dharmaprani et al., 2019), and based on a previously reported algorithm that is widely used in cardiac electrophysiology (Shkurovich et al., 1998). It starts with baseline correction by subtracting the ECG signal from its mean voltage. Then, the Pan-Tompkins algorithm by was used to detect and mark the fiducial points (timing) of the QRS complexes in the baseline corrected signal (Pan and Tompkins, 1985). The detected QRS complexes were then aligned at their fiducial points and averaged to create 'median complexes', which essentially represent an averaged template of all the ventricular components that occur over a short time window. Those median complexes were then subtracted from the electrogram to achieve the QRS subtracted signal.

3.3.3 Filtering

A 4th order Butterworth filter with 1-30 Hz band pass was used to remove power line interference and low-frequency components of the QRS-subtracted signal. Phase distortion was minimised by performing the filtering process in forward and reverse mode (Child et al., 2018).

3.3.4 Sinusoidal recomposition

In order to apply the renewal theory, phase mapping (which converts voltage into phase) is required as later described in section 3.4. However, this relies on the Hilbert Transform, which typically works best on signals with a sinusoidal shape. Therefore, transformation of QRS-subtracted signals into sinusoidal wavelets was performed to achieve higher accuracy of the Hilbert transform for phase reconstruction. The procedure for sinusoidal recomposition was as described in the previous study (Dharmaprani et al., 2019). It uses a previously published method to transform atrial electrograms into wavelets with a sinusoidal morphology (Kuklik et al., 2014). It starts by calculating the derivative of the signal. Then it looks for negative derivatives, which are the result of negative slopes (indicate the passing of wavefronts) in the signal. The resulting sinusoidal wavelets had amplitudes proportional to the negative slope of the signal and the period equal to mean cycle length of the signal.

3.4 Phase mapping using electrogram data

Figure 12. Phase mapping procedure

3.4.1 Reshaping

QRS-subtracted signals are stored in a 16 x *n* numeric matrix (where *n* = number of time samples), and therefore do not reflect the spatial dimensionality of the original HD-grid catheter, and the positioning of electrodes against the atrial wall. QRS subtracted signals were therefore transformed into a 4x4 grid, which also facilitates interpolation in the later stages of the code. The procedure to import the raw data from Excel files to MATLAB was as described in a previous study (Dharmaprani et al., 2019).In the resulting 4x4 array, each element contains a single instantaneous phase value. As a result, the 4x4 array models the electrical activity of atrial regions being recorded.

3.4.2 Phase mapping

Phase mapping was previously demonstrated to be effective in the analysis of cardiac fibrillation (Umapathy et al., 2010). Typically, phase mapping is used to help visualise the propagation of electrical activity within the heart, as it gives the relative timing of when electrical activity occurs within the action potential cycle. For example, as shown in Figure 13 (right), electrical activity occurring early in the cardiac action potential cycle is denoted in blue ($-\pi$) and activity occurring late in the cycle is denoted by red ($+\pi$). This is achieved by transforming voltage into phase using a transformation such as the 'Hilbert Transform' (further described in section 3.4.2.1). In the context of the current study, this allows identification of patterns such as endocardial breakthroughs.

Figure removed due to copyright restriction

Figure 13. Mapping of ventricular fibrillation using electrode data (Umapathy et al., 2010)

A simple way to understand phase computation is phase-space plots. A phase space plot simultaneously visualises the signal at the current time and time-shifted version of the same signal. From a phase space plot, the random relation is determined by the trajectory of the curve. A phase space plot also allows computing the phase at each instant in time, which is called instantaneous phase.

Figure removed due to copyright restriction

Figure 14. Phase computation by phase-space plots of ventricular fibrillation (Umapathy et al., 2010)

3.4.2.1 Hilbert transform

As described in previous study (Dharmaprani et al., 2019), Hilbert transform was performed to computer the instantaneous phase of the signal. It is a robust approach for phase computation as it does not require the choice of delayed time, which is a critical value in phase-space plots. Its computes the instantaneous phase using the original signal and its phase-shifted signal.

3.4.2.2 Spatial interpolation

Subsequently to phase analysis, spatial interpolation is performed to increase the resolution of phase patterns. As phase is derived from the electrogram data, the spatial resolution is limited to the number of electrodes. Different from optical imaging, electrodes only record the electrical activity at its position so it is impossible to capture every point on the cardiac surface. Hence, the interpolated values from electrode data are used to generate phase maps with better spatial resolution. It is a standard approach used in the field of cardiac electrophysiology to enhance the spatial resolution and visualisation of phase maps, which has notably been demonstrated to not lead to significant error (Jacquemet, 2018).

Figure removed due to copyright restriction

Figure 15. Enhancement of phase map resolution using spatial interpolation (Umapathy et al., 2010)

As described in previous study, spatial interpolation was performed to increase the phase map resolution from 4x4 to 13x13 (Dharmaprani et al., 2019). The electrogram data was interpolated both horizontally and vertically. Linear interpolation was performed separately on the real part of imaginary part of instantaneous phase. There were two stages of linear interpolation on the electrogram data. The first interpolation increased the resolution from 4x4 to 7x7. The second interpolation continue to increase the resolution from 7x7 to 13x13.

3.5 Wavefront processing

The automatic process of detecting wavefronts on phase maps was performed by the provided code as described below.

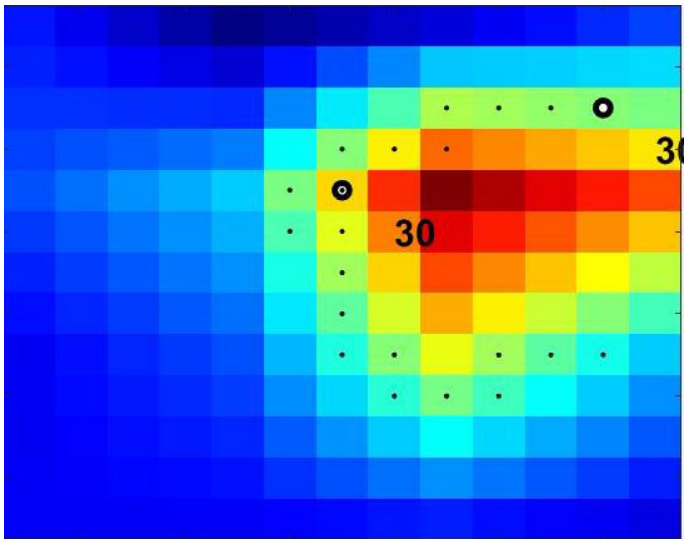

Figure 16. Wavefront detection on phase map

3.5.1 Wavefront detection

Wavefronts were identified as green areas on the phase map, which represent zero phase. The procedure for wavefronts detection on instantaneous phase map was as described in the previous study (Dharmaprani et al., 2019). The process starts by tracking for the first pixel with a zero phase. It then performs the Grassfire algorithm to track for the entire wavefront. It continuously finds and tests 8 nearest neighbouring pixels until the wavefront is fully detected. The detected wavefront is displayed on the phase map by marking the pixels located along it (Figure 14).

3.5.2 Wavefront tracking

As wavefront detection was performed separately on each frame, wavefront tracking was performed to identify wavefronts that are related to each other. The procedure for wavefront tracking was similar to previous study (Dharmaprani et al., 2019). It starts by checking the distance between the first end point of the wavefront in the current frame and the first end point of the wavefront in the next frame. Then it continues checking the distance between the second end points. If the first distance meets the tracking criteria, the wavefront in the next frame will be set as first child. If the second distance meets the tracking criteria, that wavefront will be set as second child. Subsequently, identification numbers were assigned to all the wavefronts. Children wavefronts were assigned to the same identification number of their respective parents. Figure 14 shows a wavefront identification number displayed on the phase map.

3.6 Novel custom image algorithm

In this study, a novel custom image algorithm was developed. Currently, there is no automatic methods of detecting endocardial breakthroughs that have been described. The algorithm was developed based on the binary image processing toolbox in MATLAB. Its basic operation is to cycle through all phase maps, detect and validate the wavefronts propagating from endocardial breakthroughs, search for the frames at which endocardial breakthroughs initiate. Full MATLAB codes can be found in Appendix A.

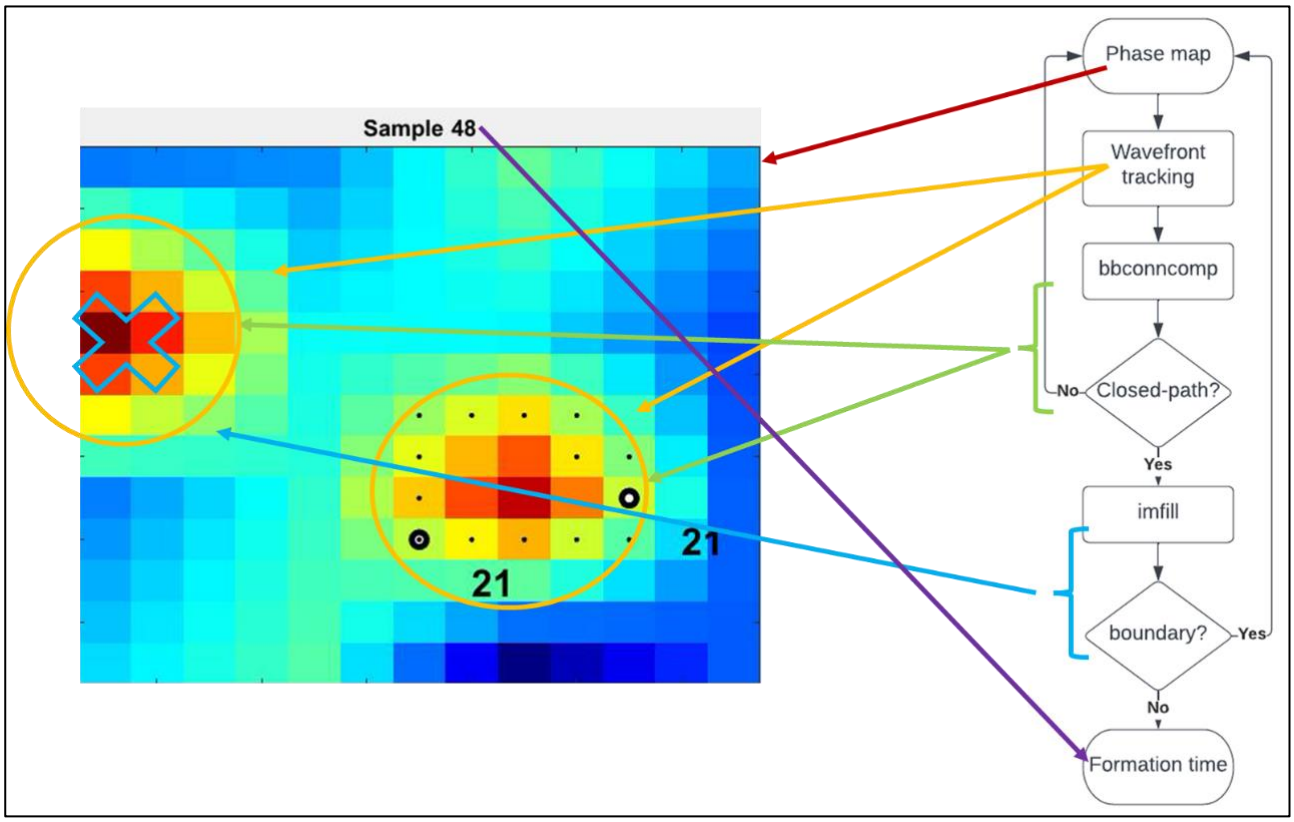

Figure 17. Novel custom image algorithm for endocardial breakthrough detection

Figure 16 describes a single cycle of the automatic process used to detect the wavefronts propagating from endocardial breakthroughs in a single phase map, which was as described below.

3.6.1 Construction of binary phase map

A binary phase map with no colour pixels representing voltage values was used to help detect endocardial breakthroughs, as it provides a better visualisation of the path of wavefronts (Figure 17). Binary phase maps were constructed based on the original phase maps. At each frame, the process starts by checking the wavefront data associated with the current phase map. If wavefront data is found, it creates a 13x13 phase map with all the pixels set to ‘1’ (turn on). Then it assigns ‘0’ to all the pixels (turns off) located along the wavefront based on the wavefront data.

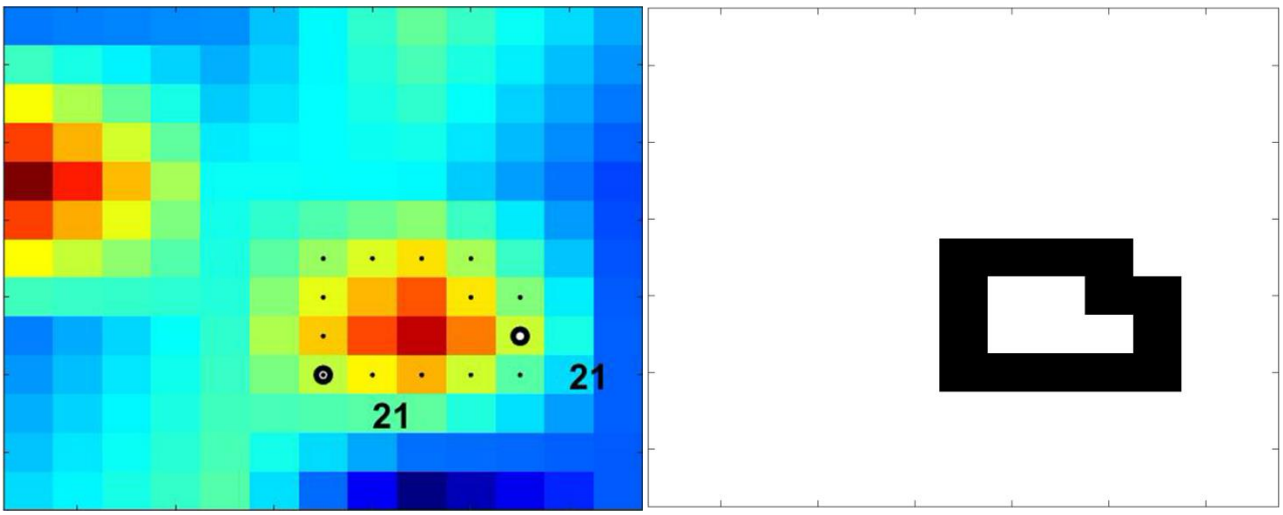

Figure 18. Original phase map with color pixels representing voltage values (left) and binary phase map with black and white pixels showing clearly the path of a wavefront (right)

3.6.2 Detection of closed-path wavefront

As a breakthrough event is defined as localised electrical activity whereas wavefront eliminates from the breakthrough site in focal pattern, which then propagates onto the endocardial surface in a circular pattern (Verheule et al., 2014). Based on this concept, the algorithm developed in the current study reasoned that the wavefront of a breakthrough wave can be identified as a closed-path object a binary phase map (Figure 17, right). Detection of closed-path wavefront was performed using `bwconncomp`, a MATLAB image processing function to finds and counts the number of objects or regions in a binary image. It works by checking the connectivity of pixels on that image. In this study, each phase map is a binary image, and the number of regions is determined by the interruption of the wavefront on the connectivity of pixels. If there is no wavefront on the phase map, the number of regions is 1 as there is no disconnection at any pixels. If there is an open-path wavefront, the number of regions is still 1 as the connectivity of neighbouring pixels around the wavefront is maintained. If there is a closed-path wavefront, the number of regions is 2 as it disconnects the pixels located at its interior from the pixels located at its exterior.

3.6.3 Validation of detected wavefront

The previously reported criteria were applied to validate if detected wavefronts propagate from the breakthrough sites. The first criterion is that a breakthrough site is located at the boundary of the phase map (Eckstein et al., 2013). The second criterion is that a breakthrough site is activated earlier than the surrounding area (de Groot et al., 2010). The first validation was performed using the combination of `imfill` and `bwconncomp`. `imfill` is a MATLAB image processing function to fill holes or regions in a binary image. The closed-path wavefront forms a hole (smaller region) when it locates within the phase map. If the detected wavefront is located at the boundary of the phase map, it cannot form a hole as its path is partly missing. Subsequent to `imfill`, `bwconncomp` is performed to

check the number of regions in the binary phase map. If the region number changes from 2 to 1, it means that the detected wavefront is located within the phase map. If the region number remains, then that wavefront is located at the boundary of the phase map. The second validation was performed by checking whether the pixel with the highest phase located at the interior of the detected wavefront is the pixel having the highest phase on the phase map. To find that pixel, the original phase map was used with all the pixels located at the filled hole were turned on while other pixels were turned off. If that pixel matches to the pixel with highest phase when all pixels are on, then the detected wavefront propagates from a breakthrough site.

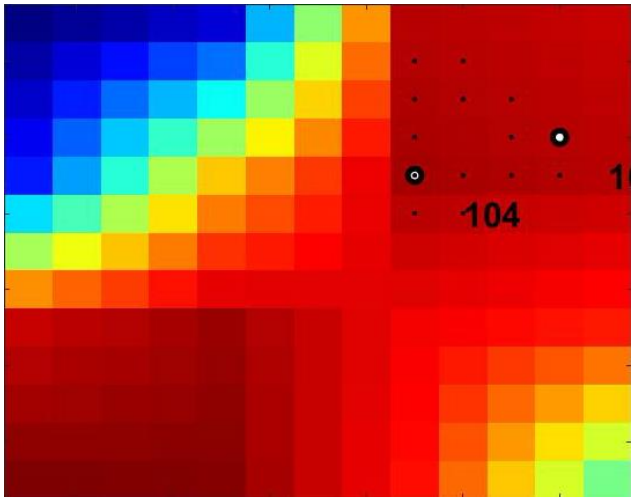

Figure 19. Example of a closed-path wavefront detected by the algorithm

3.6.4 Search for initiation frame

The identification number of each detected wavefront was used to search for frames at which a breakthrough event initiates. The algorithm cycles through all frames and looks for the first frame that has a wavefront with the identification number matches to the detected wavefront. The initiation of breakthrough is normally represented by a pattern of 2x2 pixels on a phase map (Figure 19). It then saves the frame number into the data table for the calculation of inter-formation times.

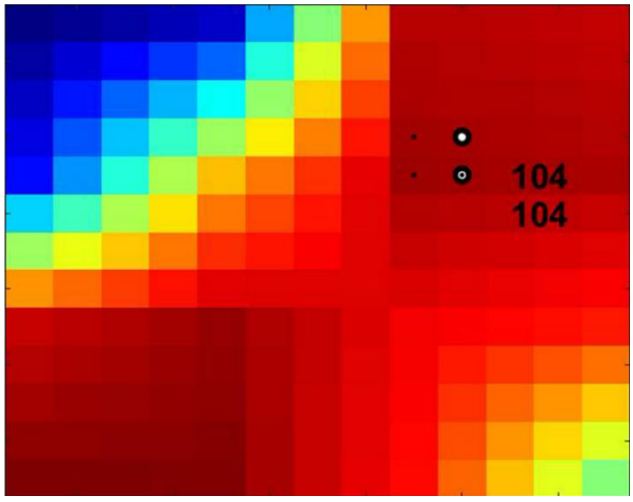

Figure 20. Example of breakthrough initiation detected by the algorithm

3.7 Statistical Analyses

To test the hypothesis that endocardial breakthroughs occur randomly in time and can therefore be modelled as a renewal process, several tests were conducted to assess for the characteristic motifs of a renewal process. This included: i) testing for statistical independence, which was assessed by looking at the autocorrelation of inter-event times; and ii) assessing the distribution of inter-event times.

3.7.1 Testing autocorrelation

To test whether inter-formation times were independently distributed, Ljung-box Q-test was performed on the autocorrelation of inter-formation times at all lags. The autocorrelation values were expected to be 1 at lag 0 and approach 0 at all other lags.

3.7.2 Testing distribution

To test whether inter-formation times were exponentially distributed, Chi-square goodness of fit test was performed on the distribution of inter-formation times.

Bonferroni correction was also performed in both tests to counteract the multiple testing problem.

3.7.3 Testing the influence of different clinical factors

To test the hypothesis that different clinical factors have influence on the formation of endocardial breakthroughs, comparison tests were performed on formation rates of endocardial breakthroughs between comparing groups. These groups were anatomical regions, gender, lifestyles and clinical subtypes of AF. The formation rates were calculated by the cumulative distribution function (CDF) of inter-formation times of endocardial breakthroughs. Unpaired t-tests were also performed to evaluate the significance of the comparing results.

4 RESULTS

There were 47/387 cases discarded prior to statistical analyses as the data was insufficient.

4.1 Autocorrelation of endocardial breakthroughs

Figure 11 shows an example correlogram from a single patient. Full correlograms for all patients can be found in appendix B. Collectively, the results showed that 335/340 (98.53%) were not rejected by the Ljung-box Q-test at a significance level of 0.05 (mean p-value = 0.47 (95%CI, 0.45 - 0.50)), after Bonferroni correction for multiple tests. It indicates that autocorrelation values approached 0 at all non-zero lags. In other words, inter-formation times of endocardial breakthroughs in 98.53% cases were statistically independent.

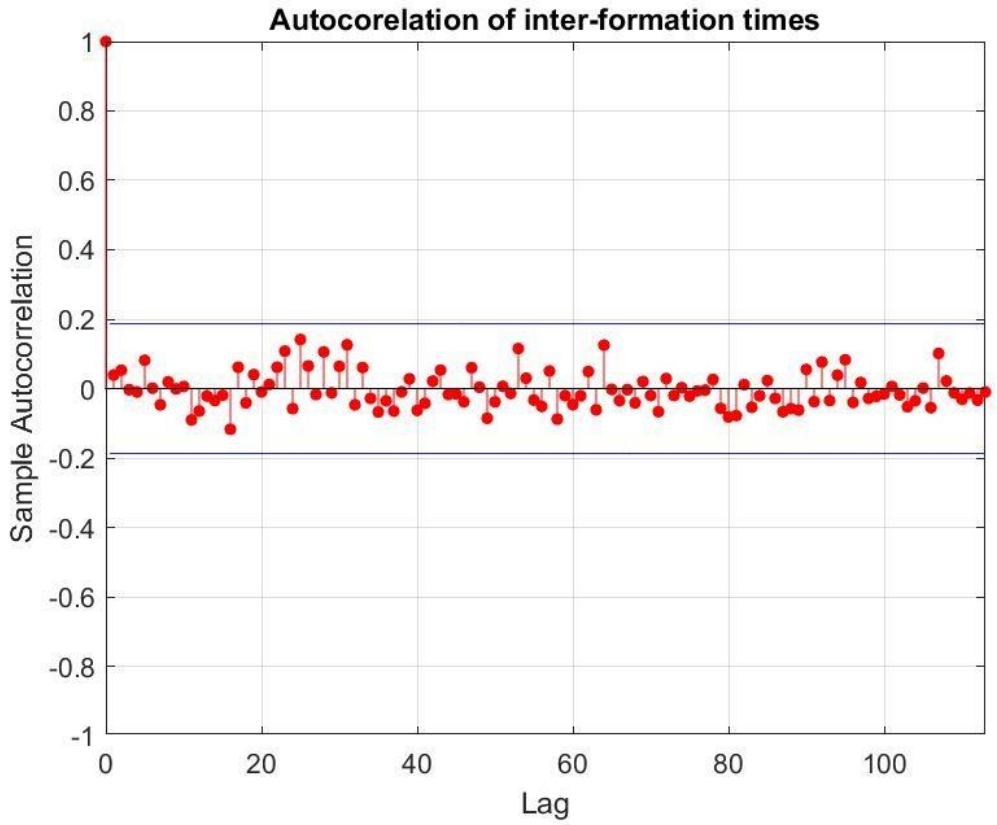

Figure 21. Autocorrelation of inter-formation times of endocardial breakthroughs within the anterior left atrium of an AF patient

The x-axis represents the lag, ranging from 0 to the number of endocardial breakthroughs within the region. The y-axis represents the degree of similarity, ranging from -1 (perfect negative correlation) to 1 (perfect positive correlation). The red dot points represent the autocorrelation at each lag, calculated using the autocorrelation function. The blue lines represent the upper and lower confidence bounds, calculated from the estimated standard error of the autocorrelation (p-value = 0.99)

In regards to the test rejection, it was found that the autocorrelation of all the rejected cases has a similar feature. The correlogram of those cases show that the autocorrelation at certain lags exceeded the confident bounds (Figure 12). The source of outliers in the autocorrelation of these cases will be discussed in Section 5.4.

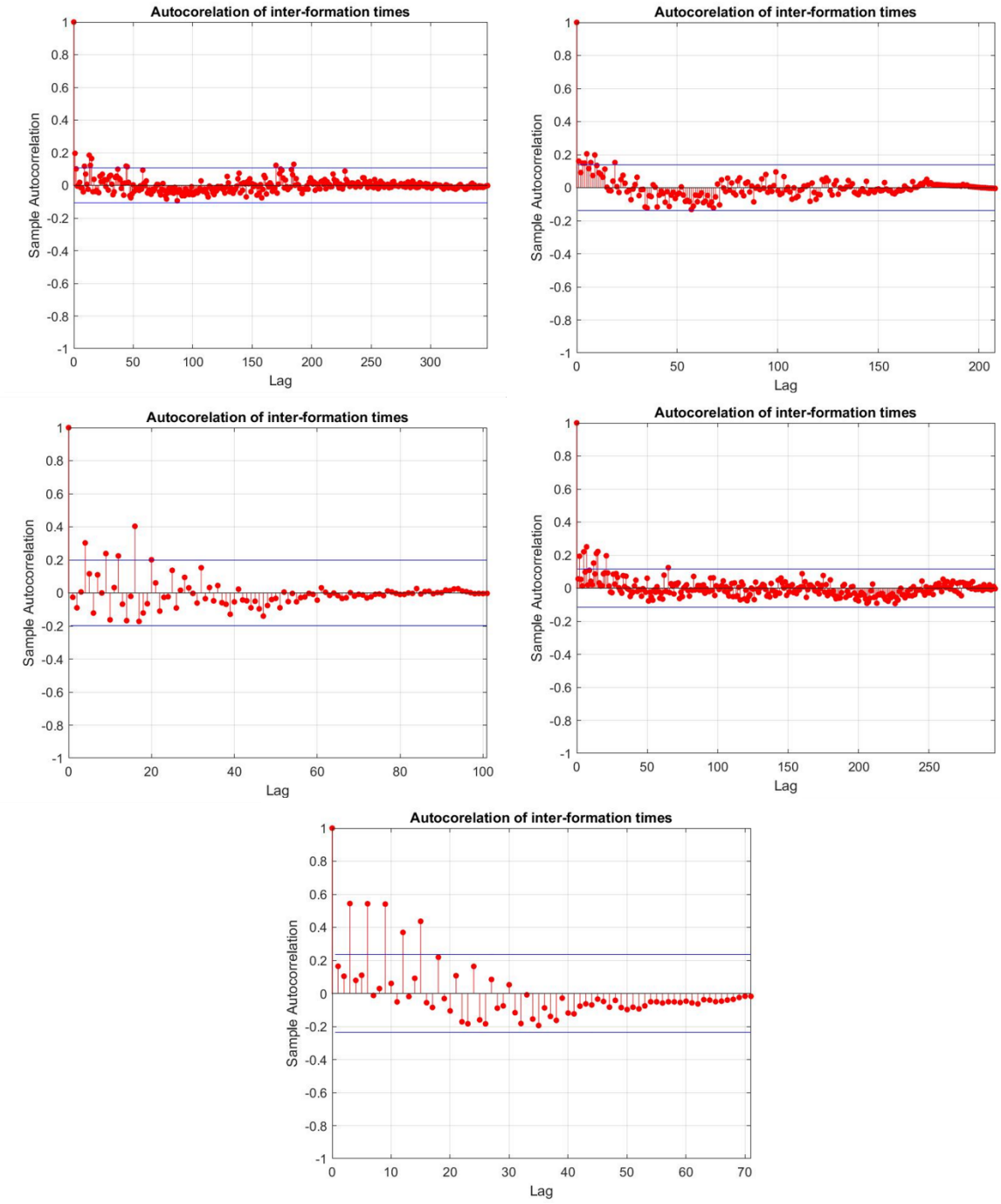

Figure 22. Autocorrelation of all the cases rejected by Ljung-box Q-test

4.2 Exponential distribution of endocardial breakthroughs

Figure 13 shows an example histogram from a single patient. Full histograms for all patients can be found in appendix C. Collectively, the results showed that 312/340 (91.76%) were not rejected by the Chi-square goodness-of-fit test at a significance level of 0.05 (give mean value and 95% confidence interval (i.e., mean p-value = 0.42 (95%CI, 0.39 - 0.45)), after Bonferroni correction for multiple tests. It indicates that inter-formation times of endocardial breakthroughs in 91.76% cases fits to an exponential distribution.

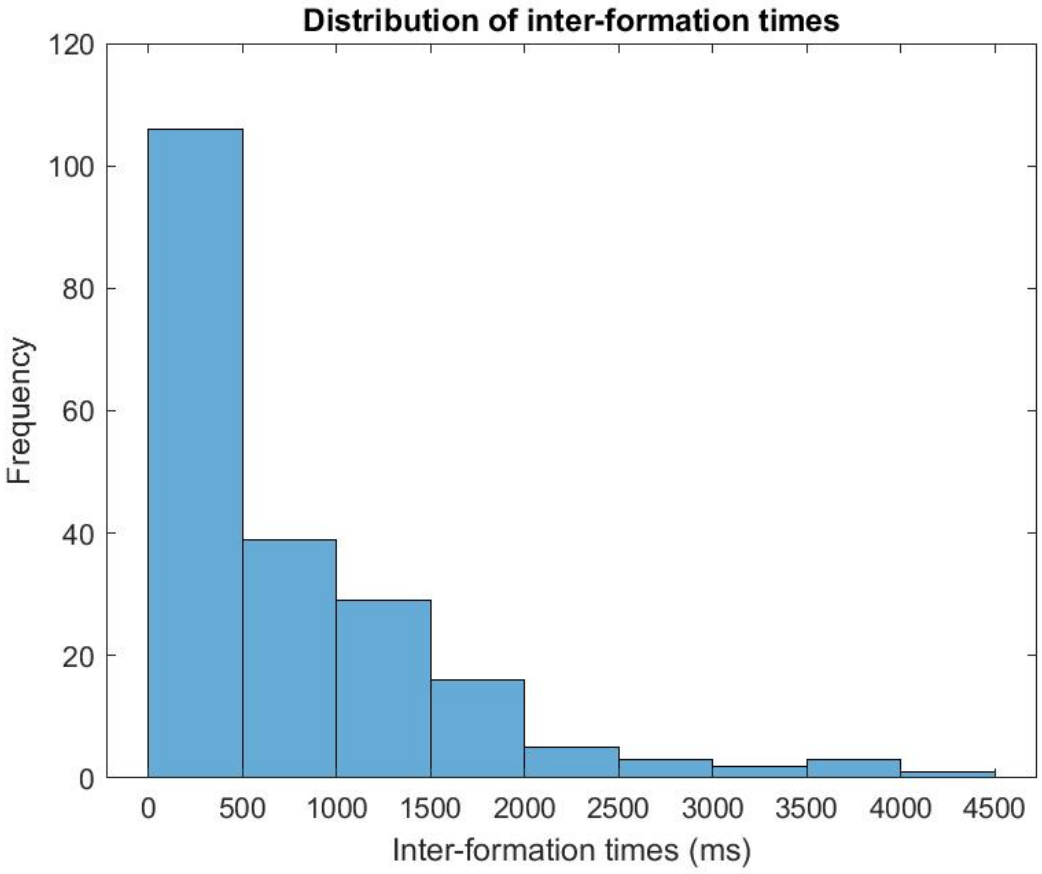

Figure 23. Exponential distribution of inter-formation times of endocardial breakthroughs within the left superior pulmonary vein of AF patients (p-value = 0.99)

In regards to the test rejection, the statistical distribution of all the rejected cases has the same feature. As the second bin outpaces the first bin, the statistical distribution of these cases was unable to be fitted to an exponential distribution (Figure 13). The source of outliers in the statistical distribution of these cases will be discussed in Section 5.4.

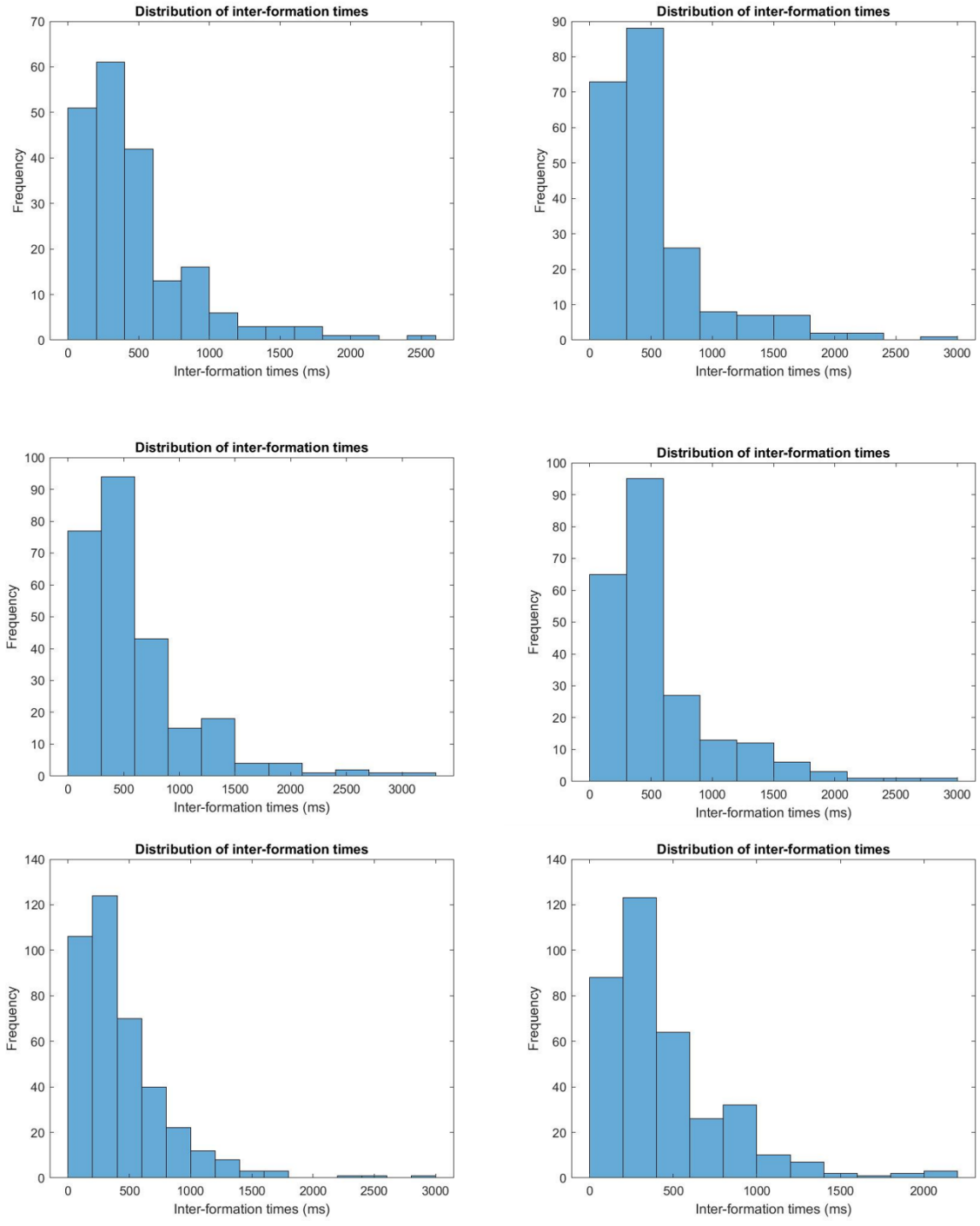

Figure 24. Examples of the cases rejected by Chi-square goodness-of-fit test

4.3 Impacts of clinical types of AF

The results show that there was a significant difference between paroxysmal AF and persistent AF. The box plot shows that the mean formation rate of endocardial breakthroughs in patients with paroxysmal AF is slightly higher than that in patients with persistent AF (Figure 17). This interesting finding will be discussed further in Section 5.2.

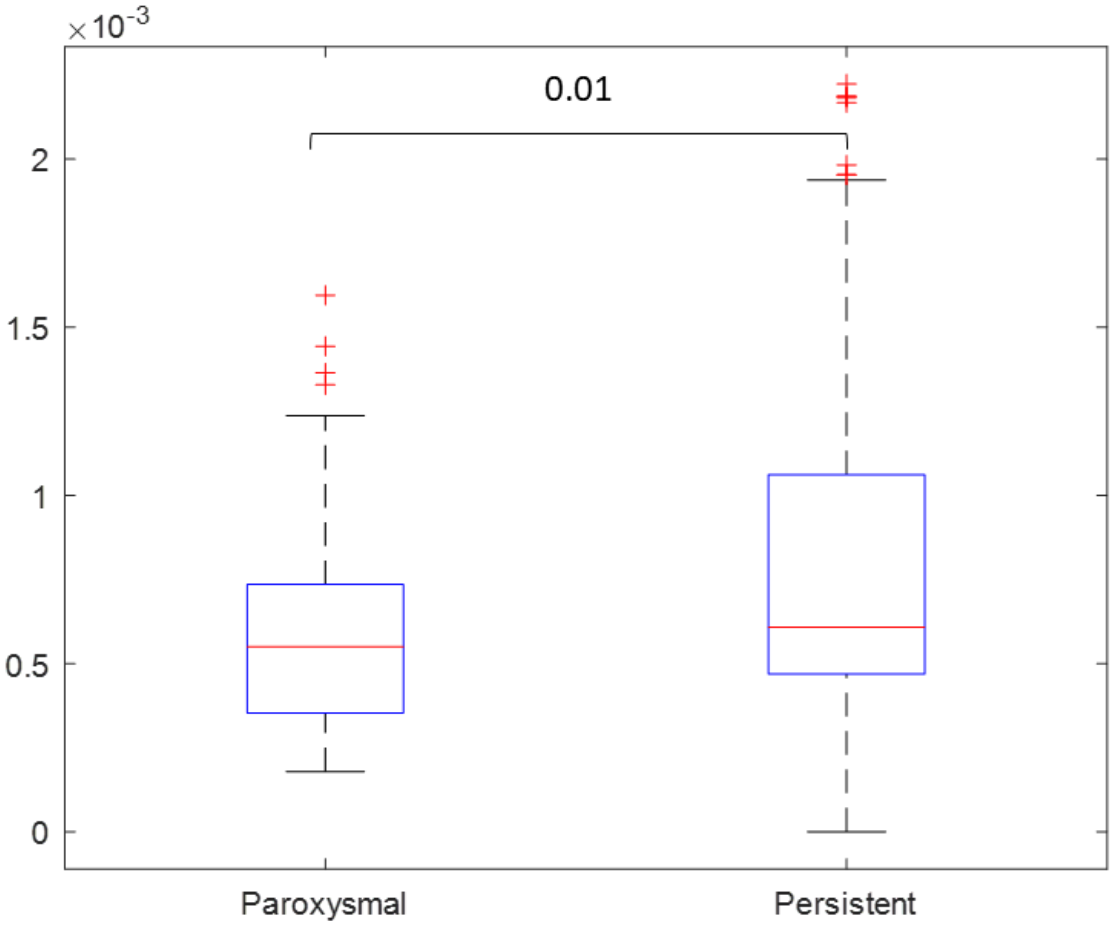

Figure 25. Comparison of the formation rates calculated by the CDF of inter-formation times of endocardial breakthroughs in patients with different clinical types of AF

4.4 Impacts of other factors

4.4.1 Anatomical regions

The results showed that there was no significant difference between the left atrium and the right atrium (p-value = 0.37). However, the box plot shows that the mean formation rate of endocardial breakthroughs in the left atrium was slightly higher than that in the right atrium.

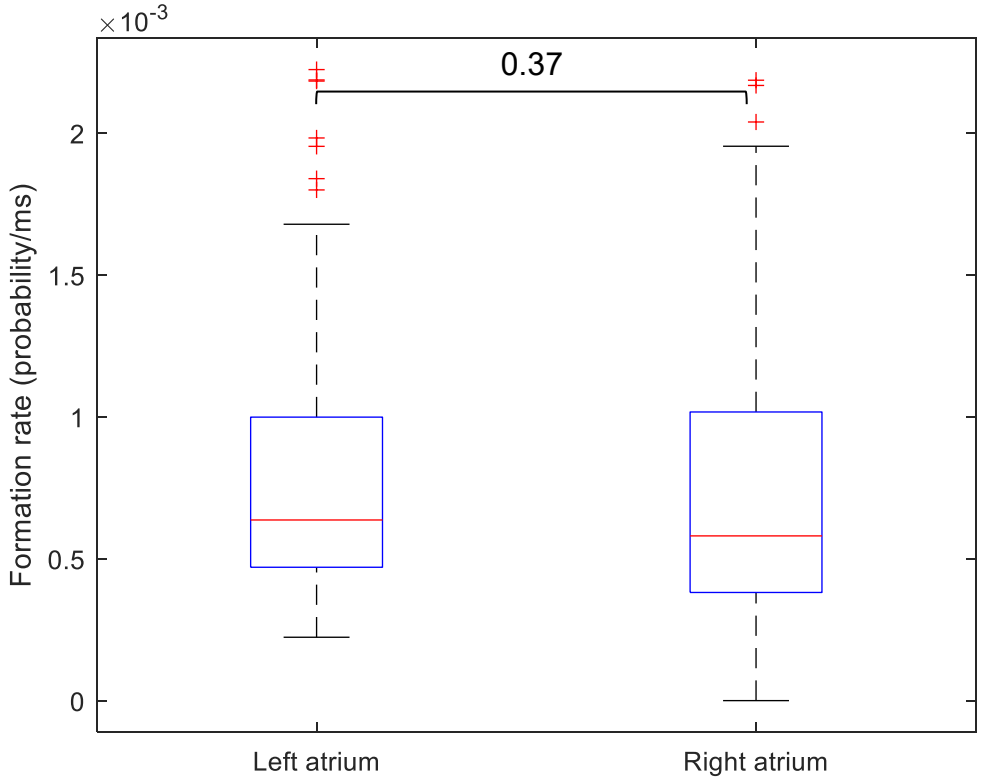

Figure 26. Comparison of the formation rates calculated by the CDF of inter-formation times of endocardial breakthroughs in the left atrium and in the right atrium (p-value = 0.37)

The x-axis represents the comparing group. The y-axis represents the formation rate calculated by the CDF of inter-formation times of endocardial breakthroughs. The red lines represent the median of the scores. The blue boxes represent the upper and lower quartile of the scores. The extending lines represents the upper and lower whiskers of scores. The red crosses at the end of the top whiskers represent the outliers of the comparison. The value and the bracket at the top of the graph represents the p-value of the unpaired t-test.

In the left atrium, there was no significant difference between anatomical regions (p-values > 0.05). However, the box plot shows that the mean formation rate of endocardial breakthroughs in the anterior region was considerably lower than those in other regions (Figure 14).

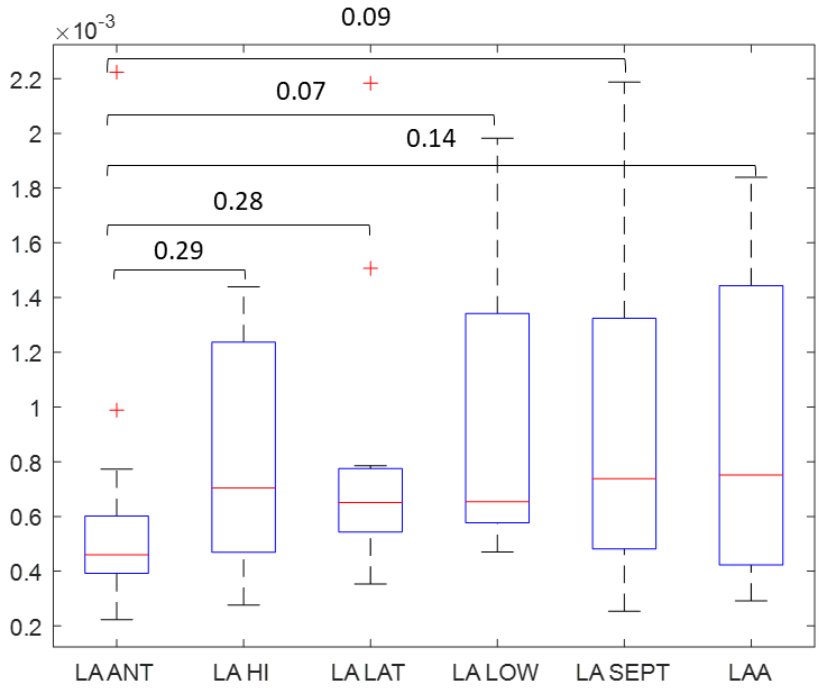

Figure 27. Comparison of the formation rates calculated by the CDF of inter-formation times of endocardial breakthroughs in different anatomical regions in the left atrium

In the right atrium, there was no significant difference between regions (p-values > 0.05). However, the box plot shows that the mean formation rate of endocardial breakthroughs in the right atrial appendage was considerably lower than those in other regions (Figure 15).

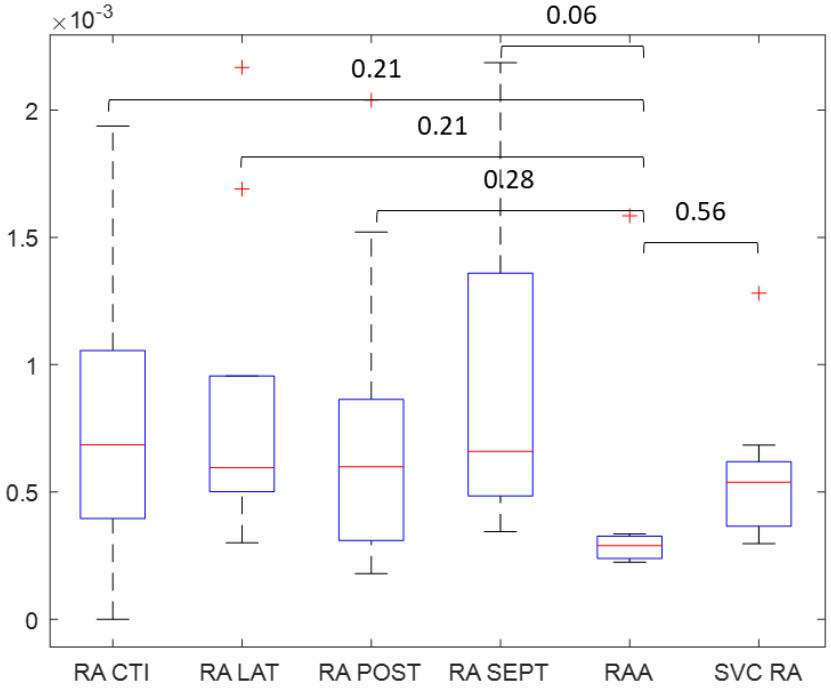

Figure 28. Comparison of the formation rates calculated by the CDF of inter-formation times of endocardial breakthroughs in different anatomical regions in the right atrium

4.4.2 Genders and lifestyles

The results showed that there was no significant difference between males and females. However, the box plot shows that the mean formation rate of endocardial breakthroughs in the females is slightly lower than that in males (Figure 16).

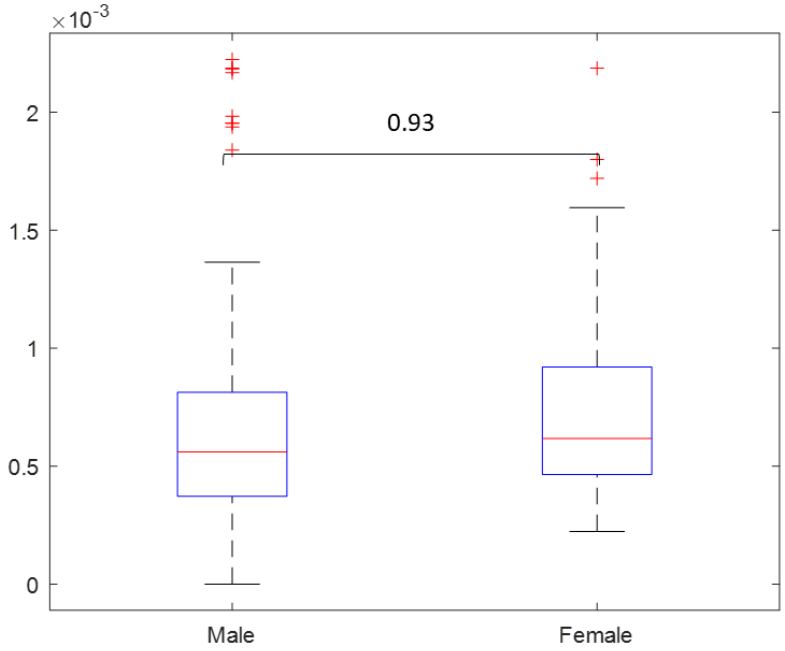

Figure 29. Comparison of the formation rates calculated by the CDF of inter-formation times of endocardial breakthroughs in different in male AF patients and in female AF patients

The results showed that there were no significant differences between not smoking and drinking alcohol, drinking alcohol only, and alcohol plus smoking. However, the box plot shows that the mean formation rate of endocardial breakthroughs for alcohol and smoking is slightly lower than the others (Figure 17).

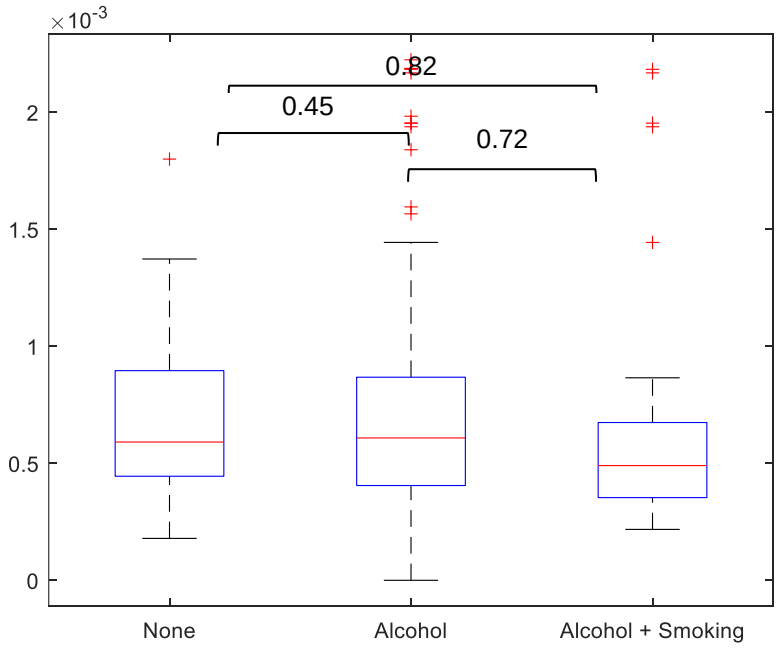

Figure 30. Comparison of the formation rates calculated by the CDF of inter-formation times of endocardial breakthroughs in AF patients with different lifestyles

5 DISCUSSION

5.1 Renewal theory for characterising electrical activities in AF

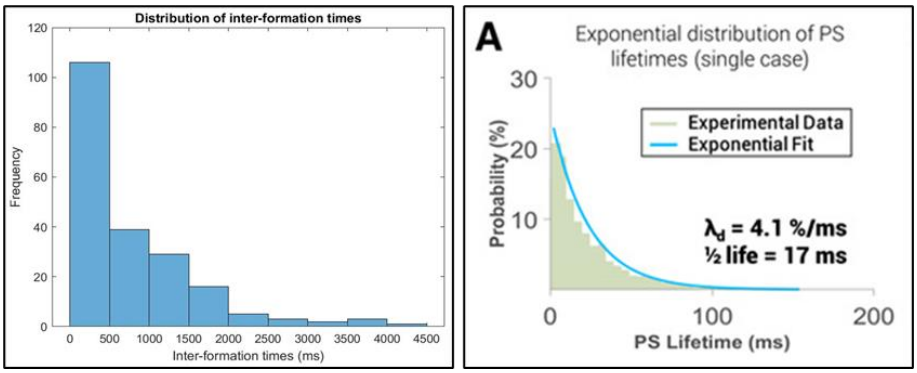

Figure 31. Renewal process models of A. Endocardial breakthroughs and B. phase singularities in AF

In this research, endocardial breakthroughs in AF patients were found to be consistent with renewal processes. Evidence for this is shown by the correlation analysis, which demonstrated that this chaotic electrical activity in AF occurs randomly in time (i.e. with statistical independence). Hence, it suggests that endocardial breakthroughs can be modelled as a stochastic process. The distribution analysis also showed that the inter-formation times associated with endocardial breakthroughs produce exponential probability distributions. The implication of this is that the formation of endocardial breakthroughs can be quantified, and thus the formation rate can be estimated using the exponential rate constant λ.

In previous studies, renewal theory was found to be a universal framework to characterise rotors and wavelets in AF (Dharmaprani et al., 2019, Quah et al., 2020, Quah et al., 2021, Jenkins et al., 2022). It challenged two long standing theories of AF, in that it has been hypothesised that either long lasting rotors are responsible for sustaining AF, or that the presence of multiple wavelets drive AF. However, previous work by Dharmaprani et al. (2019), used the Renewal theory framework to show that these two proposed mechanisms essentially co-exist, and both simply occur randomly in time due to underlying spatiotemporal chaos. Importantly, this work further suggests that rather than specific rotors and wavelets driving AF, it is the continual regeneration process of rotors and wavelets that is responsible for sustaining the condition. This has consequences for the clinical treatment of AF, as it explains why treatments that focus on eliminating these drivers as a means to terminate AF (i.e., high frequency source ablation) do not work (Atienza et al., 2014).

Hence, renewal theory can revolutionise the medical perspective that AF is chaotic and unpredictable. This perspective comes from the fact that AF is characterised by chaotic electrical activity in the atria. This has made it difficult to explore the mechanisms of AF. However, as shown in recent studies and

the current project, renewal theory has the potential to characterise the complicated electrical behaviour of AF. It is also potentially powerful in that it can be extended to other electrical patterns that have also been observed in AF outside of rotors, wavelets and endocardial breakthroughs. This has the potential to bridge the multiple competing theories of AF under one quantitative framework.

It can be noted however that some recordings demonstrated a high autocorrelation at from lags ~0-50 (i.e., at the start of the recording), indicative of correlation between the timings of new endocardial breakthrough events (Figure 21). These instances therefore do not fit to the renewal theory model whereby endocardial breakthroughs occur randomly in time. Potential explanations for these outliers may be artifacts that occur early in the recording, such as 'pacing spikes' that are present at the start of an electrophysiology study due to periodic pulses of electricity being applied to pace the heart and initiate a patient's AF. Another potential source could be from the recording capturing some sinus rhythm activity at the beginning, prior to the patients AF being initiated. However, further analysis will be required to determine this.

5.2 Endocardial breakthroughs relate to AF progression

The fact that clinical subtypes of AF was the only factor to show a statistically significant difference on the formation rate of endocardial breakthroughs aligns with previous studies on the role of breakthrough events in the progression of AF (de Groot et al., 2010, Verheule et al., 2013). The maintenance of AF and the incidence of breakthrough events are elements of a closed cycle contributing to the progression of AF (Figure 20).

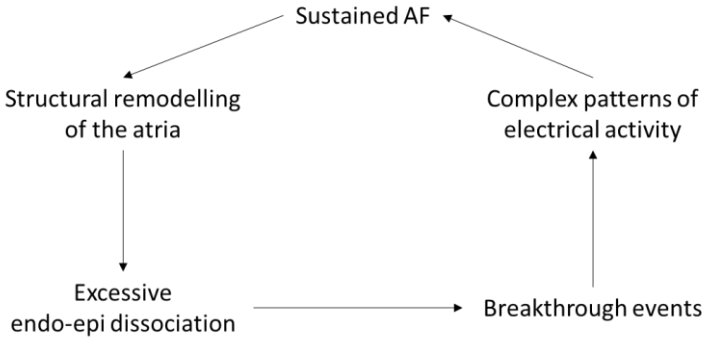

Figure 32. Closed cycle for maintenance of AF

The long-term chaotic and rapid electrical activity of sustained AF cause damages to the structural organisation of the atria walls. In response to the tissue damage, atrial fibrosis occurs and alters the trabecular network between the endocardium and the epicardium. Structural remodelling then results in excessive EED between the two walls (Verheule et al., 2013, Hansen et al., 2015). Newly born fibrous tissue interrupts the synchronous activation between cardiac cells of the opposing walls. The sudden change in the electrical activity of the atrial walls results in the incidence of breakthrough

waves. The number of breakthrough sites and the frequency of breakthrough events are proportional to the magnitude and the frequency of EED.

The incidence of breakthrough waves increases the complexity of the chaotic electrical activity of the heart during AF (Allessie et al., 2010). Highly complex electrical patterns contribute to the maintenance of AF and thus prevent the self-termination of AF. In paroxysmal AF, the episode is short so there is no measurable damage to the atrial walls and thus negligible number of breakthroughs. However, when paroxysmal AF repeats certain times, the damage increases and thus the incident of breakthroughs increases. The breakthrough waves and the resulting complex electrical patterns increase the episode length of AF, which is subsequently becomes persistent AF.

5.3 The effect of anatomical, gender, and lifestyle factors on the occurrence of breakthroughs

In this study, anatomical regions, genders and lifestyles was shown to not have a significant impact on endocardial breakthroughs inter-formation times in the results of the t-test. However, the box plots show that there are certain numerical differences between the respective factors. It indicates that the test might be limited by data size and population. The results are also affected by the fact that the number of cases between the comparing factors are different. Hence, larger data size and population are needed for further investigation.

Currently, there is no study focusing on the variations of EED and breakthroughs between different anatomical regions. The majority of previous studies were about the complex pattern of EED and breakthroughs on the entire atria (Schuessler et al., 1993, de Groot et al., 2010, Eckstein et al., 2013, Parameswaran et al., 2020). Structural characteristics of different anatomical regions in the atria were actually taken into consideration. The geometry of atrial appendages and septum, two main cavities in the atria, was normally approached for modelling EED and breakthrough (Krueger et al., 2011, Uldry et al., 2012, Colman et al., 2013). However, no study on the correlation between regional differences and the feature of EED and breakthroughs was done.

There is also no study focusing on gender differences in EED and breakthroughs. The electrophysiological differences between males and females were reported to differentiate the characteristics of AF (Westerman and Wenger, 2019). Sex hormone have an effect on the atrial pacing (Surawicz and Parikh, 2003). Atrial pacing is an important factor triggering structural remodelling of the atrial walls (Allessie et al., 2002). A higher tendency of structural remodelling leads to a higher incident of EED and breakthroughs (Verheule et al., 2014). Hence, more investigation is needed to explore how gender differences differentiate EED and breakthroughs.

Similar to other factors, there is no study focusing on the effects of alcohol and smoking on EED and breakthroughs. Alcohol and smoking were previously reported to be associated with the incident of AF (Liang et al., 2012, Chamberlain et al., 2011). The substances in alcohol and smoking stimulate the activity of the heart. Heavy intake of those substances results in irregularly rapid atrial pacing. As mentioned above, rapid atrial pacing is closely associated with the incident of EED and breakthroughs. Hence, more investigation is needed to understand further the effects of alcohol and smoking on the increase of EED and breakthroughs in the atria.

5.4 Limitations of the research

Sample size and resolution is the limitation of mapping methods using electrogram data (Umapathy et al., 2010). Those parameters are dependent on the size of the catheter and the number of the electrodes on the catheter. Optical mapping is an alternative for higher spatial resolution. However, it is currently not available for clinical usage due to the requirements of voltage-sensitive dyes, which causes the toxicity to human health.

Interpolation is a common method to overcome the limitation in the resolution of electrogram-based mapping methods, but it also affects the reliability of the data (Umapathy et al., 2010). The quality of the interpolation is dependent on the distance of the electrodes on the catheter. Larger proximity of the electrodes results in poorer quality of interpolated data, and thus no sufficient information to represent the surface of the atrial walls.

Although phase mapping is a versatile method to study the spatiotemporal chaos during sustained AF, it has the limitations in studying endocardial breakthroughs in atrial fibrillation. Breakthrough events have been found as highly localised activation patterns on the surface of the atrial walls (Verheule et al., 2014). Those events are the result of atrial fibrosis as the scar tissue interrupts increase EED between the opposing walls of the atria. The characteristics of breakthrough events might result in the biased spatial distribution of phase (Umapathy et al., 2010).

2-dimensional surface mapping has the limitations for performing phase mapping and studying endocardial breakthrough (Umapathy et al., 2010, Parameswaran et al., 2020). Although previous studies applied phase mapping on the single surface of the atrial walls, this technique actually requires simultaneous mapping of the epicardium and the endocardium. It is an important factor for studying fibrillation dynamics at the anatomical regions with the high thickness of cardiac walls such as ventricular fibrillation. As breakthrough events involve fibrillation waves propagate through the atrial walls as the result of excessive endo-epi dissociation, simultaneous analysis of the electrical activity across 3-dimensional structure of the atrial walls is required.

The criteria to detect breakthrough events in 2-dimensional surface mapping are varied between previous studies (de Groot et al., 2010, Verheule et al., 2013). It was mainly based on the observation and the limited demonstration of the single-surface mapping. Moreover, the origin of breakthrough events is also a debating topic. Two previously reported principles are ectopic focal discharges and transmural conduction (Mahida et al., 2015, Eckstein et al., 2013). They are also distinguishable through the morphology of unipolar electrograms. However, the computational algorithm to distinguish those principles based on electrogram data are not readily available.

5.5 Future Work

Larger sample size and higher resolution of cardiac mapping is expected in further study. Basket catheter provides better mapping data as it has a total of 64 electrodes. An 8x8 grid of electrodes will increases the resolution of mapping array by the factor of 4. Higher resolution of mapping array will require less interpolated data and thus increase the reliability of results. Higher density of electrodes on the catheter also outputs a higher quality of interpolated electrograms.

Simultaneous mapping of the endocardium and the epicardium is to validate the detection of excessive EED and breakthrough events by referring to the activation time of the endocardial surface and the epicardial surface. It is also to explore the formation and propagation of breakthrough waves between the opposing walls through the trabecular network of the atrial walls. Furthermore, it is to distinguish breakthrough events from other electrical patterns such as ectopic beats and focal discharges, as well as any other disturbances from the electrogram data. Promisingly, the principle of breakthrough events can be distinguished or validated without referring to the morphology of unipolar electrograms.

Further work can be done to enhance the computational algorithm developed in this study, as it has a potential in working with highly localised electrical patterns, e.g., breakthrough events. In this study, it was efficient in detecting endocardial breakthroughs and calculating inter-formation times on the provided data source. Testing with different sample size and resolution is needed to evaluate the performance of this algorithm. Furthermore, it is expected implemented in the combination with endo-epi simultaneous mapping to advance the study of breakthrough events.

Renewal theory is expected to expand to gain more insight into the mechanism of breakthrough events during sustained AF. Further study on the measurable rate of the probability distribution of endocardial breakthroughs is needed to characterise those events in the maintenance of AF. Moreover, the formation rate of endocardial breakthroughs can be integrated with the formation and destruction rates of phase singularities in AF to study further on the mechanism of sustained AF.

The role of breakthrough events in the progression of AF has been widely reported but it needs to be evidenced by the statistical characterisation of inter-formation times. In this study, the statistical analyses have found the significance difference in endocardial breakthroughs in paroxysmal AF and persistent AF on the provided data source. Further study on different sample size and population is needed to confirm this significance difference. Moreover, the statistical characterisation of endocardial breakthroughs can be extended to patients with permanent AF. It is needed to emphasise the correlation between breakthrough events and the episode of sustained AF.

6 CONCLUSIONS

This study found that the inter-formation times of endocardial breakthroughs were statistically independent and has an exponential distribution in AF patient's hearts. The statistical independence of inter-formation times means that endocardial breakthrough is a stochastic process. There is no underlying constant driver of those events, and AF is not sustained by the constant formation of endocardial breakthroughs. It also means that Renewal theory is applicable to understand endocardial breakthroughs by modelling its probability distribution of inter-formation times. The exponential probability distribution of inter-formation times means that the formation rate of endocardial breakthroughs is measurable. The measurable rate allows the characterisation of endocardial breakthroughs during the maintenance of AF.

Another finding was that clinical types of AF have a significant impact on the formation of endocardial breakthroughs. It is consistent with previous studies on the mechanistic correlation between endocardial breakthroughs and the progression of AF. The fact that persistent AF has a higher formation rate of endocardial breakthroughs than paroxysmal is aligned with current literature. The incidence of breakthrough events was reported to relate to atrial fibrosis, which involves structural remodelling of the atrial walls triggered by the damage of sustained AF. Then the propagation of breakthrough waves between the endo-epi surfaces through the trabecular network contributes to the complexity of electrical patterns sustaining AF.

Limitations of the study, which might be the source of outliers in statistical analyses have been addressed. Sample size and resolution are the typical concerns of electrogram-based cardiac mapping. Interpolation has certain issues with the quality and reliability of interpolated electrograms. Phase mapping are quite limited in studying localised electrical patterns and AF. Studying of breakthrough events is also limited by 2-dimensional surface mapping. It leads to various and unclear criteria for detecting breakthrough events that requires validation with unipolar electrograms.

Future work is expected to expand the study of breakthrough events and overcome the limitation so the current study. Basket catheter data is needed to increase the resolution of cardiac mapping. Simultaneous mapping should be performed to improve the detection and validation of breakthrough events. The computational algorithm developed in this study has a good performance in studying breakthrough events and a potential in applying to other localised electrical patterns during sustained AF, so its use needs to be expanded and enhanced. Renewal theory can be expanded to characterise breakthrough events in the sustenance of progressive AF.

7 REFERENCES

ALLESSIE, M., AUSMA, J. & SCHOTTEN, U. 2002. Electrical, contractile and structural remodeling during atrial fibrillation. *Cardiovascular research,* 54**,** 230-246.

ALLESSIE, M. A. 1985. Experimental evaluation of Moe's multiple wavelet hypothesis of atrial fibrillation. *Cardiac electrophysiology and arrhythmias***,** 265-275.

ALLESSIE, M. A., BONKE, F. & SCHOPMAN, F. 1977. Circus movement in rabbit atrial muscle as a mechanism of tachycardia. III. The" leading circle" concept: a new model of circus movement in cardiac tissue without the involvement of an anatomical obstacle. *Circulation research,* 41**,** 9-18.

ALLESSIE, M. A., DE GROOT, N. M., HOUBEN, R. P., SCHOTTEN, U., BOERSMA, E., SMEETS, J. L. & CRIJNS, H. J. 2010. Electropathological substrate of long-standing persistent atrial fibrillation in patients with structural heart disease: longitudinal dissociation. *Circulation: Arrhythmia and Electrophysiology,* 3**,** 606-615.

ARONIS, K. N. & TRAYANOVA, N. A. 2020. Endocardial-Epicardial Dissociation in Persistent Atrial Fibrillation. *Circulation: Arrhythmia and Electrophysiology,* 13**,** e009110.

ATIENZA, F., ALMENDRAL, J., ORMAETXE, J. M., MOYA, Á., MARTÍNEZ-ALDAY, J. D., HERNÁNDEZ-MADRID, A., CASTELLANOS, E., ARRIBAS, F., ARIAS, M. Á., TERCEDOR, L., PEINADO, R., ARCOCHA, M. F., ORTIZ, M., MARTÍNEZ-ALZAMORA, N., ARENAL, Á., FERNÁNDEZ-AVILÉS, F. & JALIFE, J. 2014. Comparison of Radiofrequency Catheter Ablation of Drivers and Circumferential Pulmonary Vein Isolation in Atrial Fibrillation: A Noninferiority Randomized Multicenter RADAR-AF Trial. *Journal of the American College of Cardiology,* 64**,** 2455-2467.

BURSTEIN, B. & NATTEL, S. 2008. Atrial fibrosis: mechanisms and clinical relevance in atrial fibrillation. *Journal of the American College of Cardiology,* 51**,** 802-809.

CAMPBELL, S. L. & DUARTE, J. M. 2008. Poisson statistics of radioactive decay. *Prepr. MIT Dep. Phys***,** 3-6.

CENSI, F., CORAZZA, I., REGGIANI, E., CALCAGNINI, G., MATTEI, E., TRIVENTI, M. & BORIANI, G. 2016. P-wave variability and atrial fibrillation. *Scientific reports,* 6**,** 1-7.

CHAMBERLAIN, A. M., AGARWAL, S. K., FOLSOM, A. R., DUVAL, S., SOLIMAN, E. Z., AMBROSE, M., EBERLY, L. E. & ALONSO, A. 2011. Smoking and incidence of atrial fibrillation: results from the Atherosclerosis Risk in Communities (ARIC) study. *Heart Rhythm,* 8**,** 1160-1166.

CHEN, S.-A., HSIEH, M.-H., TAI, C.-T., TSAI, C.-F., PRAKASH, V., YU, W.-C., HSU, T.-L., DING, Y.-A. & CHANG, M.-S. 1999. Initiation of atrial fibrillation by ectopic beats originating from the pulmonary veins: electrophysiological characteristics, pharmacological responses, and effects of radiofrequency ablation. *Circulation,* 100**,** 1879-1886.

CHENITI, G., VLACHOS, K., PAMBRUN, T., HOOKS, D., FRONTERA, A., TAKIGAWA, M., BOURIER, F., KITAMURA, T., LAM, A., MARTIN, C., DUMAS-POMMIER, C., PUYO, S., PILLOIS, X., DUCHATEAU, J., KLOTZ, N., DENIS, A., DERVAL, N., JAIS, P., COCHET, H., HOCINI, M., HAISSAGUERRE, M. & SACHER, F. 2018. Atrial Fibrillation Mechanisms and Implications for Catheter Ablation. *Frontiers in Physiology,* 9.

CHILD, N., CLAYTON, R. H., RONEY, C. R., LAUGHNER, J. I., SHUROS, A., NEUZIL, P., PETRU, J., JACKSON, T., PORTER, B. & BOSTOCK, J. 2018. Unraveling the underlying arrhythmia mechanism in persistent atrial fibrillation: results from the STARLIGHT study. *Circulation: Arrhythmia and Electrophysiology,* 11**,** e005897.

COLMAN, M. A., ASLANIDI, O. V., KHARCHE, S., BOYETT, M. R., GARRATT, C., HANCOX, J. C. & ZHANG, H. 2013. Pro-arrhythmogenic effects of atrial fibrillation-induced electrical remodelling: insights from the three-dimensional virtual human atria. *The Journal of physiology,* 591**,** 4249-4272.

DALEY, D. J. & VERE-JONES, D. 2003. Basic properties of the Poisson process. *An Introduction to the Theory of Point Processes: Volume I: Elementary Theory and Methods***,** 19-40.

DANILOV, V. V., LITVINOV, R. G. & GERGET, O. M. 2016. Mathematical modelling the electrical activity of the heart. *Information Technologies in Science, Management, Social Sphere and Medicine***,** 361-365.

DE GROOT, N. M., HOUBEN, R. P., SMEETS, J. L., BOERSMA, E., SCHOTTEN, U., SCHALIJ, M. J., CRIJNS, H. & ALLESSIE, M. A. 2010. Electropathological substrate of longstanding persistent atrial fibrillation in patients with structural heart disease: epicardial breakthrough. *Circulation,* 122**,** 1674-1682.

DHARMAPRANI, D., SCHOPP, M., KUKLIK, P., CHAPMAN, D., LAHIRI, A., DYKES, L., XIONG, F., AGUILAR, M., STRAUSS, B. & MITCHELL, L. 2019. Renewal theory as a universal quantitative framework to characterize phase singularity regeneration in mammalian cardiac fibrillation. *Circulation: Arrhythmia and Electrophysiology,* 12**,** e007569.

DONG, J., SCHREIECK, J., NDREPEPA, G. & SCHMITT, C. 2002. Ectopic tachycardia originating from the superior vena cava. *Journal of cardiovascular electrophysiology,* 13**,** 620-624.

DOOB, J. L. 1948. Renewal theory from the point of view of the theory of probability. *Transactions of the American Mathematical Society,* 63**,** 422-438.

ECKSTEIN, J., MAESEN, B., LINZ, D., ZEEMERING, S., VAN HUNNIK, A., VERHEULE, S., ALLESSIE, M. & SCHOTTEN, U. 2011. Time course and mechanisms of endo-epicardial electrical dissociation during atrial fibrillation in the goat. *Cardiovascular research,* 89**,** 816-824.

ECKSTEIN, J., ZEEMERING, S., LINZ, D., MAESEN, B., VERHEULE, S., HUNNIK, A. V., CRIJNS, H., ALLESSIE, M. A. & SCHOTTEN, U. 2013. Transmural Conduction Is the Predominant Mechanism of Breakthrough During Atrial Fibrillation. *Circulation: Arrhythmia and Electrophysiology,* 6**,** 334-341.

EVERETT IV, T. H. & OLGIN, J. E. 2007. Atrial fibrosis and the mechanisms of atrial fibrillation. *Heart Rhythm,* 4**,** S24-S27.

GHARAVIRI, A., BIDAR, E., POTSE, M., ZEEMERING, S., VERHEULE, S., PEZZUTO, S., KRAUSE, R., MAESSEN, J. G., AURICCHIO, A. & SCHOTTEN, U. 2020. Epicardial fibrosis explains increased endo–epicardial dissociation and epicardial breakthroughs in human atrial fibrillation. *Frontiers in physiology,* 11**,** 68.

GRANEK, R. & CATES, M. 1992. Stress relaxation in living polymers: Results from a Poisson renewal model. *The Journal of chemical physics,* 96**,** 4758-4767.

HAÏSSAGUERRE, M., HOCINI, M., SANDERS, P., TAKAHASHI, Y., ROTTER, M., SACHER, F., ROSTOCK, T., HSU, L.-F., JONSSON, A. & O'NEILL, M. D. 2006. Localized sources maintaining atrial fibrillation organized by prior ablation. *Circulation,* 113**,** 616-625.

HAISSAGUERRE, M., JAÏS, P., SHAH, D. C., TAKAHASHI, A., HOCINI, M., QUINIOU, G., GARRIGUE, S., LE MOUROUX, A., LE MÉTAYER, P. & CLÉMENTY, J. 1998. Spontaneous initiation of atrial fibrillation by ectopic beats originating in the pulmonary veins. *New England Journal of Medicine,* 339**,** 659-666.

HANSEN, B. J., CSEPE, T. A., ZHAO, J., IGNOZZI, A. J., HUMMEL, J. D. & FEDOROV, V. V. 2016. Maintenance of atrial fibrillation: are reentrant drivers with spatial stability the key? *Circulation: Arrhythmia and Electrophysiology,* 9**,** e004398.

HANSEN, B. J., ZHAO, J., CSEPE, T. A., MOORE, B. T., LI, N., JAYNE, L. A., KALYANASUNDARAM, A., LIM, P., BRATASZ, A., POWELL, K. A., SIMONETTI, O. P., HIGGINS, R. S. D., KILIC, A., MOHLER, P. J., JANSSEN, P. M. L., WEISS, R., HUMMEL, J. D. & FEDOROV, V. V. 2015. Atrial fibrillation driven by micro-anatomic intramural re-entry revealed by simultaneous sub-epicardial and sub-endocardial optical mapping in explanted human hearts. *European Heart Journal,* 36**,** 2390-2401.

HOCINI, M., SHAH, A. J., NAULT, I., SANDERS, P., WRIGHT, M., NARAYAN, S. M., TAKAHASHI, Y., JAÏS, P., MATSUO, S. & KNECHT, S. 2011. Localized reentry within

the left atrial appendage: arrhythmogenic role in patients undergoing ablation of persistent atrial fibrillation. *Heart Rhythm,* 8**,** 1853-1861.

JACQUEMET, V. 2018. Phase singularity detection through phase map interpolation: Theory, advantages and limitations. *Computers in Biology and Medicine,* 102**,** 381-389.

JALIFE, J., BERENFELD, O. & MANSOUR, M. 2002. Mother rotors and fibrillatory conduction: a mechanism of atrial fibrillation. *Cardiovascular research,* 54**,** 204-216.

JENKINS, E. V., DHARMAPRANI, D., SCHOPP, M., QUAH, J. X., TIVER, K., MITCHELL, L., POPE, K. & GANESAN, A. N. 2022. Understanding the origins of the basic equations of statistical fibrillatory dynamics. *Chaos: An Interdisciplinary Journal of Nonlinear Science,* 32**,** 032101.

KASHOU, A. H., BASIT, H. & CHHABRA, L. 2021. *Physiology, Sinoatrial Node,* StatPearls Publishing, Treasure Island (FL).

KLABUNDE, R. E. 2017. Cardiac electrophysiology: normal and ischemic ionic currents and the ECG. *Advances in Physiology Education,* 41**,** 29-37.

KRUEGER, M. W., SEVERI, S., RHODE, K., GENOVESI, S., WEBER, F. M., VINCENTI, A., FABBRINI, P., SEEMANN, G., RAZAVI, R. & DÖSSEL, O. 2011. Alterations of atrial electrophysiology related to hemodialysis session: insights from a multiscale computer model. *Journal of electrocardiology,* 44**,** 176-183.

KUKLIK, P., ZEEMERING, S., MAESEN, B., MAESSEN, J., CRIJNS, H. J., VERHEULE, S., GANESAN, A. N. & SCHOTTEN, U. 2014. Reconstruction of instantaneous phase of unipolar atrial contact electrogram using a concept of sinusoidal recomposition and Hilbert transform. *IEEE transactions on biomedical engineering,* 62**,** 296-302.

LEE, E. T. & WANG, J. W. 2003. Some well-known parametric survival distributions and their applications. *Statistical methods for survival data analysis,* 3**,** 134-136.

LEE, S., KHRESTIAN, C. M., SAHADEVAN, J. & WALDO, A. L. 2020. Reconsidering the multiple wavelet hypothesis of atrial fibrillation. *Heart Rhythm,* 17**,** 1976-1983.

LIANG, Y., MENTE, A., YUSUF, S., GAO, P., SLEIGHT, P., ZHU, J., FAGARD, R., LONN, E., TEO, K. K., ONTARGET & INVESTIGATORS, T. 2012. Alcohol consumption and the risk of incident atrial fibrillation among people with cardiovascular disease. *CMAJ : Canadian Medical Association journal = journal de l'Association medicale canadienne,* 184**,** E857-E866.

LIN, W.-S., TAI, C.-T., HSIEH, M.-H., TSAI, C.-F., LIN, Y.-K., TSAO, H.-M., HUANG, J.-L., YU, W.-C., YANG, S.-P. & DING, Y.-A. 2003. Catheter ablation of paroxysmal atrial fibrillation initiated by non–pulmonary vein ectopy. *Circulation,* 107**,** 3176-3183.

MAHIDA, S., SACHER, F., DERVAL, N., BERTE, B., YAMASHITA, S., HOOKS, D., DENIS, A., AMRAOUI, S., HOCINI, M. & HAISSAGUERRE, M. 2015. Science linking pulmonary veins and atrial fibrillation. *Arrhythmia & electrophysiology review,* 4**,** 40.

MAINARDI, F., GORENFLO, R. & VIVOLI, A. 2007. Beyond the Poisson renewal process: A tutorial survey. *Journal of Computational and Applied Mathematics,* 205**,** 725-735.

MEIJLER, F. L. & JANSE, M. J. 1988. Morphology and electrophysiology of the mammalian atrioventricular node. *Physiological reviews,* 68**,** 608-647.

MOE, G. K., RHEINBOLDT, W. C. & ABILDSKOV, J. 1964. A computer model of atrial fibrillation. *American heart journal,* 67**,** 200-220.

MYLON, K. & MCBETH, G. 1983. Radioactive decay viewed through an extending dead time. *Nuclear Instruments and Methods in Physics Research,* 217**,** 459-464.

NATTEL, S. 2002. New ideas about atrial fibrillation 50 years on. *Nature,* 415**,** 219-226.

PAN, J. & TOMPKINS, W. J. 1985. A real-time QRS detection algorithm. *IEEE transactions on biomedical engineering***,** 230-236.

PARAMESWARAN, R., KALMAN, J. M., ROYSE, A., GOLDBLATT, J., LAROBINA, M., WATTS, T., WALTERS, T. E., NALLIAH, C. J., WONG, G., AL-KAISEY, A., ANDERSON, R. D., VOSKOBOINIK, A., SUGUMAR, H., CHIENG, D., SANDERS, P., KISTLER, P. M., GERSTENFELD, E. P. & LEE, G. 2020. Endocardial-Epicardial Phase

Mapping of Prolonged Persistent Atrial Fibrillation Recordings. *Circulation: Arrhythmia and Electrophysiology,* 13**,** e008512.
PETRUTIU, S., NG, J., NIJM, G. M., AL-ANGARI, H., SWIRYN, S. & SAHAKIAN, A. V. 2006. Atrial fibrillation and waveform characterization. *IEEE engineering in medicine and biology magazine,* 25**,** 24-30.
PLATONOV, P. G. 2012. P-wave morphology: Underlying mechanisms and clinical implications. *Annals of Noninvasive Electrocardiology,* 17**,** 161-169.
QUAH, J., DHARMAPRANI, D., LAHIRI, A., SCHOPP, M., MITCHELL, L., SELVANAYAGAM, J. B., PERRY, R., CHAHADI, F., TUNG, M. & AHMAD, W. 2020. Prospective cross-sectional study using Poisson renewal theory to study phase singularity formation and destruction rates in atrial fibrillation (RENEWAL-AF): Study design. *Journal of Arrhythmia,* 36**,** 660-667.
QUAH, J. X., DHARMAPRANI, D., LAHIRI, A., TIVER, K. & GANESAN, A. N. 2021. Reconceptualising atrial fibrillation using renewal theory: a novel approach to the assessment of atrial fibrillation dynamics. *Arrhythmia & Electrophysiology Review,* 10**,** 77.
RONEY, C. H., WIT, A. L. & PETERS, N. S. 2019. Challenges associated with interpreting mechanisms of AF. *Arrhythmia & Electrophysiology Review,* 8**,** 273.
SCHUESSLER, R. B., KAWAMOTO, T., HAND, D. E., MITSUNO, M., BROMBERG, B. I., COX, J. L. & BOINEAU, J. P. 1993. Simultaneous epicardial and endocardial activation sequence mapping in the isolated canine right atrium. *Circulation,* 88**,** 250-263.
SHAH, D. C., HÄISSAGUERRE, M., JÄIS, P. & CLEMENTY, J. 2002. High-resolution mapping of tachycardia originating from the superior vena cava: evidence of electrical heterogeneity, slow conduction, and possible circus movement reentry. *Journal of cardiovascular electrophysiology,* 13**,** 388-392.
SHKUROVICH, S., SAHAKIAN, A. V. & SWIRYN, S. 1998. Detection of atrial activity from high-voltage leads of implantable ventricular defibrillators using a cancellation technique. *IEEE Transactions on Biomedical Engineering,* 45**,** 229-234.
SMITH, W. L. 1958. Renewal theory and its ramifications. *Journal of the Royal Statistical Society: Series B (Methodological),* 20**,** 243-284.
SURAWICZ, B. & PARIKH, S. R. 2003. Differences between ventricular repolarization in men and women: description, mechanism and implications. *Annals of Noninvasive Electrocardiology,* 8**,** 333-340.
ULDRY, L., VIRAG, N., LINDEMANS, F., VESIN, J.-M. & KAPPENBERGER, L. 2012. Atrial septal pacing for the termination of atrial fibrillation: study in a biophysical model of human atria. *Europace,* 14**,** v112-v120.
UMAPATHY, K., NAIR, K., MASSE, S., KRISHNAN, S., ROGERS, J., NASH, M. P. & NANTHAKUMAR, K. 2010. Phase Mapping of Cardiac Fibrillation. *Circulation: Arrhythmia and Electrophysiology,* 3**,** 105-114.
VERHEULE, S., ECKSTEIN, J., LINZ, D., MAESEN, B., BIDAR, E., GHARAVIRI, A. & SCHOTTEN, U. 2014. Role of endo-epicardial dissociation of electrical activity and transmural conduction in the development of persistent atrial fibrillation. *Progress in biophysics and molecular biology,* 115**,** 173-185.
VERHEULE, S., TUYLS, E., GHARAVIRI, A., HULSMANS, S., VAN HUNNIK, A., KUIPER, M., SERROYEN, J., ZEEMERING, S., KUIJPERS, N. H. & SCHOTTEN, U. 2013. Loss of continuity in the thin epicardial layer because of endomysial fibrosis increases the complexity of atrial fibrillatory conduction. *Circulation: Arrhythmia and Electrophysiology,* 6**,** 202-211.
VIGMOND, E. J. & STUYVERS, B. D. 2016. Modeling our understanding of the His-Purkinje system. *Progress in biophysics and molecular biology,* 120**,** 179-188.
WAKS, J. W. & JOSEPHSON, M. E. 2014. Mechanisms of atrial fibrillation–reentry, rotors and reality. *Arrhythmia & electrophysiology review,* 3**,** 90.

WEISS, J. N., QU, Z., CHEN, P.-S., LIN, S.-F., KARAGUEUZIAN, H. S., HAYASHI, H., GARFINKEL, A. & KARMA, A. 2005. The dynamics of cardiac fibrillation. *Circulation,* 112**,** 1232-1240.

WESTERMAN, S. & WENGER, N. 2019. Gender Differences in Atrial Fibrillation: A Review of Epidemiology, Management, and Outcomes. *Current cardiology reviews,* 15**,** 136-144.

WIJFFELS, M. C. E. F., KIRCHHOF, C. J. H. J., DORLAND, R. & ALLESSIE, M. A. 1995. Atrial Fibrillation Begets Atrial Fibrillation. *Circulation,* 92**,** 1954-1968.

WINFREE, A. 1994. Electrical turbulence in three-dimensional heart muscle. *Science,* 266**,** 1003-1006.

WU, T. J., LIANG, K. W. & TING, C. T. 2001. Relation between the rapid focal activation in the pulmonary vein and the maintenance of paroxysmal atrial fibrillation. *Pacing and Clinical Electrophysiology,* 24**,** 902-905.

YAN, G.-X., LANKIPALLI, R. S., BURKE, J. F., MUSCO, S. & KOWEY, P. R. 2003. Ventricular repolarization components on the electrocardiogram: cellular basis and clinical significance. *Journal of the American College of Cardiology,* 42**,** 401-409.

APPENDIX A – MATLAB codes for the detection algorithm

```
%% Detect wavefronts propagating from endocardial breakthroughs

Detected_WF_IDs = zeros(1,numel(Frame));
% Create empty array for detected wavefront IDs
for i = 2:numel(Frame)  % Cycle through all frames
    fprintf('Detecting WFs triggered by EB...Frame %d out of %d...
                \n',i,numel(Frame));  % Display process status
    if ~isempty(numel(Frame(i).WF))
    % Check if wavefronts in current frame
        for j = 1:numel(Frame(i).WF)
        % Cycle through all wavefronts in current frame
            bw1 = ones(13,13);
            % Create binary map of all pixels switched on
            for k = 1:numel(Frame(i).WF(j).WFx)
            % Search for x-coordinate of current wavefront
                bw1(Frame(i).WF(j).WFy(k),Frame(i).WF(j).WFx(k)) = 0;
                % Switch off pixels at current wavefront
            end
            cc1 = bwconncomp(bw1);
            % Finds and counts regions in binary map
            if cc1.NumObjects > 1 % Check if no. of regions > 1
                bw2 = ~bw1;  % Switch all pixels to opposite status
                bw2 = imfill(bw2,'holes');  % Finds and fills holes
                bw2 = ~bw2;  % Switch all pixels back to original status
                cc2 = bwconncomp(bw2);  % Finds and counts regions
                if cc2.NumObjects == cc1.NumObjects - 1
                % Check if no. of regions decrease by 1
                    for k = 1:numel(Frame(i).WF(j).WFx)
                    % Search for x-coordinate of current wavefront
                  bw2(Frame(i).WF(j).WFy(k),Frame(i).WF(j).WFx(k)) = 1;
                  % Switch off pixels at current wavefront
                    end
                    bw3 = phase_map_all{i};
                    % Call for current phase map
                    bw3(bw2) = 0;
                    % Switch off pixels by templating binary map
                    indx = find(max(max(bw3)));
                    % find position of pixel at highest phase
                    for k = 1:length(electrodes)
                    % Cycle through all electrodes
```

```
                        if indx == electrodes(k)
                        % Check if position matches to current electrode
                            Detected_WF_IDs(i) = Frame(i).WF(j).WF_ID;
                            % Save current wavefront ID
                        end
                    end
                end
            end
        end
    end
end
Detected_WF_IDs = nonzeros(Detected_WF_IDs);  % Remove zero elements
Detected_WF_IDs = unique(Detected_WF_IDs);  % Remove repeated elements
fprintf(' // WFs detected...\n');  % Display process completed

%% Discard wavefronts not propagating from endocardial breakthroughs

for i = 1:numel(Frame)  % Cycle through all frames
    fprintf('Discarding WF not triggered by EB...Frame %d out of %d
                \n',i,numel(Frame)); % Display process status
    if ~isempty(numel(Frame(i).WF))
    % Check if wavefronts in current frame
        tag = zeros(1,numel(Frame(i).WF));
        % Create empty array for wavefront ID tags
        for j = 1:numel(Frame(i).WF)  % Cycle through all wavefronts
            for k = 1:numel(Detected_WF_IDs)
            % Cycle through all detected wavefront ID
                if Detected_WF_IDs(k) == Frame(i).WF(j).WF_ID
                % Check if detected ID matches to current ID
                    tag(j) = 1;  % Tag wavefront ID
                end
            end
        end
        indx = find(tag == 0);  % Find untagged wavefronts
        Frame(i).WF(indx) = [];  % Discard untagged wavefronts
    end
end
fprintf(' // WFs discarded...\n');  % Display process completed
```

APPENDIX B – Correlograms of inter-formation times

Correlograms of endocardial breakthroughs inter-formation times in all AF cases are provided on the following pages.

Correlograms visualise the autocorrelation of inter-formation times at all lags.

In most correlograms, the autocorrelation was 1 at lag 0 and approached zero at all non-zero lags (within the upper and lower confident bounds).

In the correlograms of the cases rejected by Ljung-box Q-test, the autocorrelation at certain non-zero lags exceeded the confident bounds.

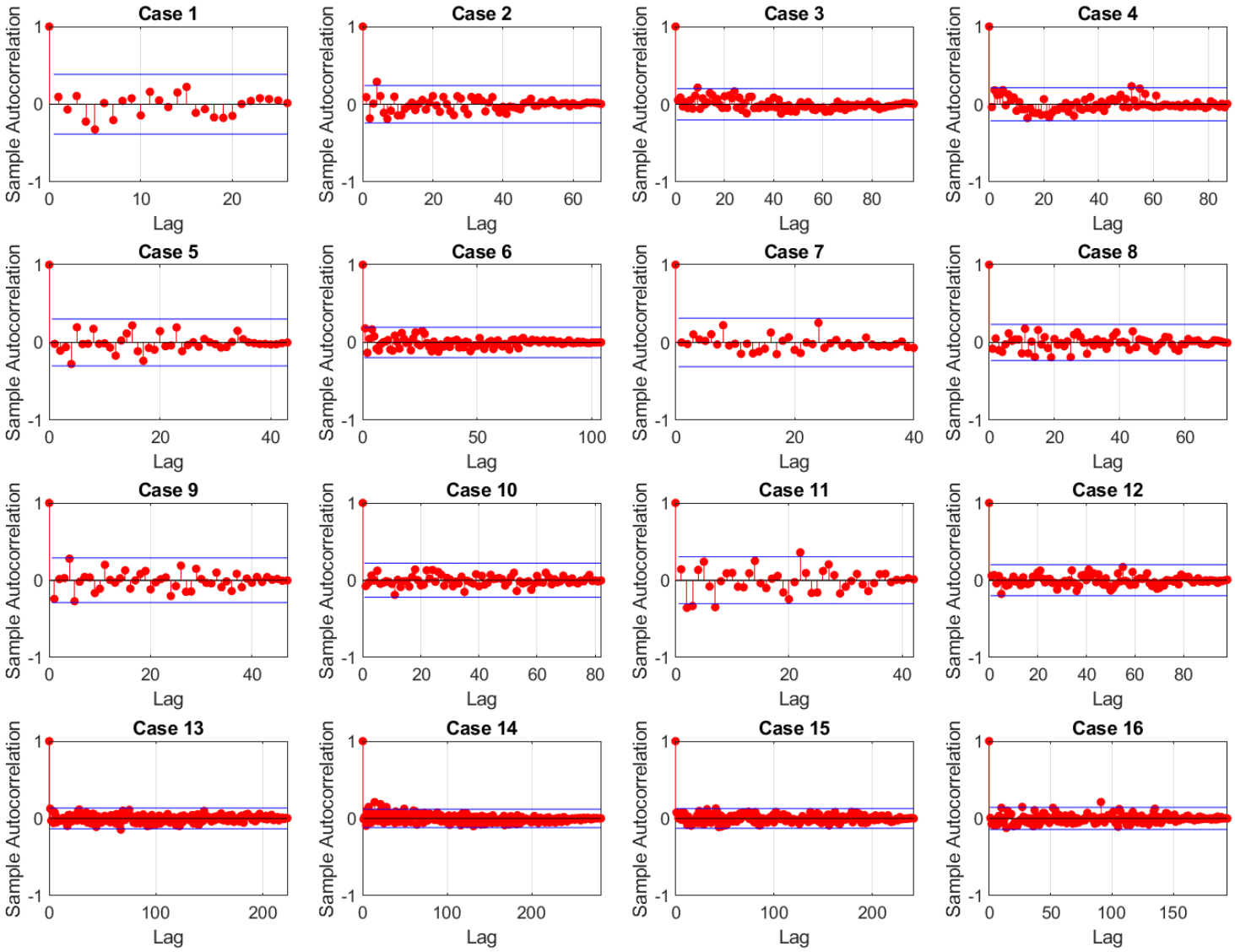
Case 1
Case 2
Case 3
Case 4
Case 5
Case 6
Case 7
Case 8
Case 9
Case 10
Case 11
Case 12
Case 13
Case 14
Case 15
Case 16
Sample Autocorrelation
Lag

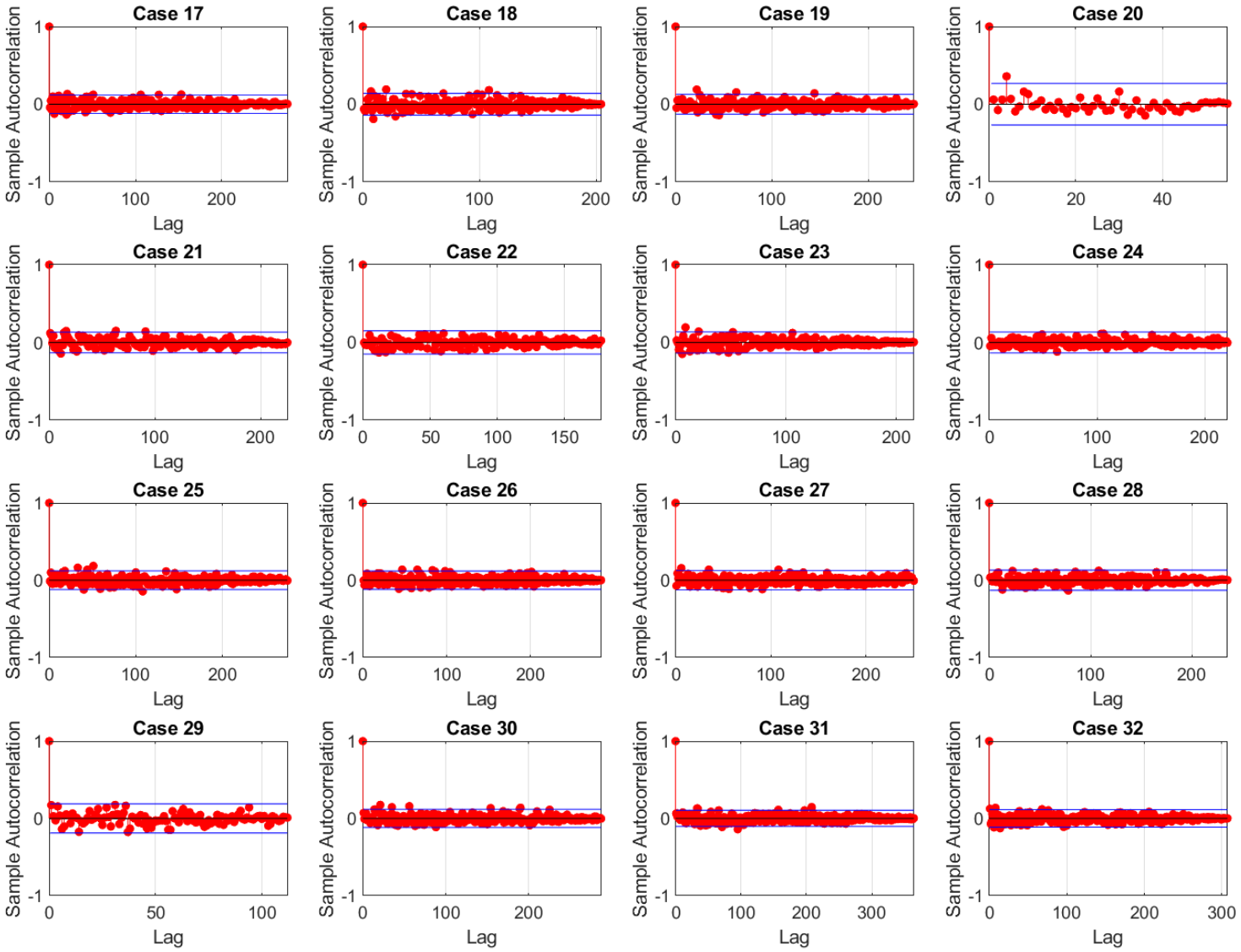
Case 17
Case 18
Case 19
Case 20
Case 21
Case 22
Case 23
Case 24
Case 25
Case 26
Case 27
Case 28
Case 29
Case 30
Case 31
Case 32
Sample Autocorrelation
Lag

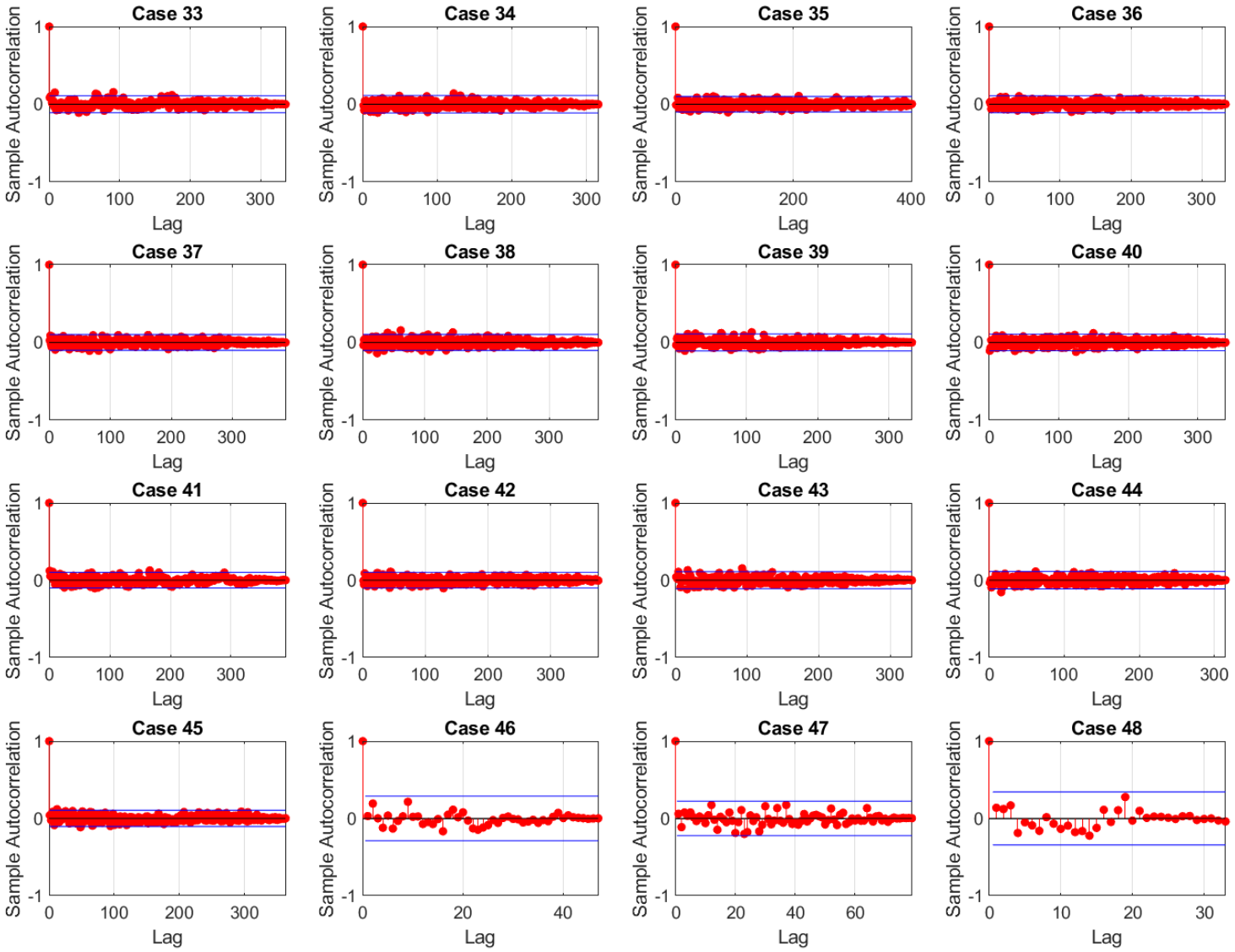
Case 33
Case 34
Case 35
Case 36
Case 37
Case 38
Case 39
Case 40
Case 41
Case 42
Case 43
Case 44
Case 45
Case 46
Case 47
Case 48
Sample Autocorrelation
Lag

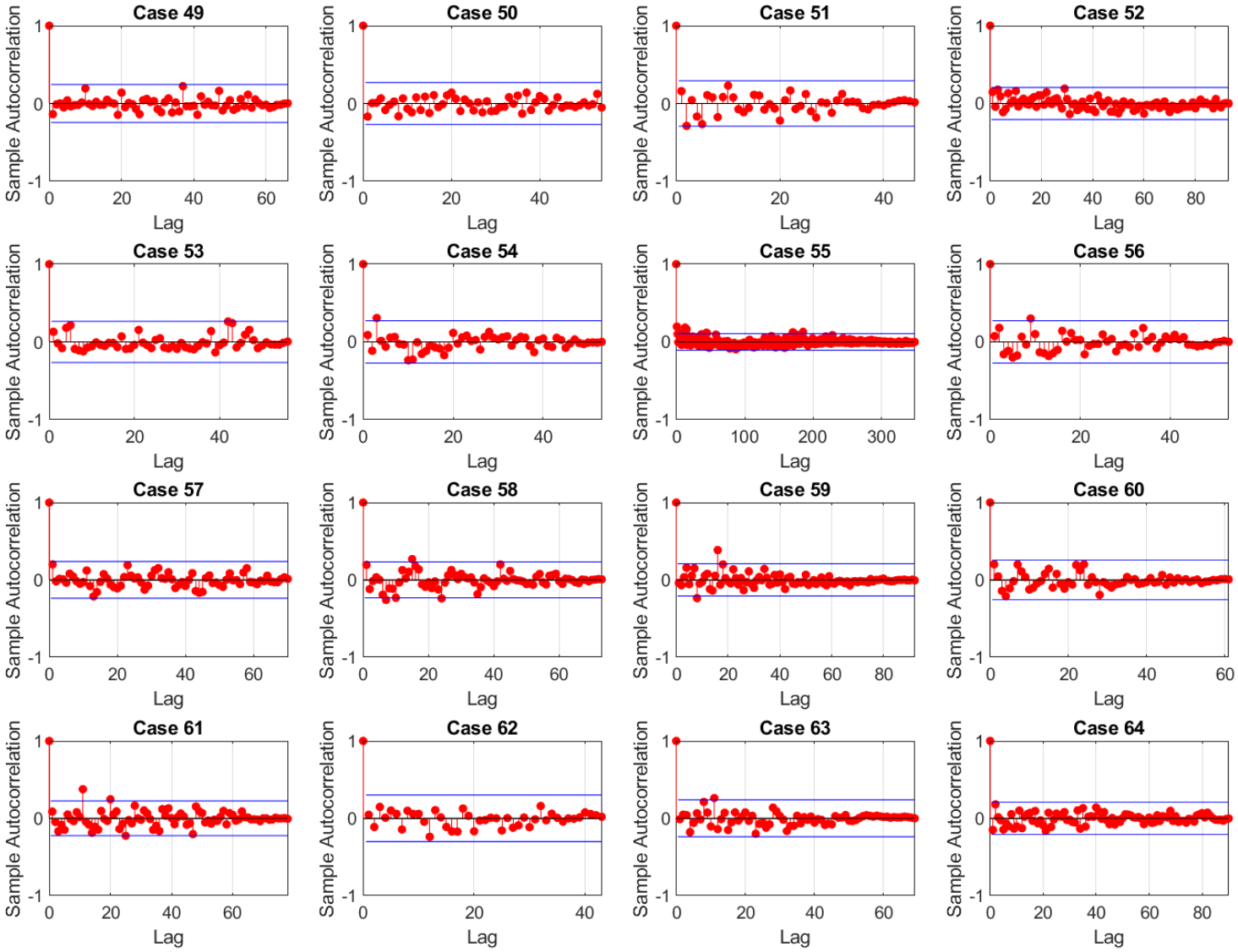
Case 49
Case 50
Case 51
Case 52
Case 53
Case 54
Case 55
Case 56
Case 57
Case 58
Case 59
Case 60
Case 61
Case 62
Case 63
Case 64
Sample Autocorrelation
Lag

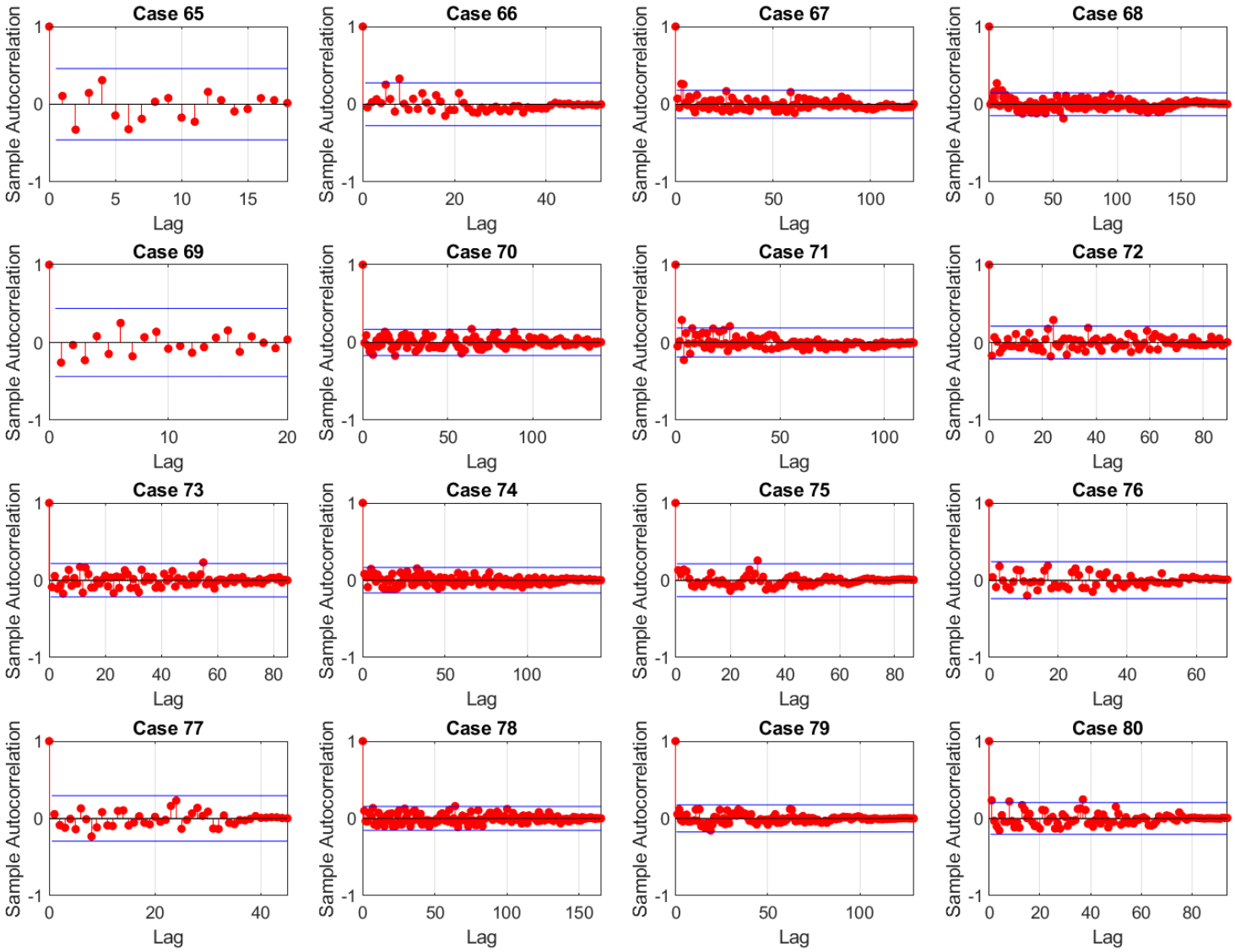
Case 65
Case 66
Case 67
Case 68
Case 69
Case 70
Case 71
Case 72
Case 73
Case 74
Case 75
Case 76
Case 77
Case 78
Case 79
Case 80
Sample Autocorrelation
Lag

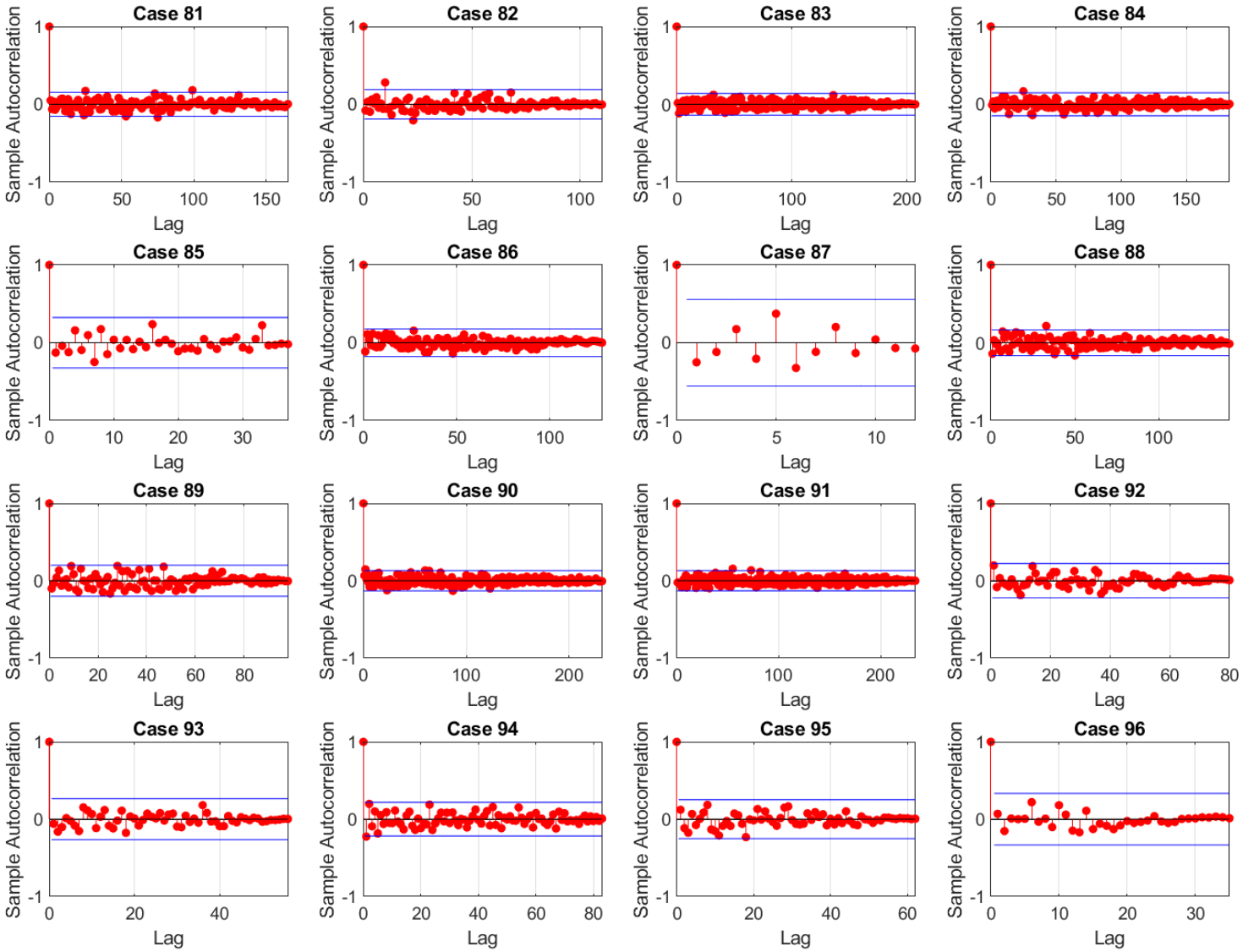
Case 81
Case 82
Case 83
Case 84
Case 85
Case 86
Case 87
Case 88
Case 89
Case 90
Case 91
Case 92
Case 93
Case 94
Case 95
Case 96
Sample Autocorrelation
Lag

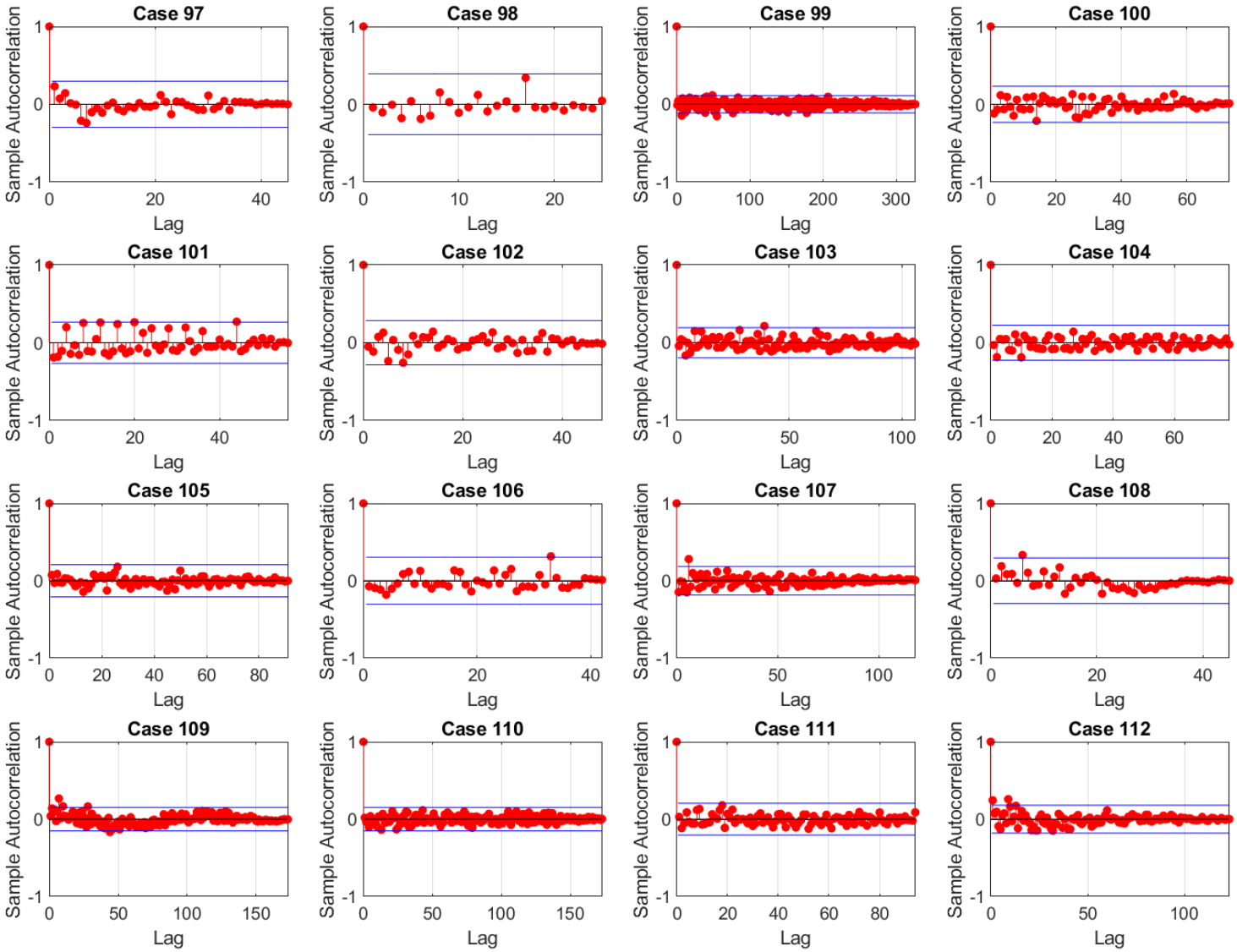
Case 97
Case 98
Case 99
Case 100
Case 101
Case 102
Case 103
Case 104
Case 105
Case 106
Case 107
Case 108
Case 109
Case 110
Case 111
Case 112
Sample Autocorrelation
Lag

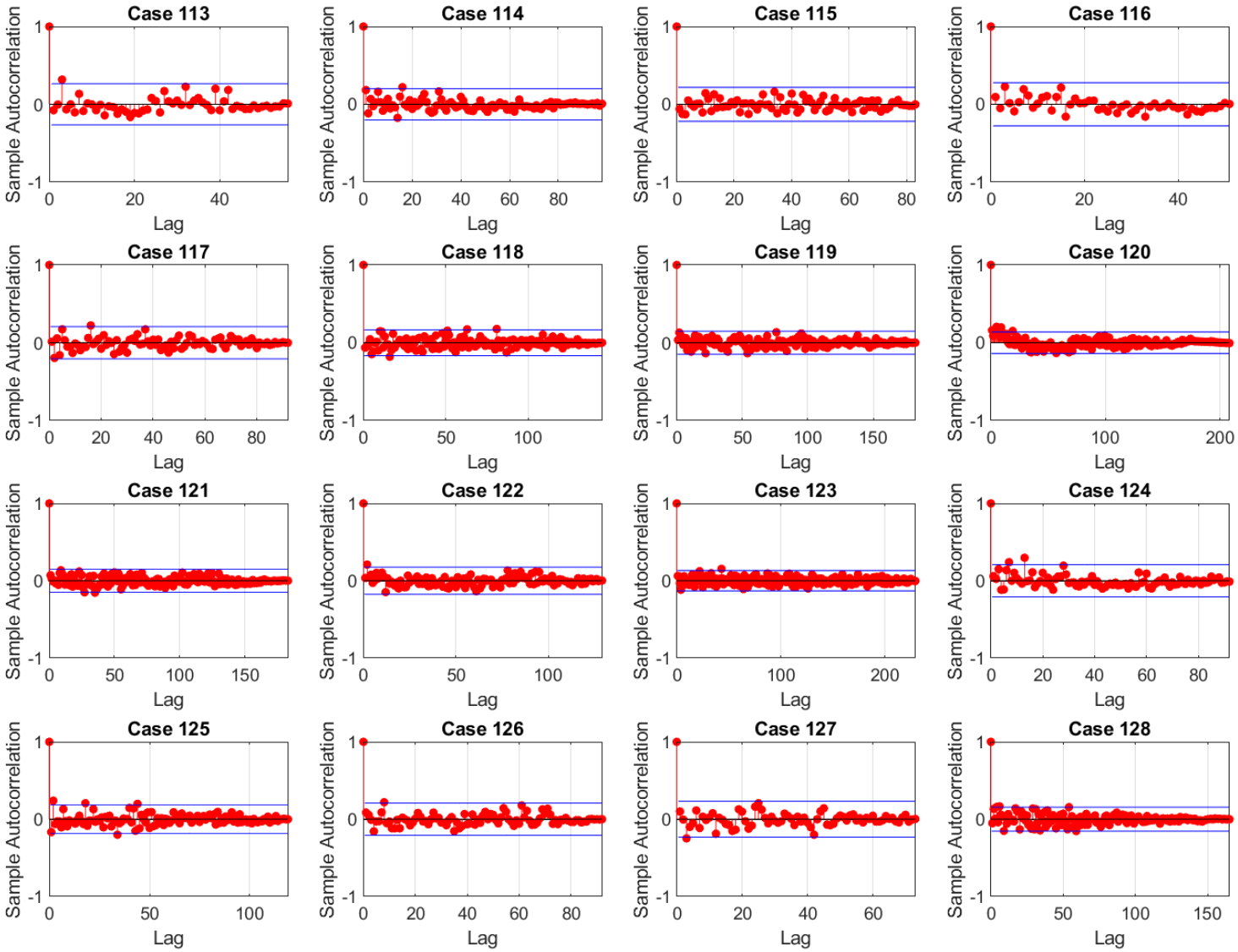
Case 113
Case 114
Case 115
Case 116
Case 117
Case 118
Case 119
Case 120
Case 121
Case 122
Case 123
Case 124
Case 125
Case 126
Case 127
Case 128
Sample Autocorrelation
Lag

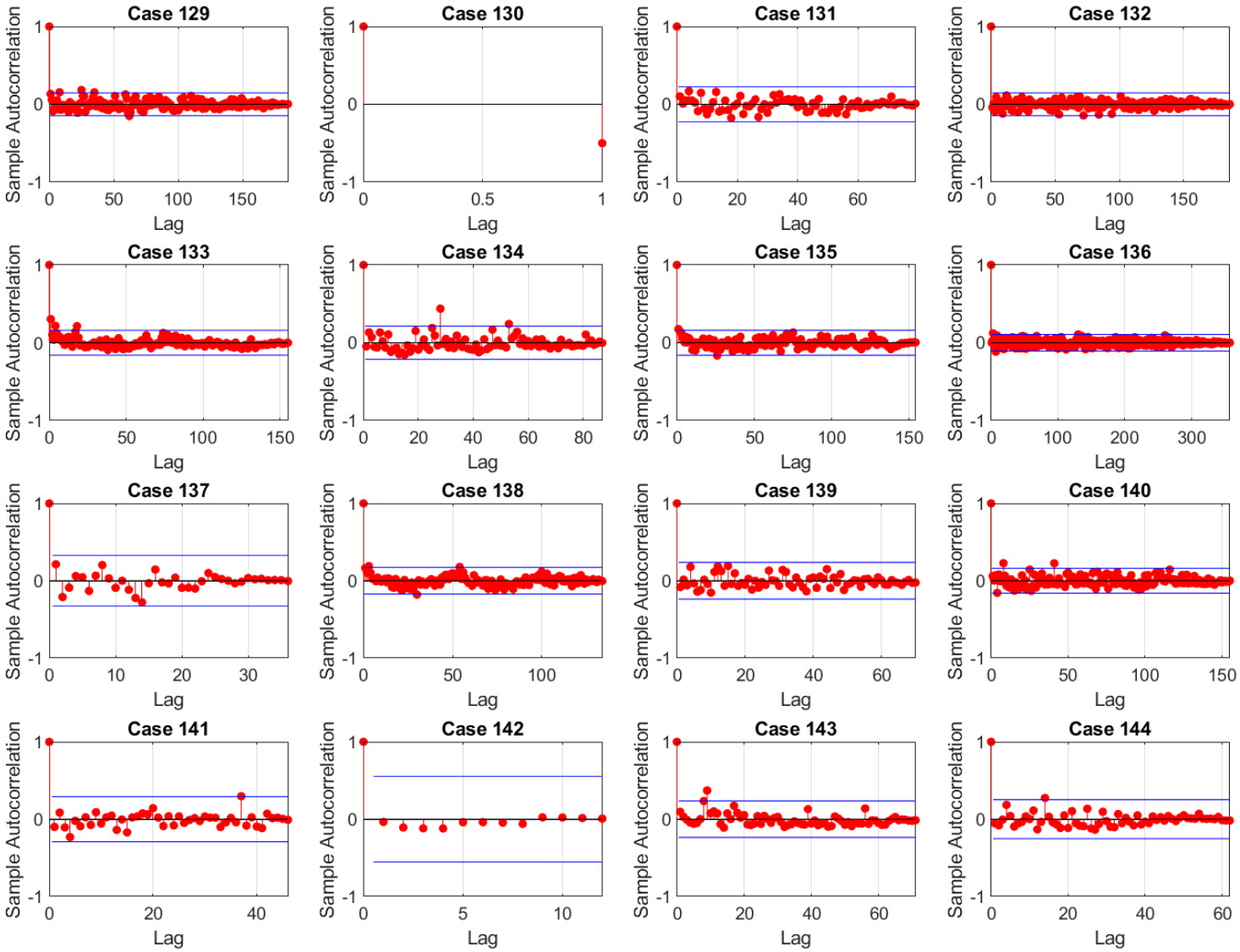
Case 129
Case 130
Case 131
Case 132
Case 133
Case 134
Case 135
Case 136
Case 137
Case 138
Case 139
Case 140
Case 141
Case 142
Case 143
Case 144
Sample Autocorrelation
Lag

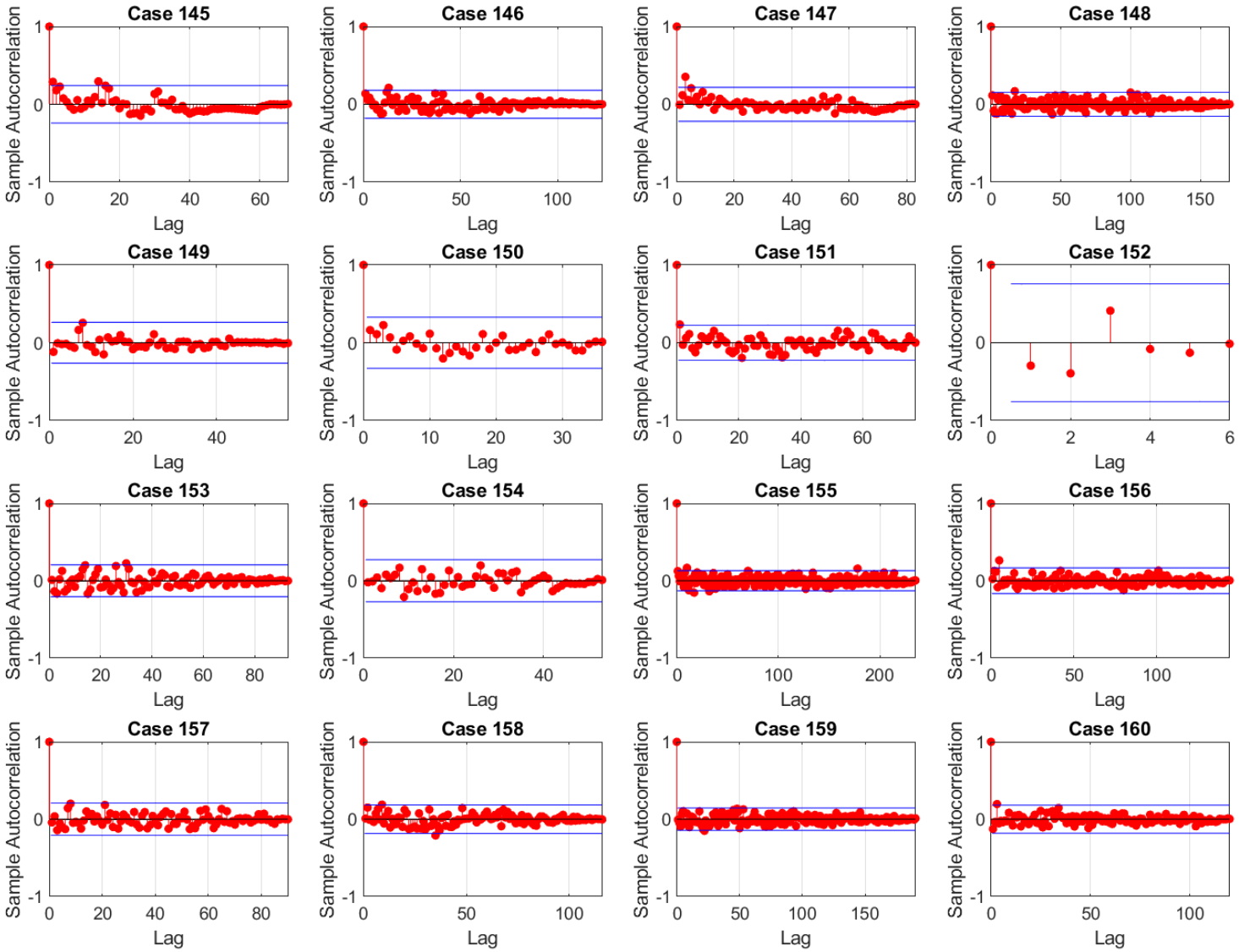
Case 145
Case 146
Case 147
Case 148
Case 149
Case 150
Case 151
Case 152
Case 153
Case 154
Case 155
Case 156
Case 157
Case 158
Case 159
Case 160
Sample Autocorrelation
Lag

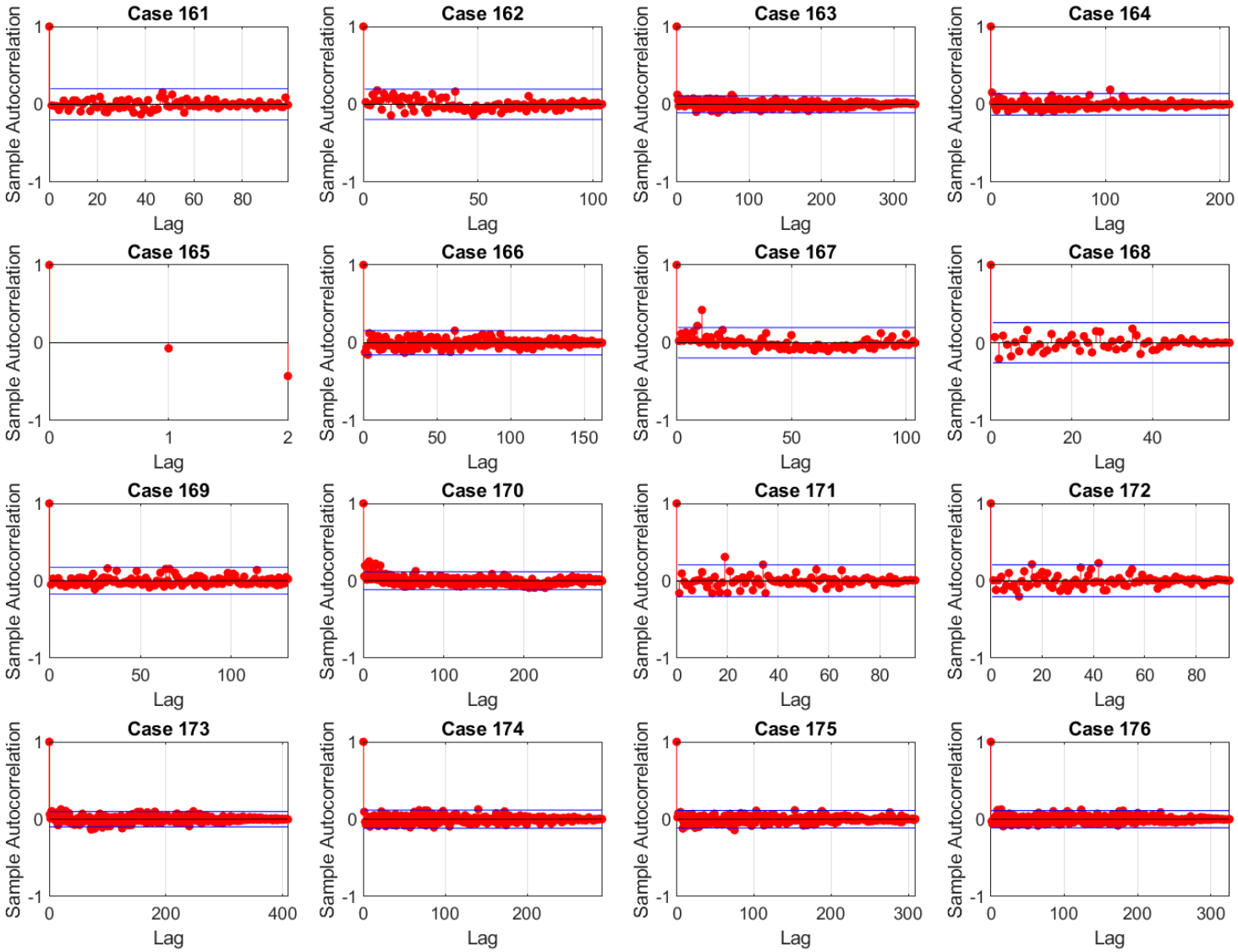
Case 161
Case 162
Case 163
Case 164
Case 165
Case 166
Case 167
Case 168
Case 169
Case 170
Case 171
Case 172
Case 173
Case 174
Case 175
Case 176
Sample Autocorrelation
Lag

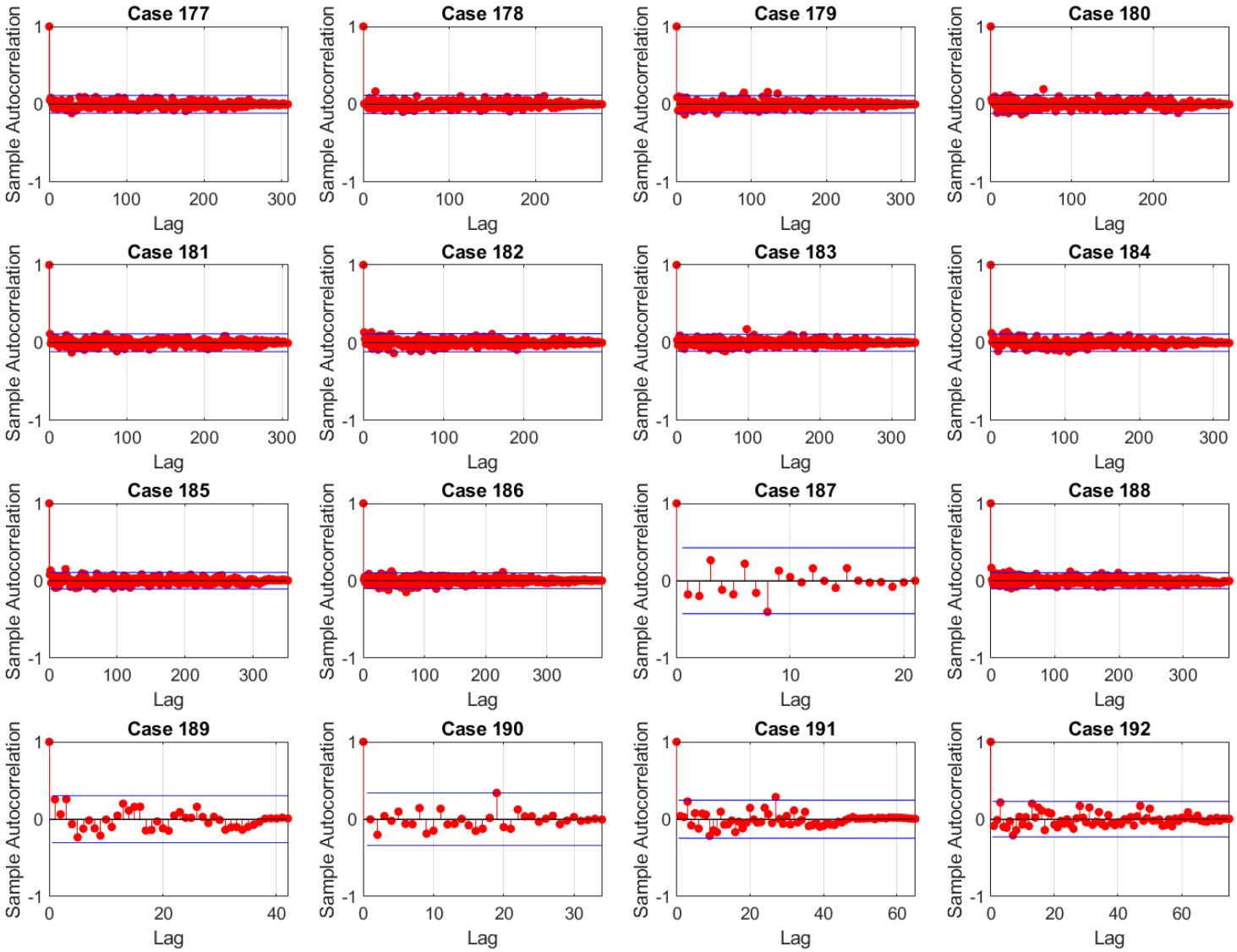
Case 177
Case 178
Case 179
Case 180
Case 181
Case 182
Case 183
Case 184
Case 185
Case 186
Case 187
Case 188
Case 189
Case 190
Case 191
Case 192
Sample Autocorrelation
Lag

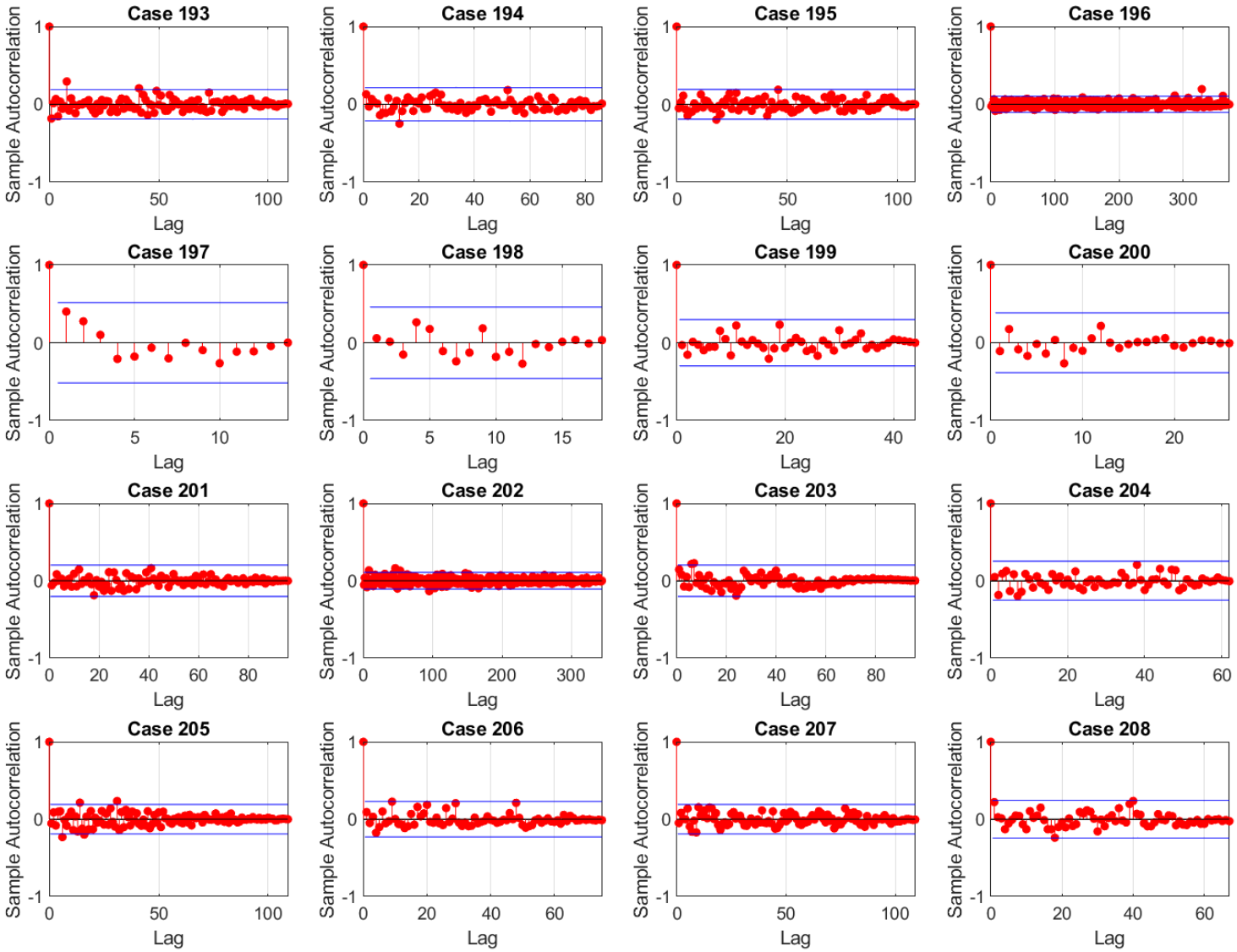
Case 193
Case 194
Case 195
Case 196
Case 197
Case 198
Case 199
Case 200
Case 201
Case 202
Case 203
Case 204
Case 205
Case 206
Case 207
Case 208
Sample Autocorrelation
Lag

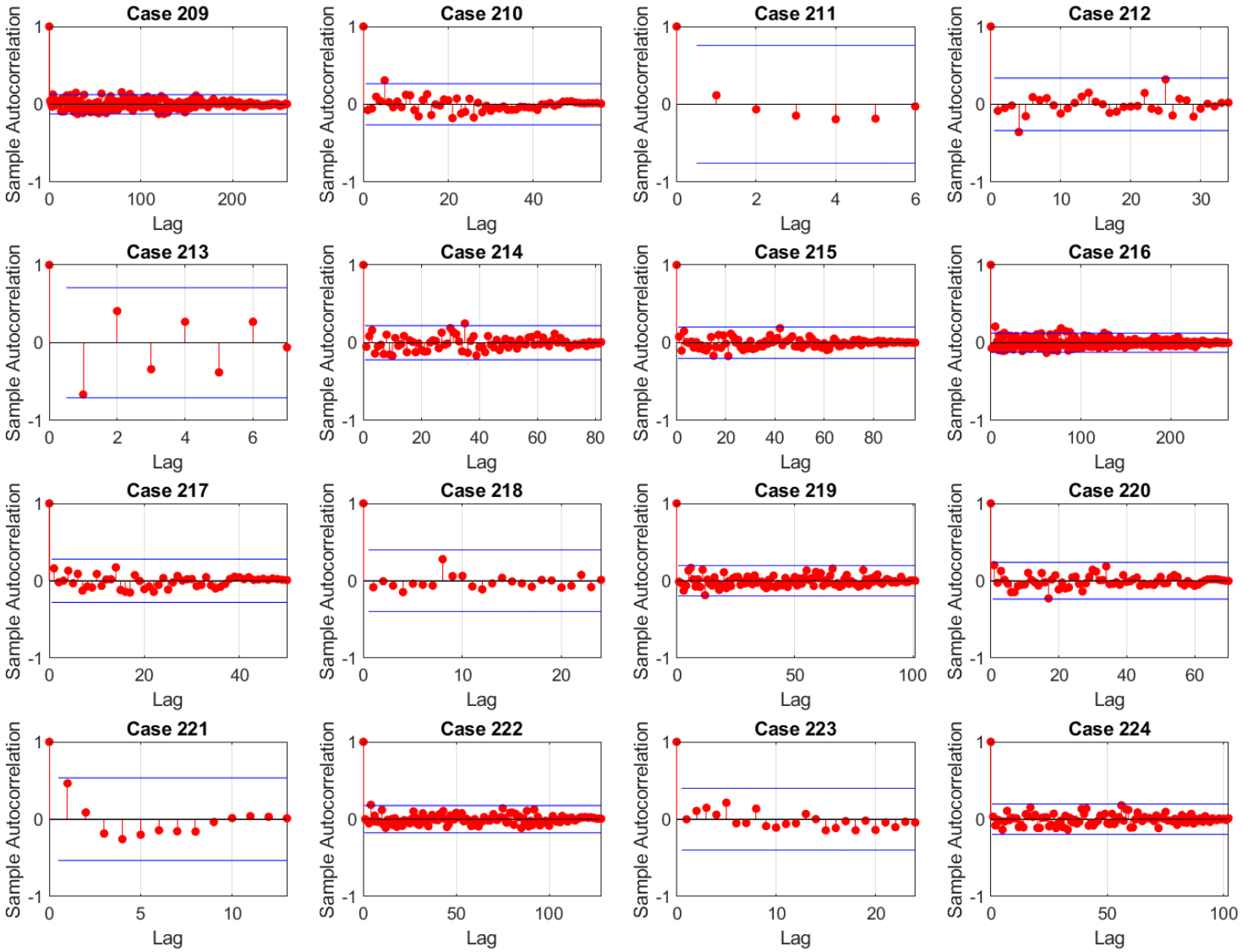
Case 209
Case 210
Case 211
Case 212
Case 213
Case 214
Case 215
Case 216
Case 217
Case 218
Case 219
Case 220
Case 221
Case 222
Case 223
Case 224
Sample Autocorrelation
Lag

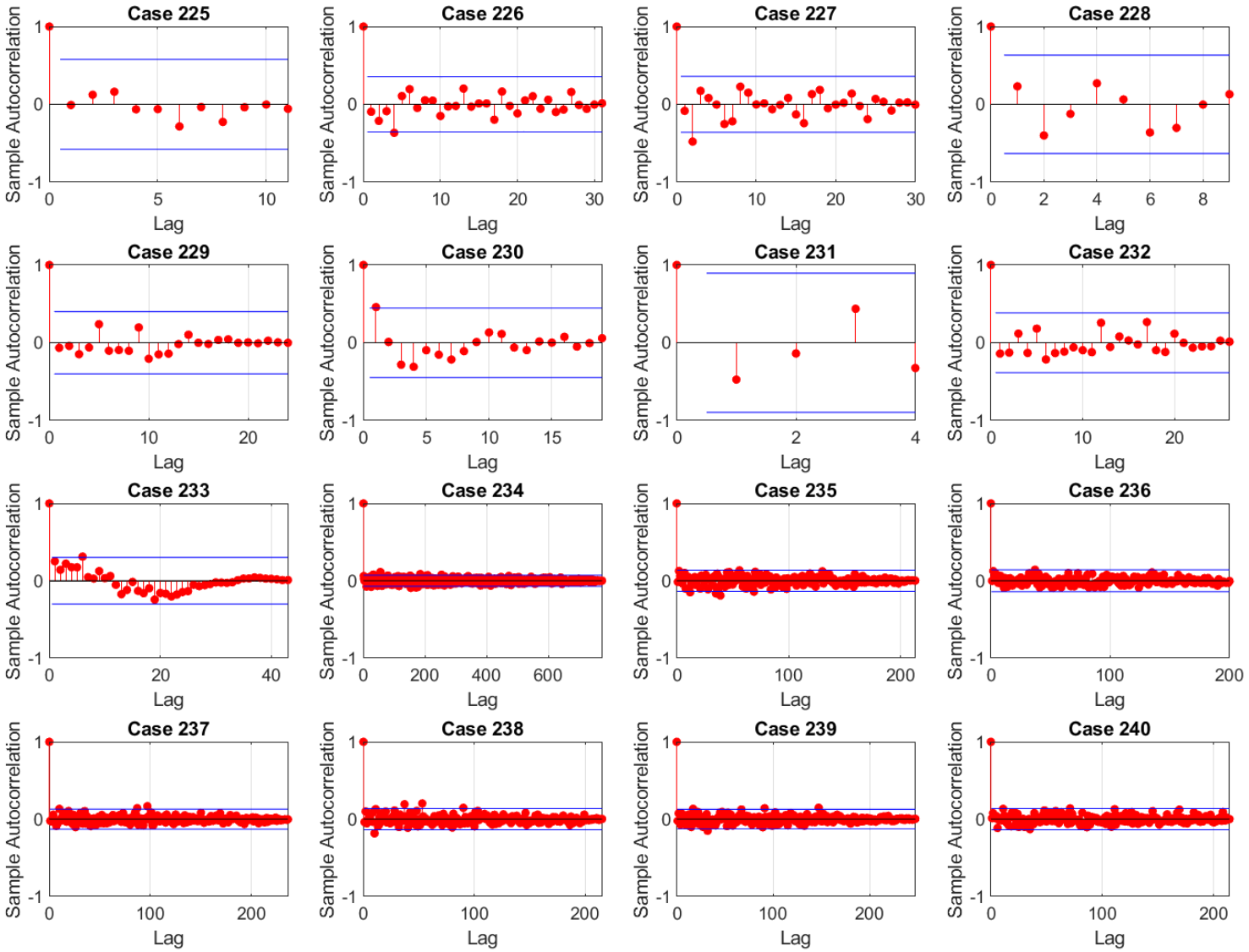
Case 225
Case 226
Case 227
Case 228
Case 229
Case 230
Case 231
Case 232
Case 233
Case 234
Case 235
Case 236
Case 237
Case 238
Case 239
Case 240
Sample Autocorrelation
Lag

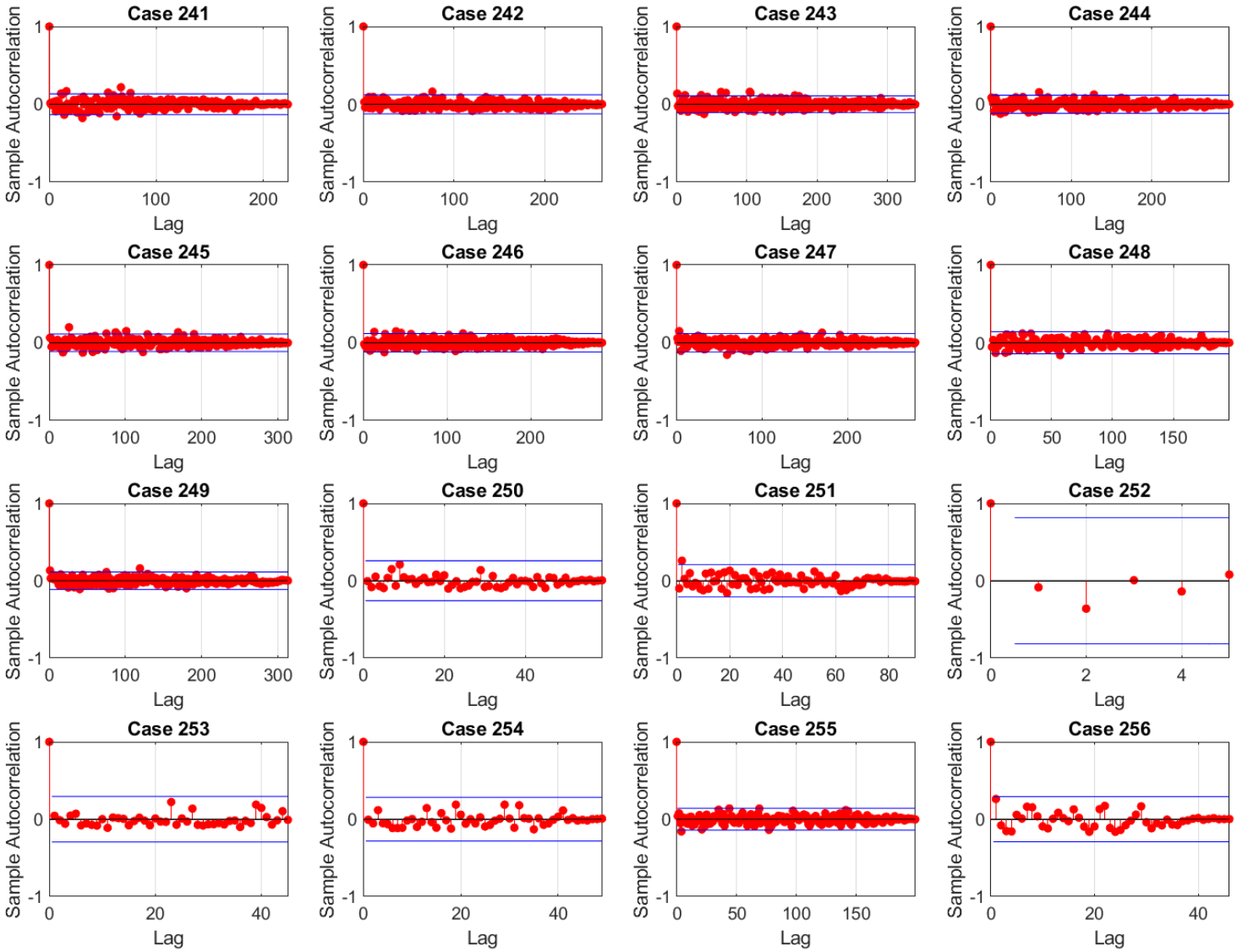
Case 241
Case 242
Case 243
Case 244
Case 245
Case 246
Case 247
Case 248
Case 249
Case 250
Case 251
Case 252
Case 253
Case 254
Case 255
Case 256
Sample Autocorrelation
Lag

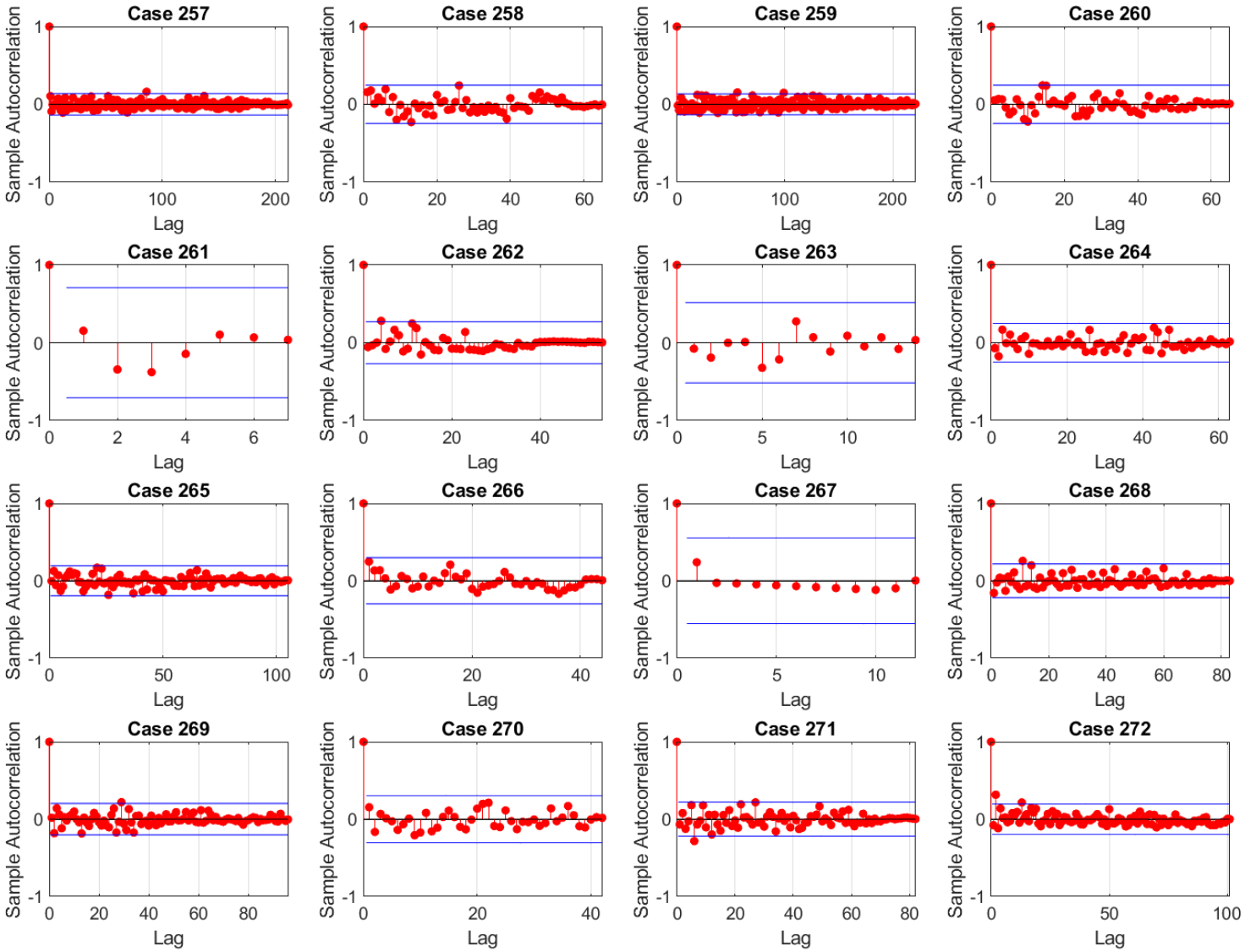
Case 257
Case 258
Case 259
Case 260
Case 261
Case 262
Case 263
Case 264
Case 265
Case 266
Case 267
Case 268
Case 269
Case 270
Case 271
Case 272
Sample Autocorrelation
Lag

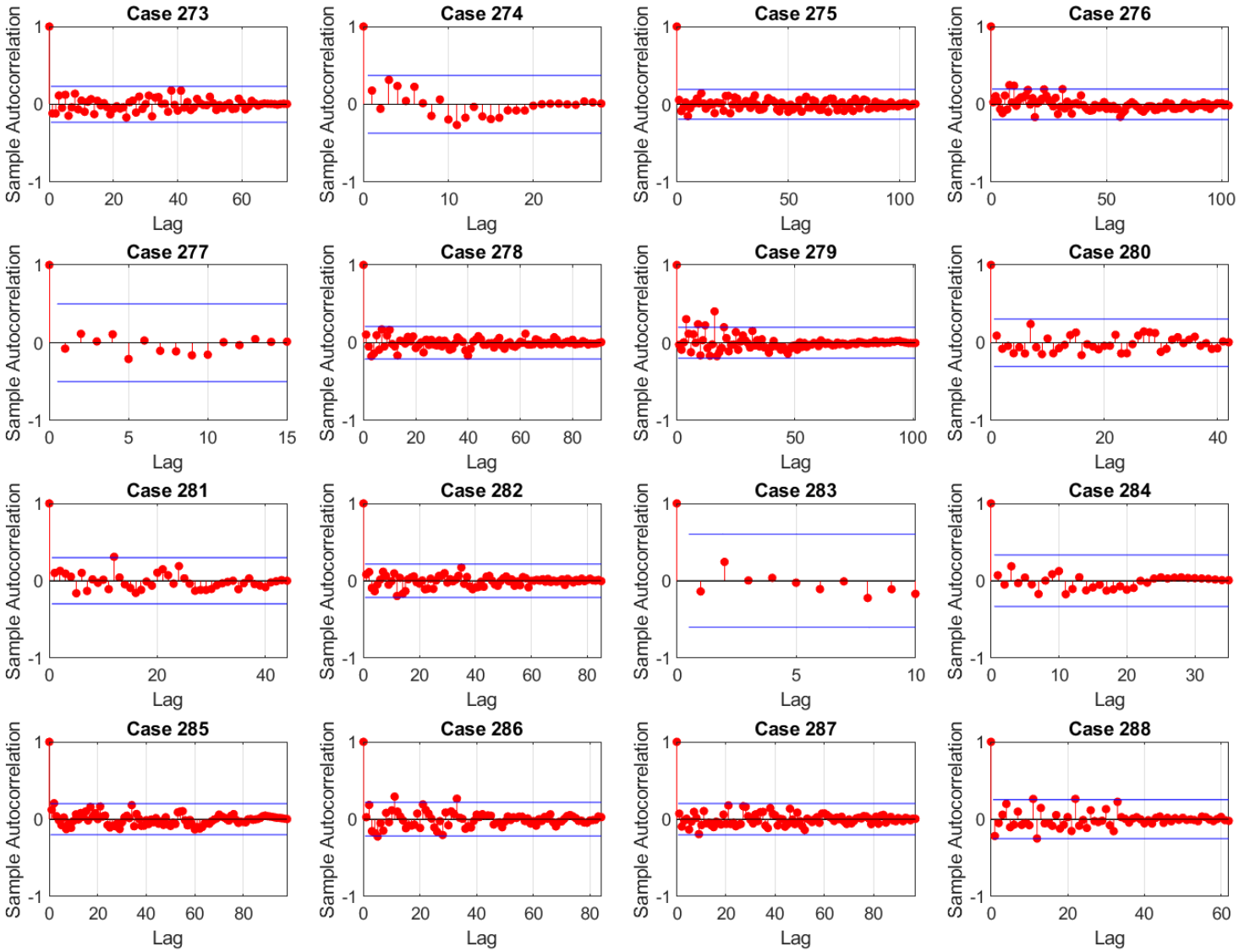
Case 273
Case 274
Case 275
Case 276
Case 277
Case 278
Case 279
Case 280
Case 281
Case 282
Case 283
Case 284
Case 285
Case 286
Case 287
Case 288
Sample Autocorrelation
Lag

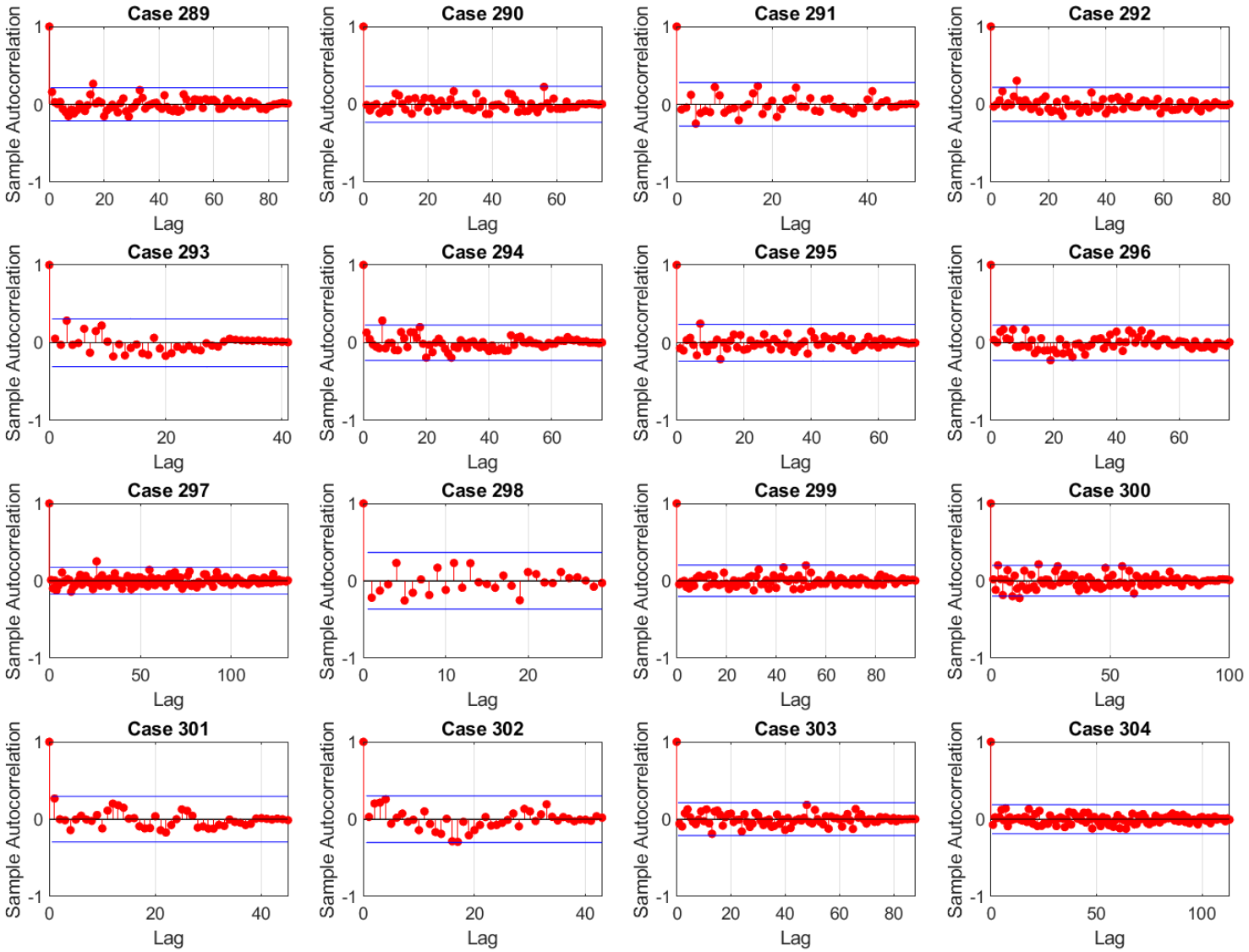
Case 289
Case 290
Case 291
Case 292
Case 293
Case 294
Case 295
Case 296
Case 297
Case 298
Case 299
Case 300
Case 301
Case 302
Case 303
Case 304
Sample Autocorrelation
Lag

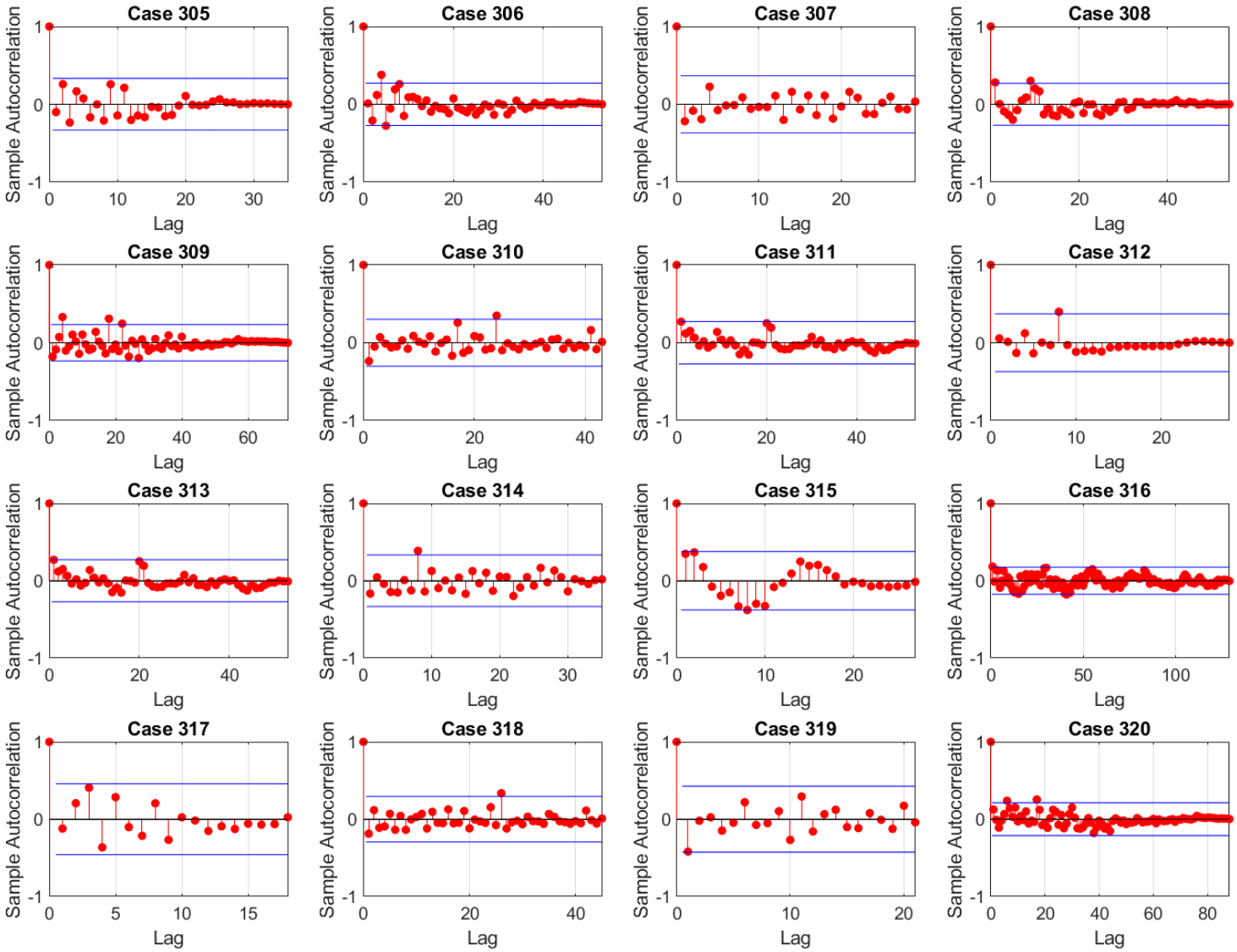
Case 305
Case 306
Case 307
Case 308
Case 309
Case 310
Case 311
Case 312
Case 313
Case 314
Case 315
Case 316
Case 317
Case 318
Case 319
Case 320
Sample Autocorrelation
Lag

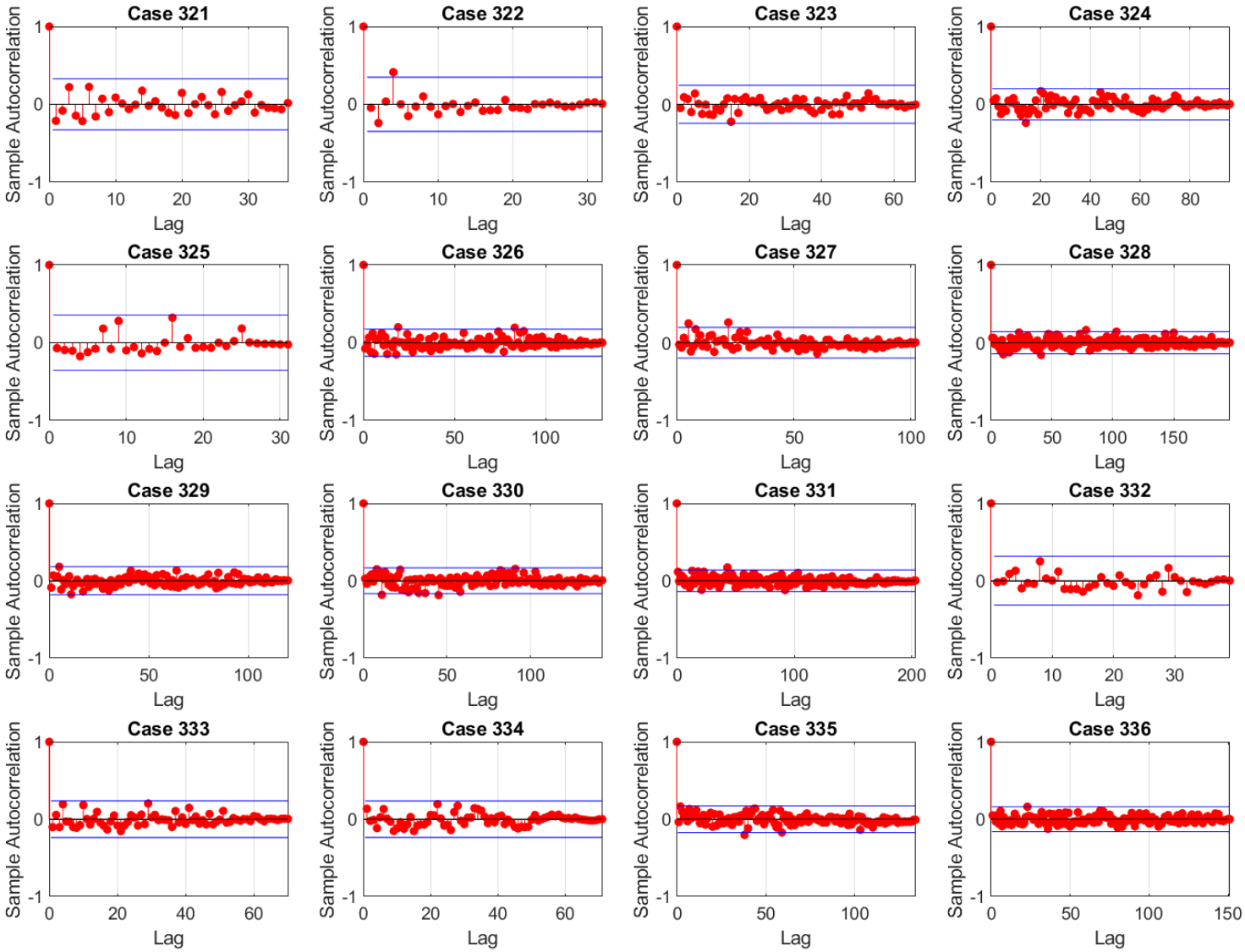
Case 321
Case 322
Case 323
Case 324
Case 325
Case 326
Case 327
Case 328
Case 329
Case 330
Case 331
Case 332
Case 333
Case 334
Case 335
Case 336
Sample Autocorrelation
Lag

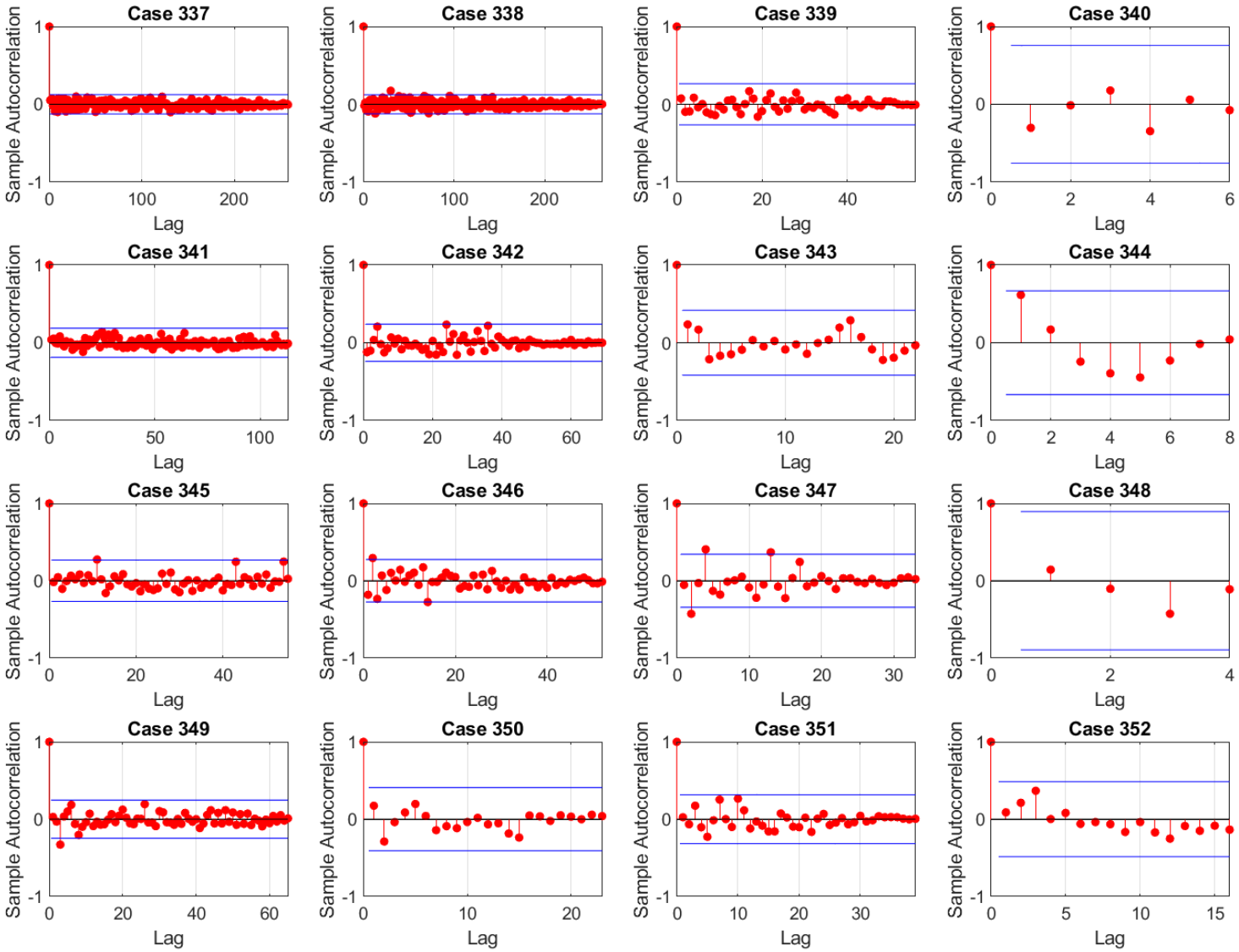
Case 337
Case 338
Case 339
Case 340
Case 341
Case 342
Case 343
Case 344
Case 345
Case 346
Case 347
Case 348
Case 349
Case 350
Case 351
Case 352
Sample Autocorrelation
Lag

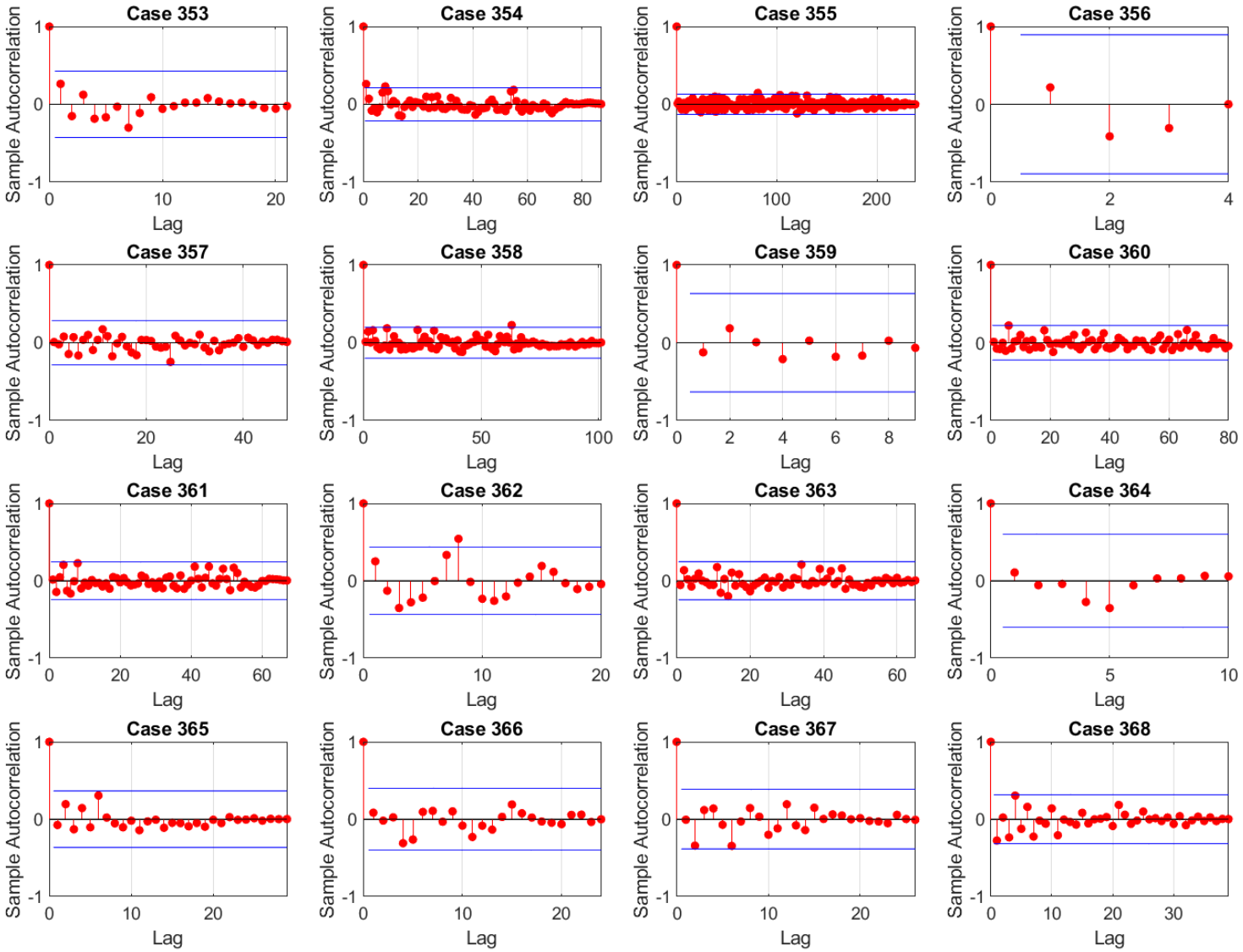
Case 353
Case 354
Case 355
Case 356
Case 357
Case 358
Case 359
Case 360
Case 361
Case 362
Case 363
Case 364
Case 365
Case 366
Case 367
Case 368
Sample Autocorrelation
Lag

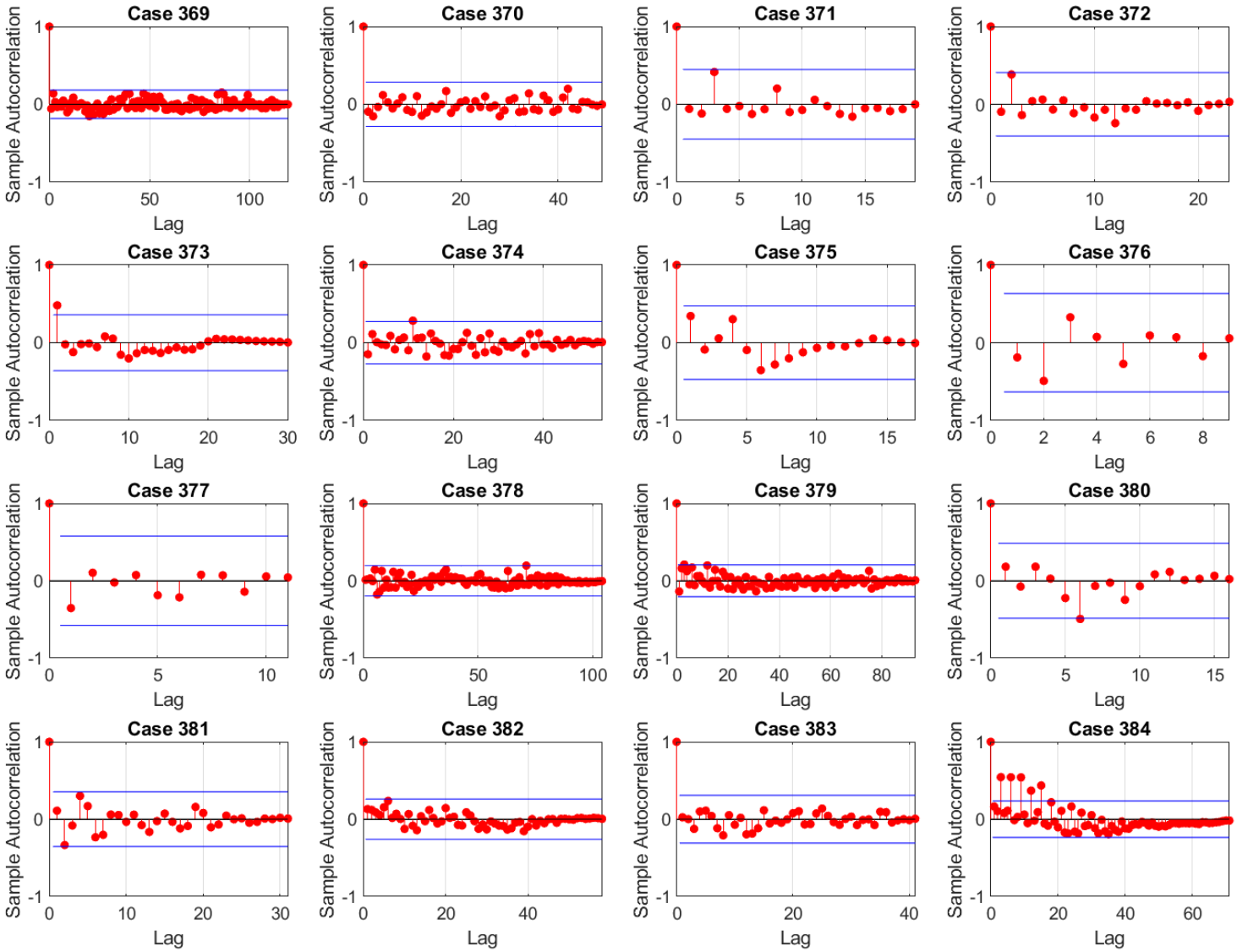
Case 369
Case 370
Case 371
Case 372
Case 373
Case 374
Case 375
Case 376
Case 377
Case 378
Case 379
Case 380
Case 381
Case 382
Case 383
Case 384
Sample Autocorrelation
Lag

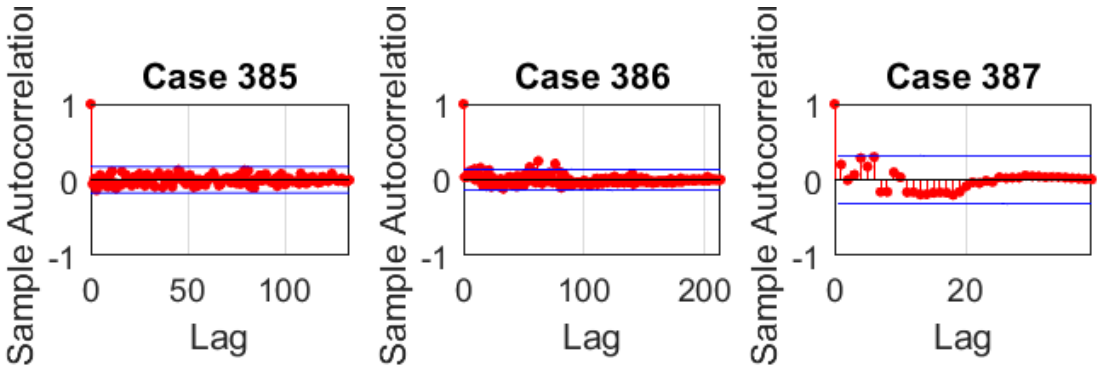
Case 385
Sample Autocorrelation
1
0
-1
0
50
100
Lag
Case 386
Sample Autocorrelation
1
0
-1
0
100
200
Lag
Case 387
Sample Autocorrelation
1
0
-1
0
20
Lag

APPENDIX C – Histograms of inter-formation times

Histograms of endocardial breakthroughs inter-formation times in all AF cases are provided on the following pages.

Histograms visualise the probability distribution of inter-formation times.

In most histograms, the probability distribution of inter-formation times was an exponential distribution.

In the histograms of the cases rejected by Chi-square goodness-of-fit test, the probability distribution of inter-formation times could not fit well to an exponential distribution as the first bin is lower than the second bin.

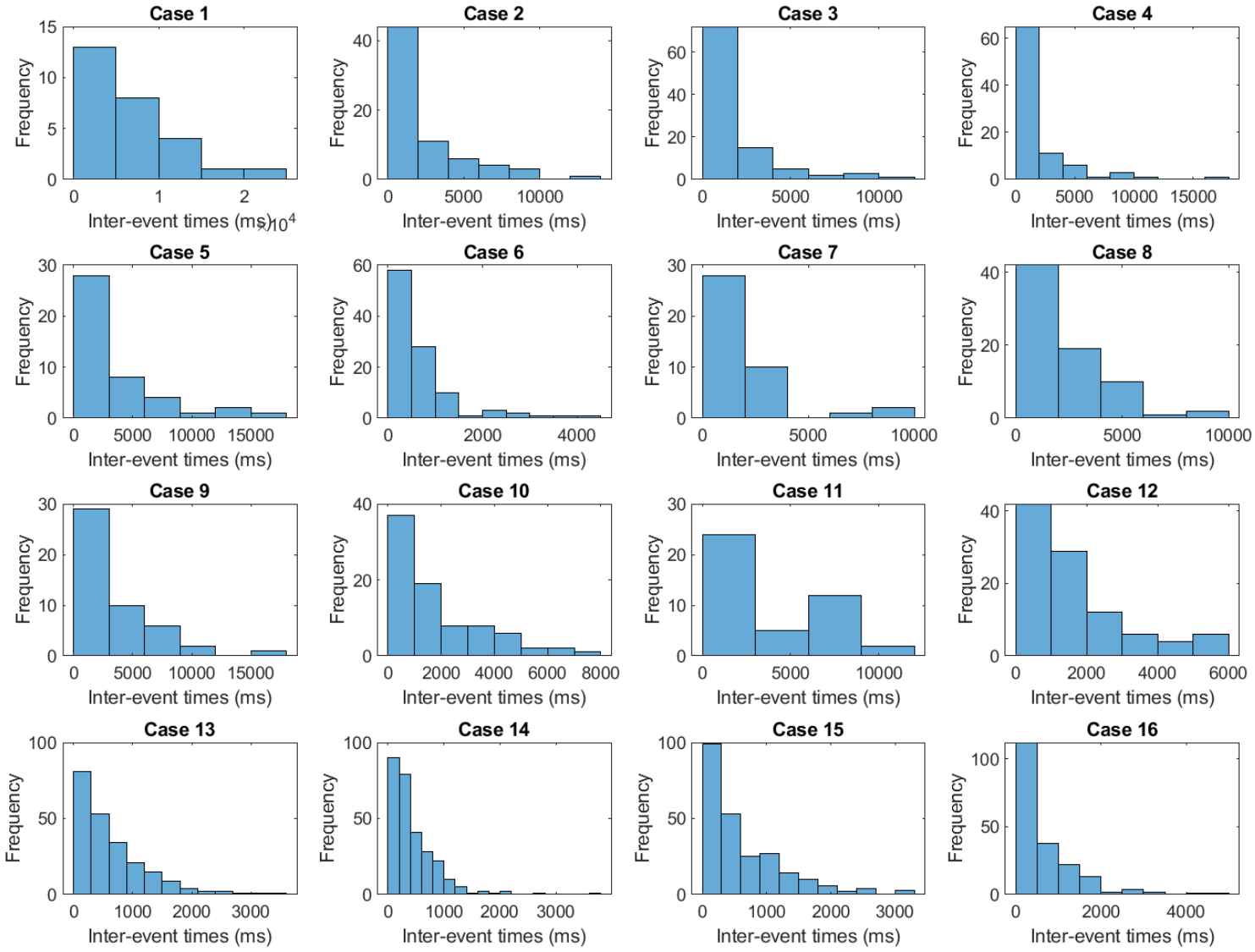
Case 1
Frequency
Inter-event times (ms)
×10^4
Case 2
Case 3
Case 4
Case 5
Case 6
Case 7
Case 8
Case 9
Case 10
Case 11
Case 12
Case 13
Case 14
Case 15
Case 16

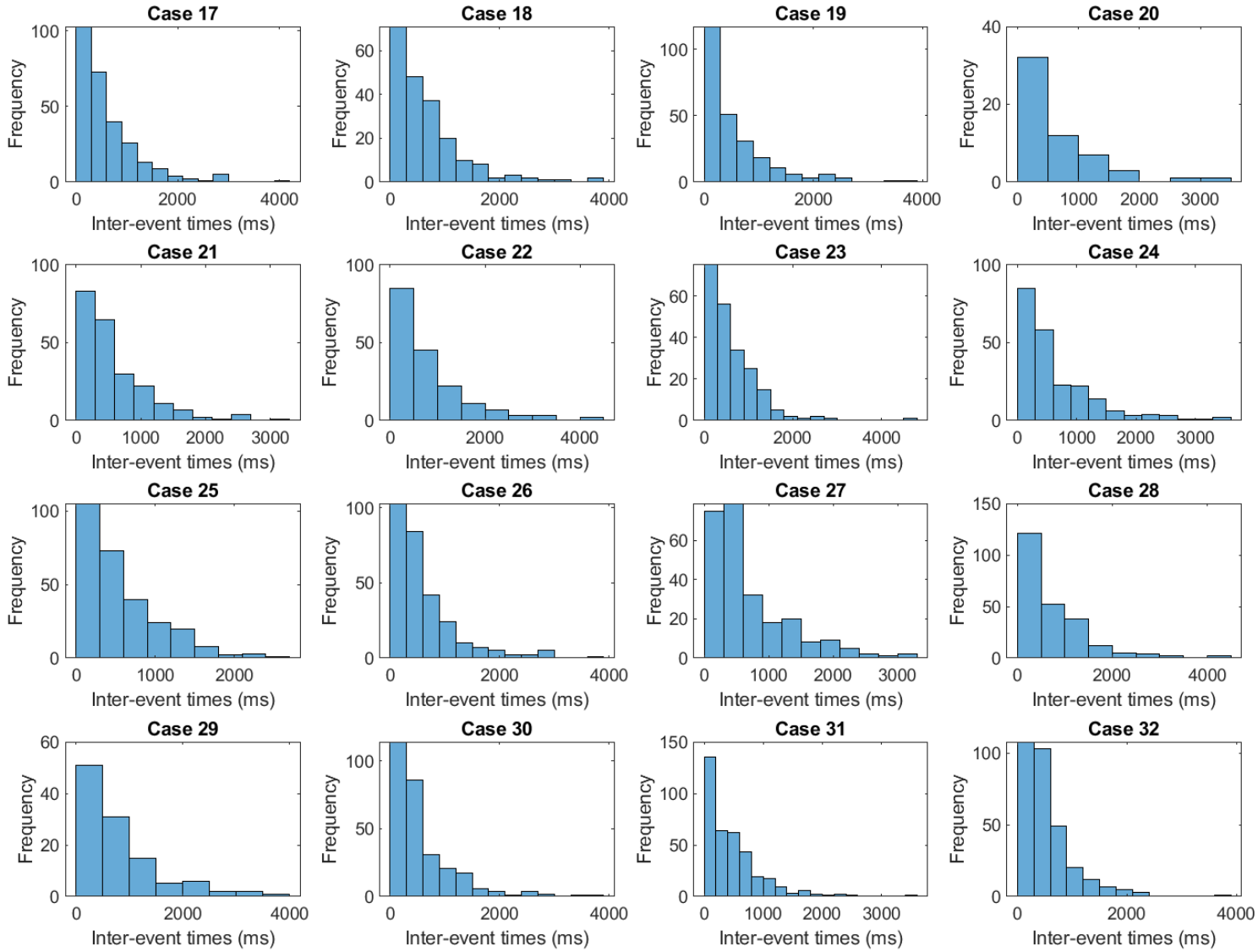
Case 17
Case 18
Case 19
Case 20
Case 21
Case 22
Case 23
Case 24
Case 25
Case 26
Case 27
Case 28
Case 29
Case 30
Case 31
Case 32
Frequency
Inter-event times (ms)

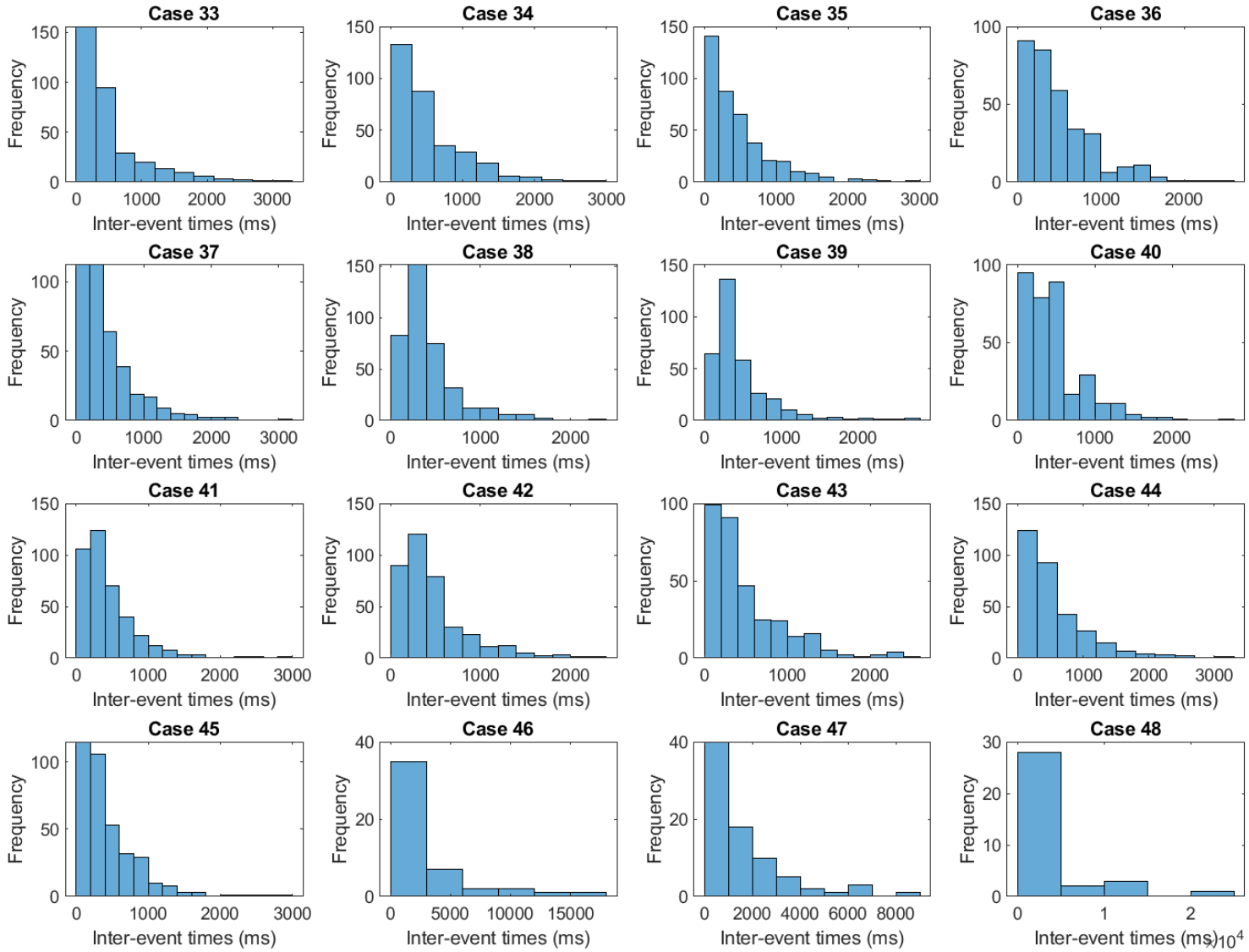
Case 33
Case 34
Case 35
Case 36
Case 37
Case 38
Case 39
Case 40
Case 41
Case 42
Case 43
Case 44
Case 45
Case 46
Case 47
Case 48
Frequency
Inter-event times (ms)
×10^4

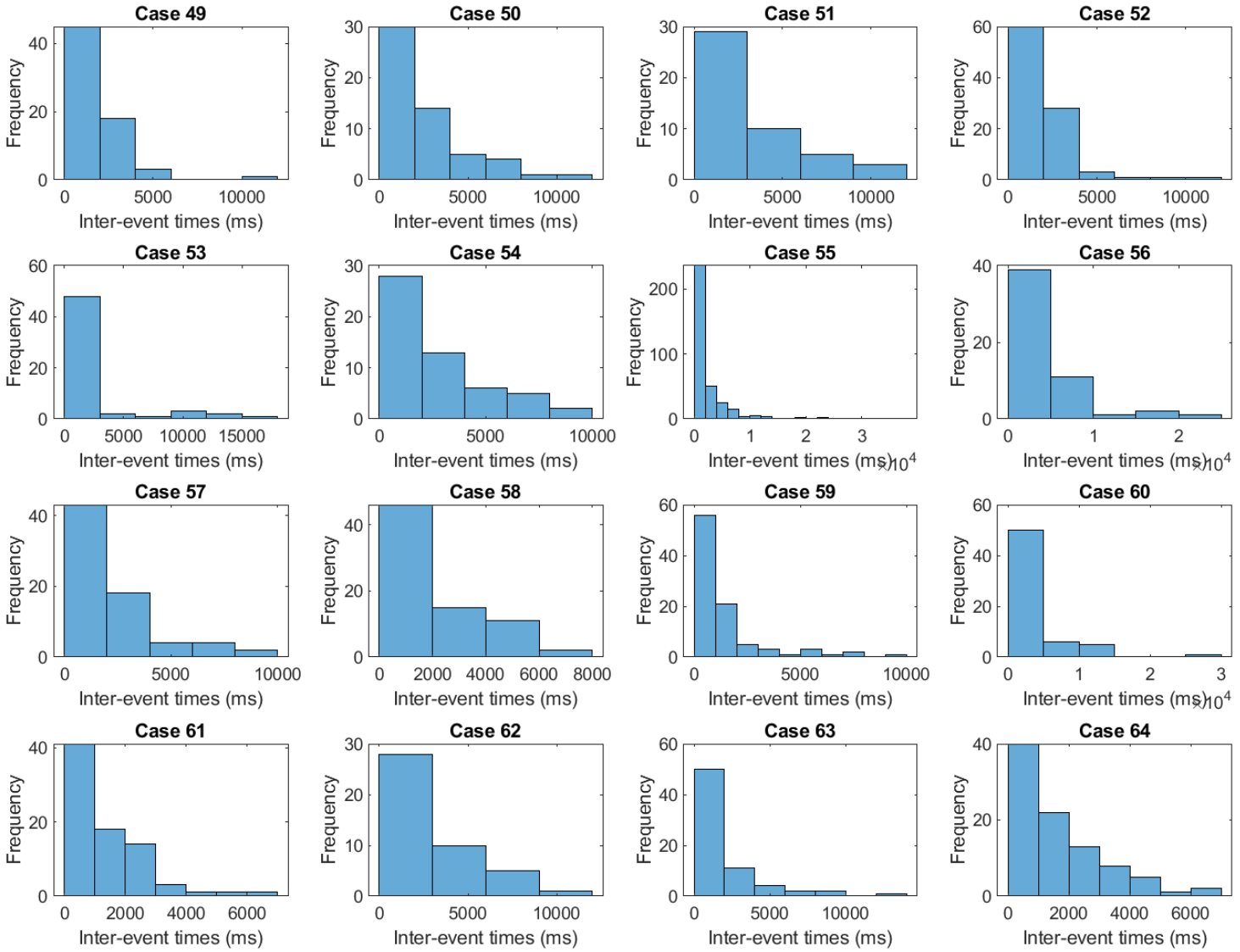
Case 49
Case 50
Case 51
Case 52
Case 53
Case 54
Case 55
Case 56
Case 57
Case 58
Case 59
Case 60
Case 61
Case 62
Case 63
Case 64
Frequency
Inter-event times (ms)
×10^4

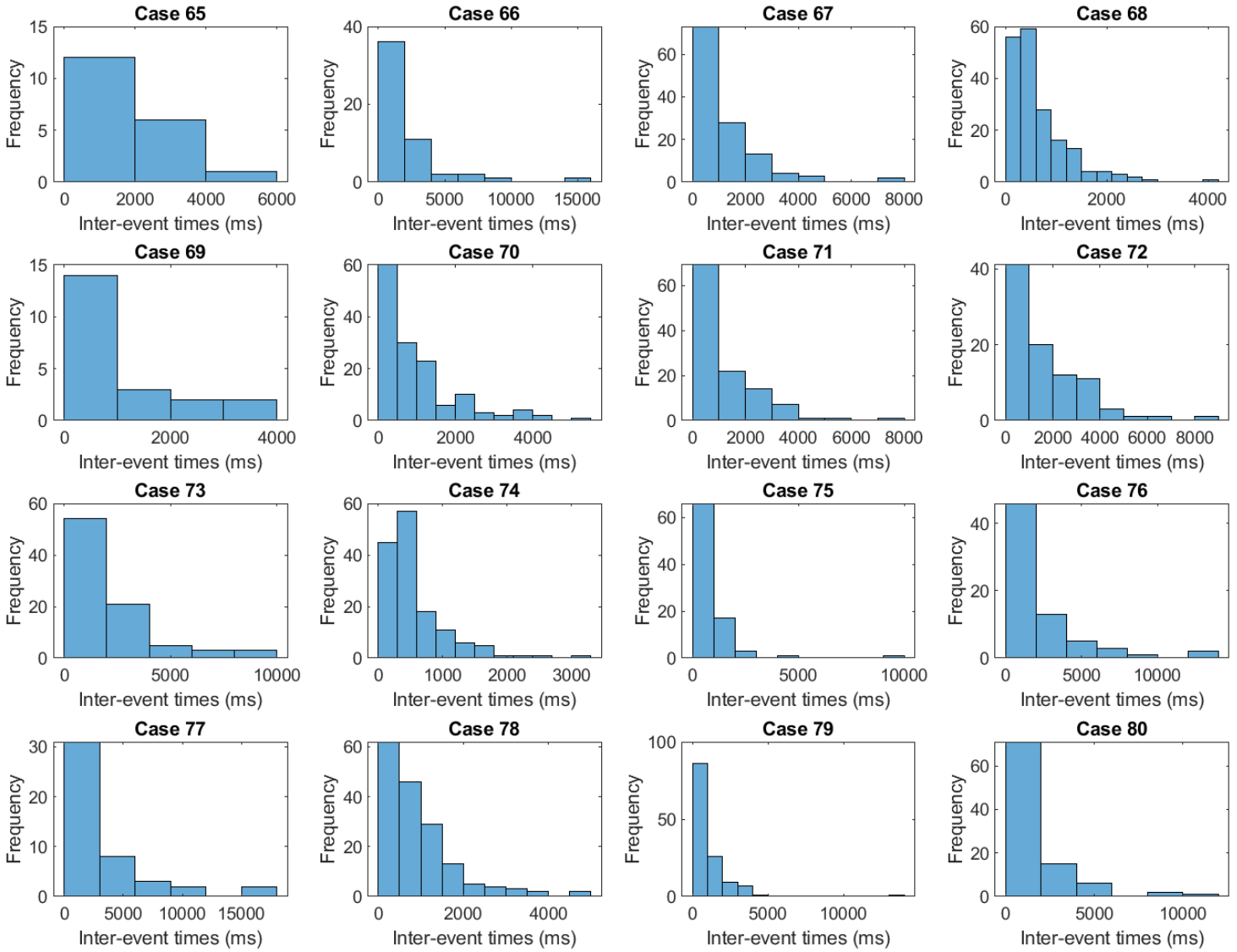
Case 65
Case 66
Case 67
Case 68
Case 69
Case 70
Case 71
Case 72
Case 73
Case 74
Case 75
Case 76
Case 77
Case 78
Case 79
Case 80
Frequency
Inter-event times (ms)

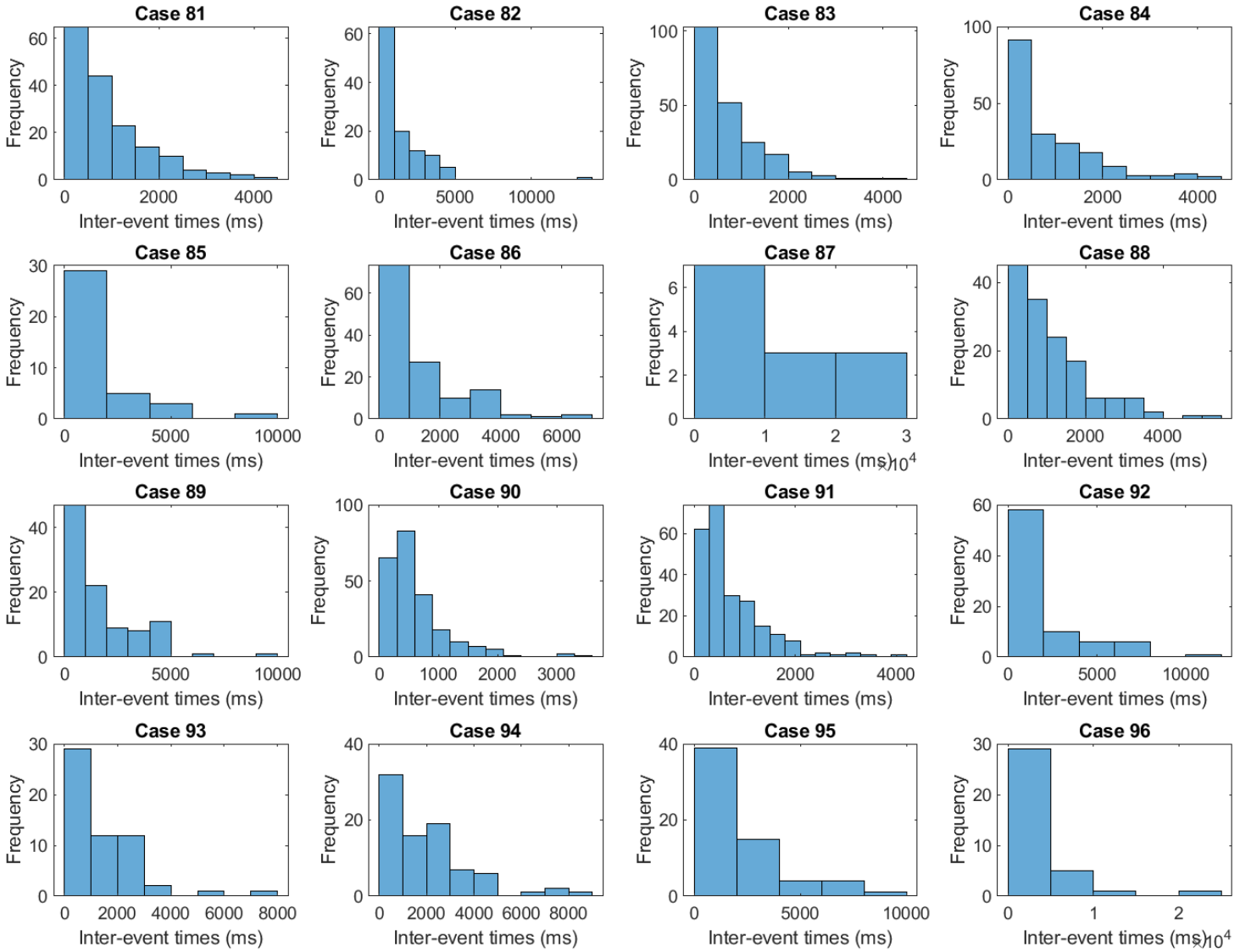
Case 81
Case 82
Case 83
Case 84
Case 85
Case 86
Case 87
Case 88
Case 89
Case 90
Case 91
Case 92
Case 93
Case 94
Case 95
Case 96
Frequency
Inter-event times (ms)
×10^4

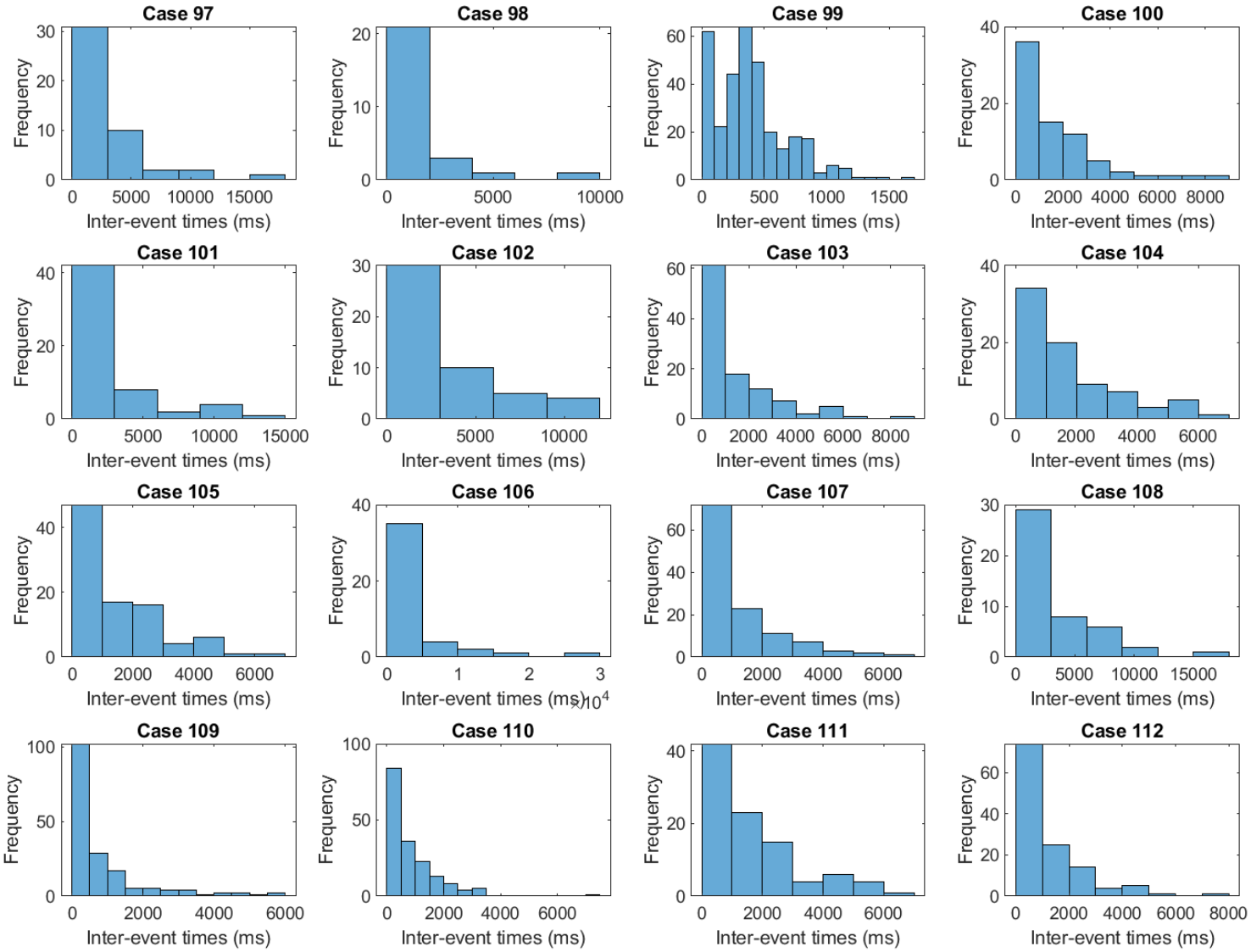
Case 97
Case 98
Case 99
Case 100
Case 101
Case 102
Case 103
Case 104
Case 105
Case 106
Case 107
Case 108
Case 109
Case 110
Case 111
Case 112
Frequency
Inter-event times (ms)
×10^4

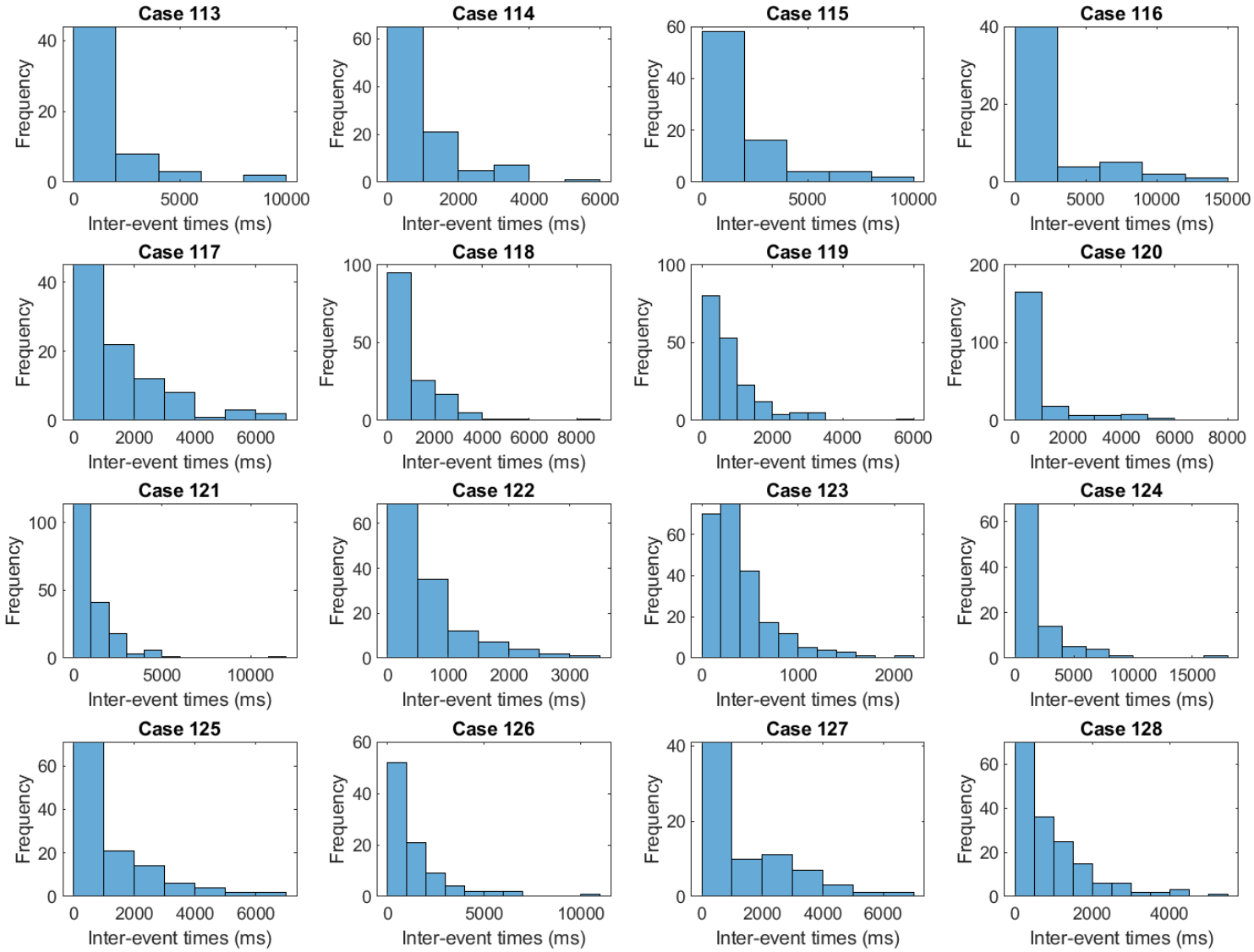
Case 113
Case 114
Case 115
Case 116
Case 117
Case 118
Case 119
Case 120
Case 121
Case 122
Case 123
Case 124
Case 125
Case 126
Case 127
Case 128
Frequency
Inter-event times (ms)

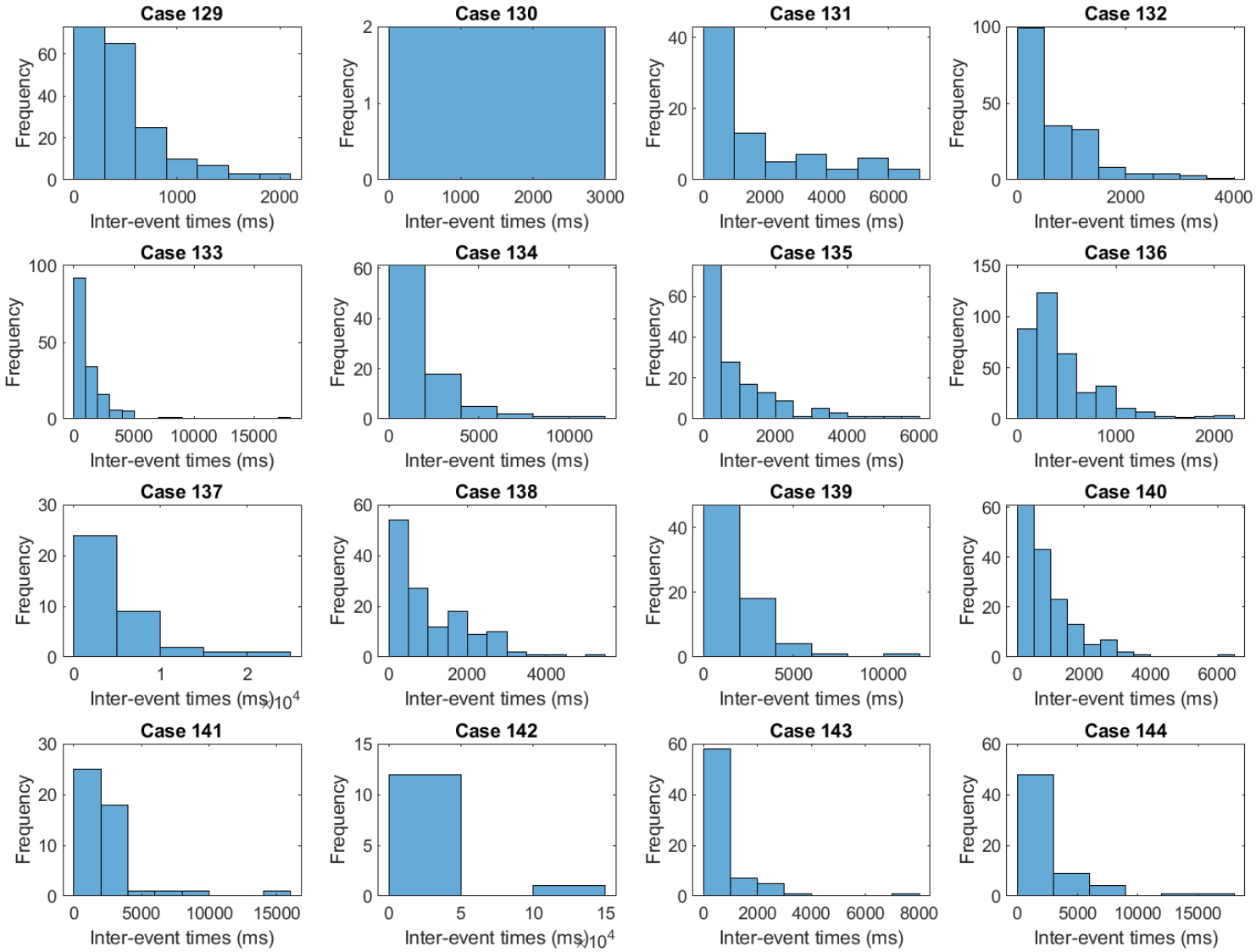
Case 129
Case 130
Case 131
Case 132
Case 133
Case 134
Case 135
Case 136
Case 137
Case 138
Case 139
Case 140
Case 141
Case 142
Case 143
Case 144
Frequency
Inter-event times (ms)
×10^4

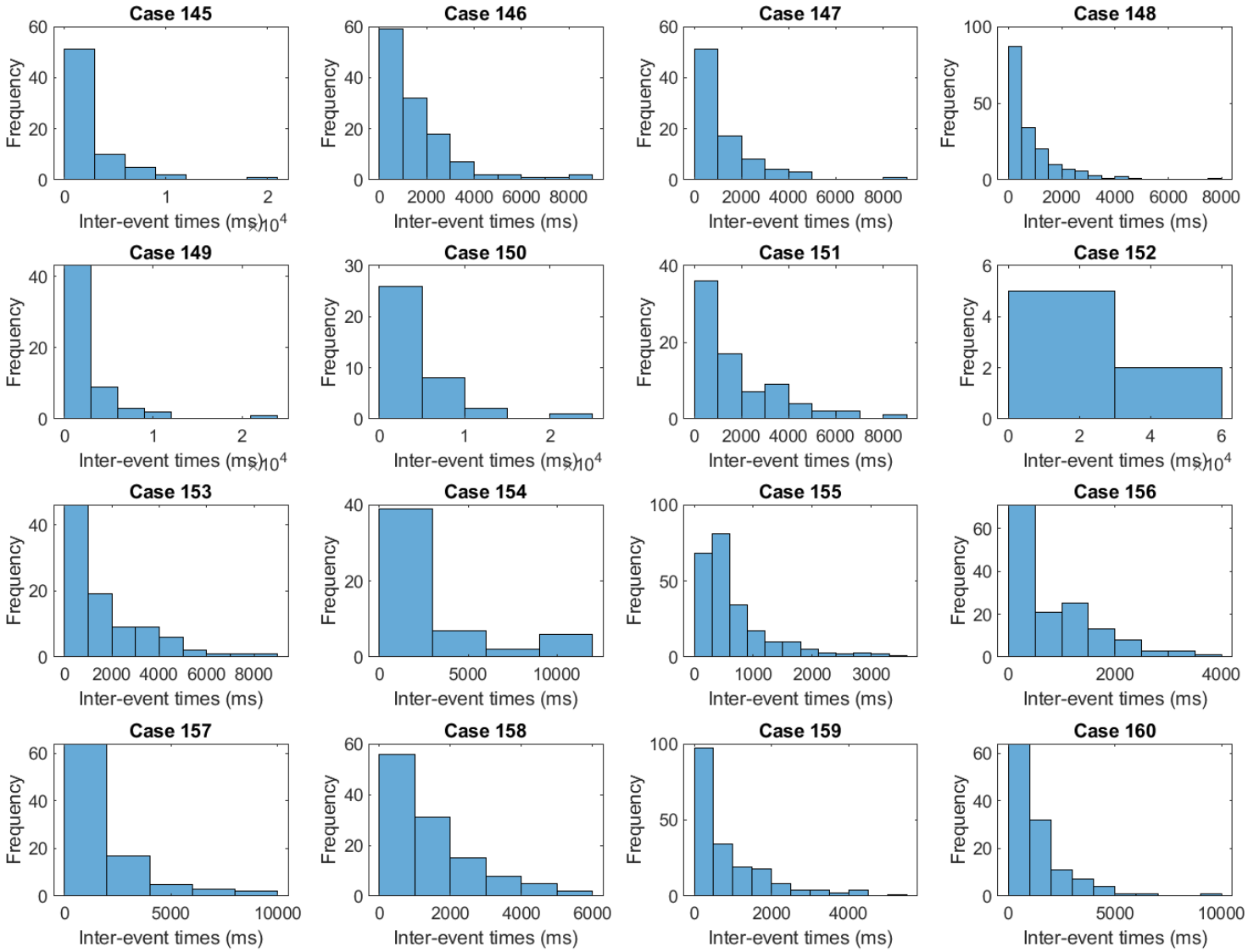
Case 145
Case 146
Case 147
Case 148
Case 149
Case 150
Case 151
Case 152
Case 153
Case 154
Case 155
Case 156
Case 157
Case 158
Case 159
Case 160
Frequency
Inter-event times (ms)
×10^4

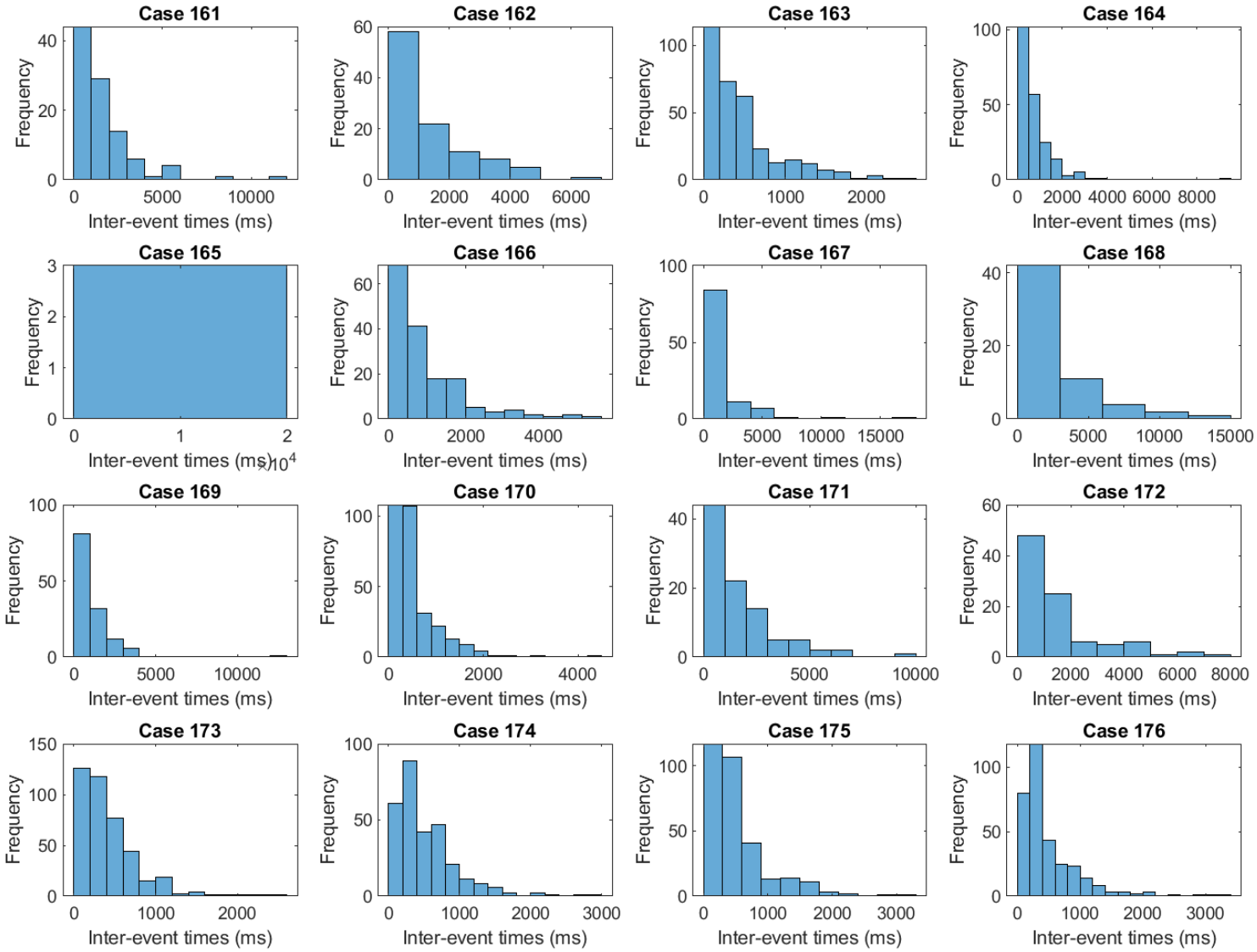
Case 161
Case 162
Case 163
Case 164
Case 165
Case 166
Case 167
Case 168
Case 169
Case 170
Case 171
Case 172
Case 173
Case 174
Case 175
Case 176
Frequency
Inter-event times (ms)
×10^4

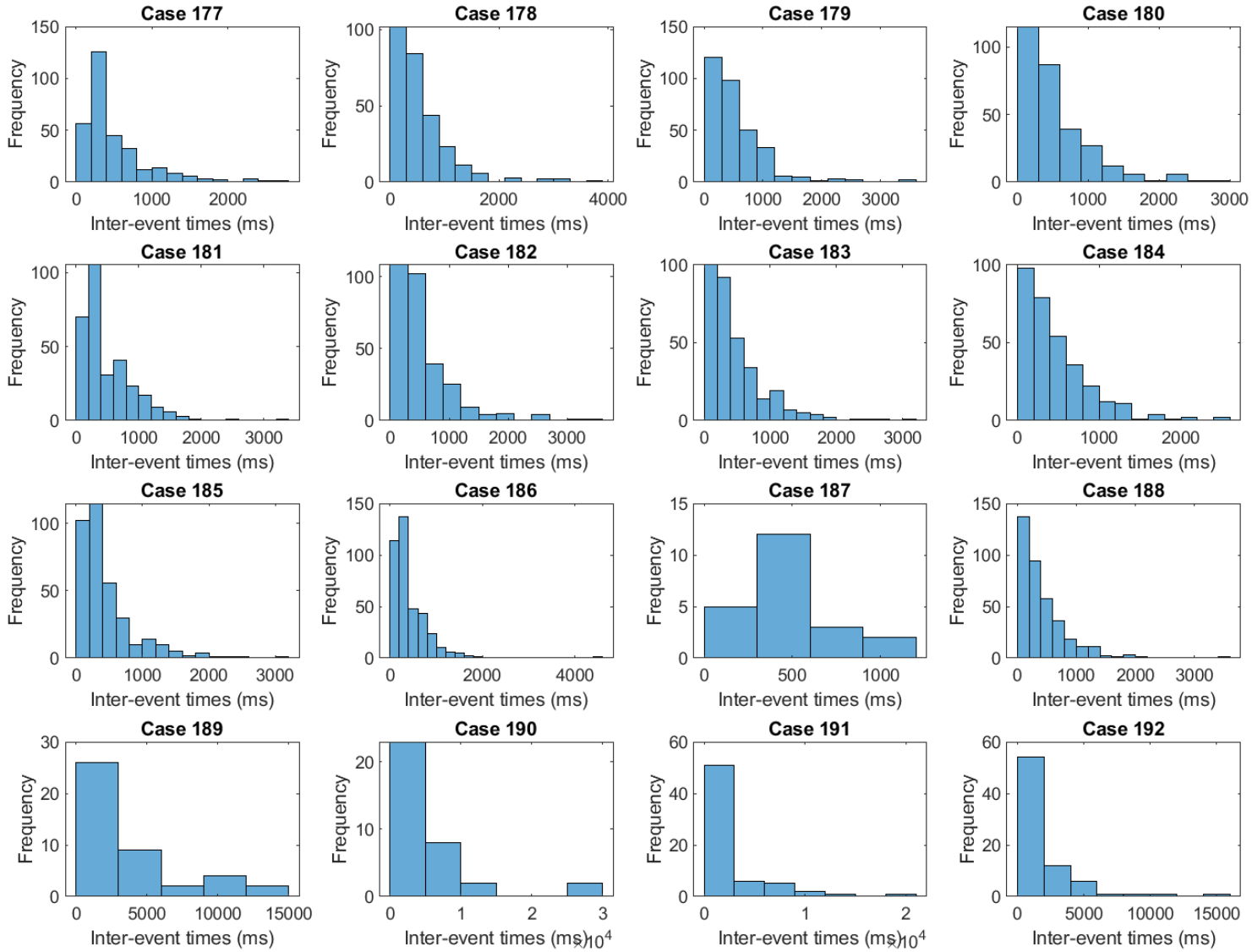
Case 177
Case 178
Case 179
Case 180
Case 181
Case 182
Case 183
Case 184
Case 185
Case 186
Case 187
Case 188
Case 189
Case 190
Case 191
Case 192
Frequency
Inter-event times (ms)
×10^4

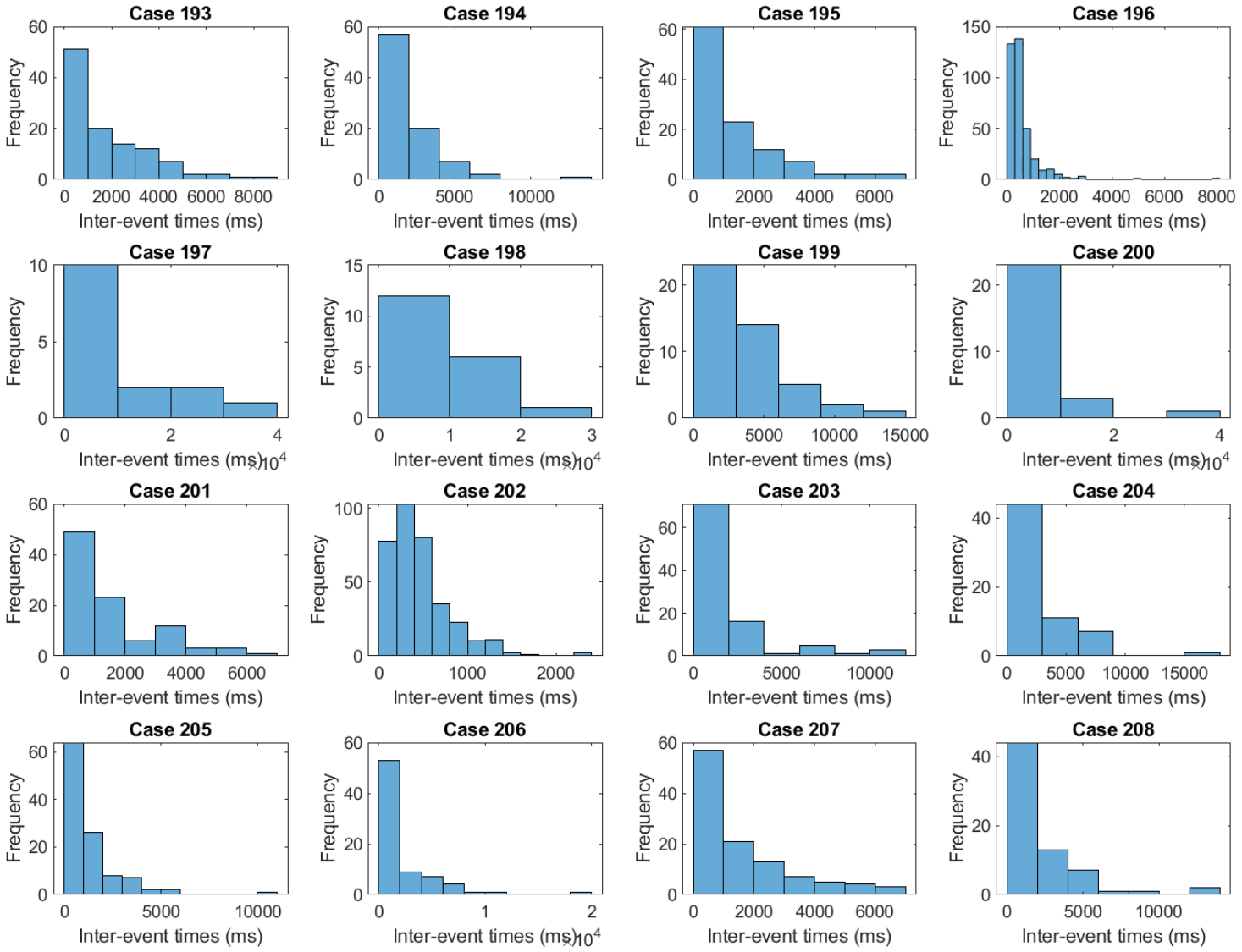
Case 193
Case 194
Case 195
Case 196
Case 197
Case 198
Case 199
Case 200
Case 201
Case 202
Case 203
Case 204
Case 205
Case 206
Case 207
Case 208
Frequency
Inter-event times (ms)
×10^4

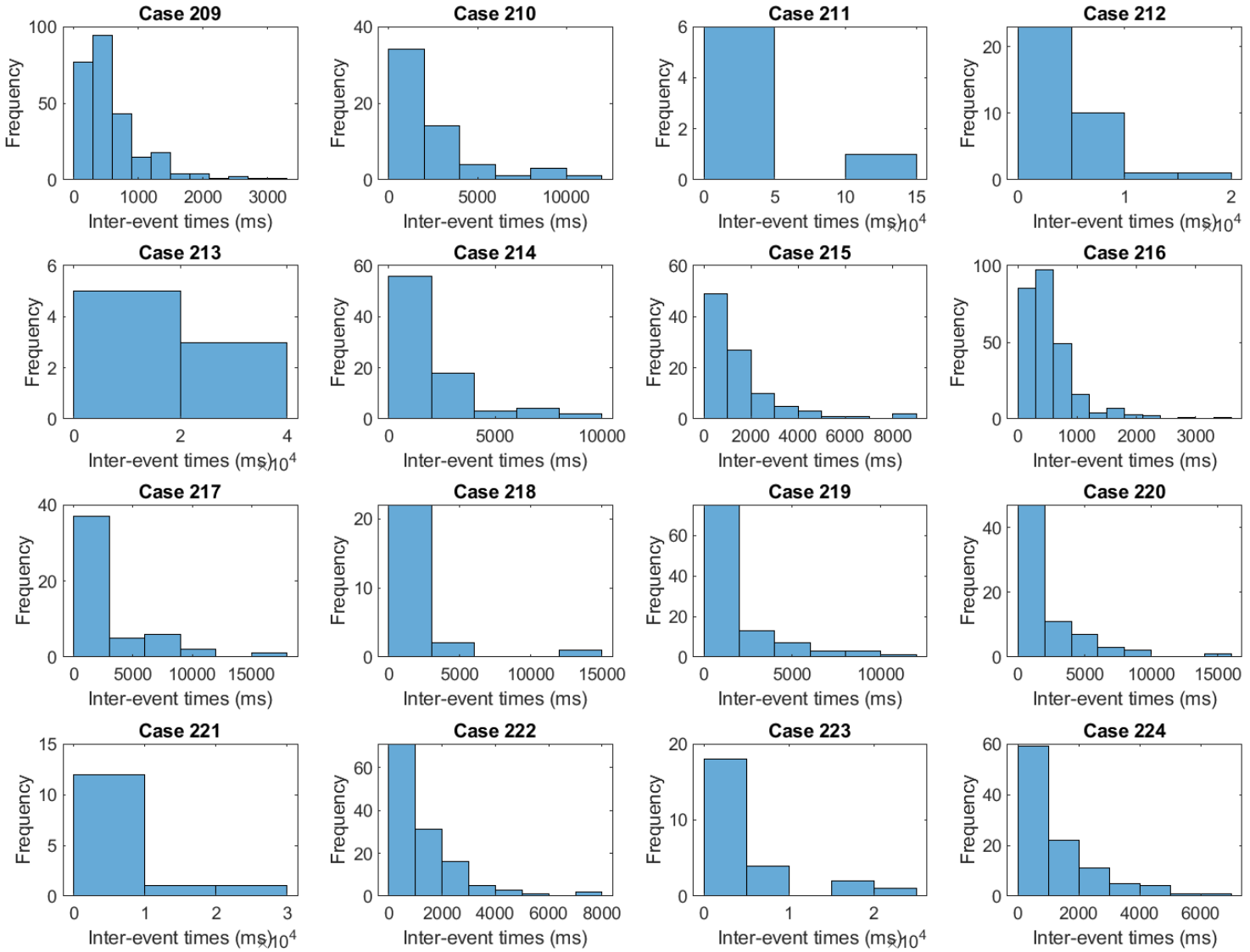
Case 209
Case 210
Case 211
Case 212
Case 213
Case 214
Case 215
Case 216
Case 217
Case 218
Case 219
Case 220
Case 221
Case 222
Case 223
Case 224
Frequency
Inter-event times (ms)
×10^4

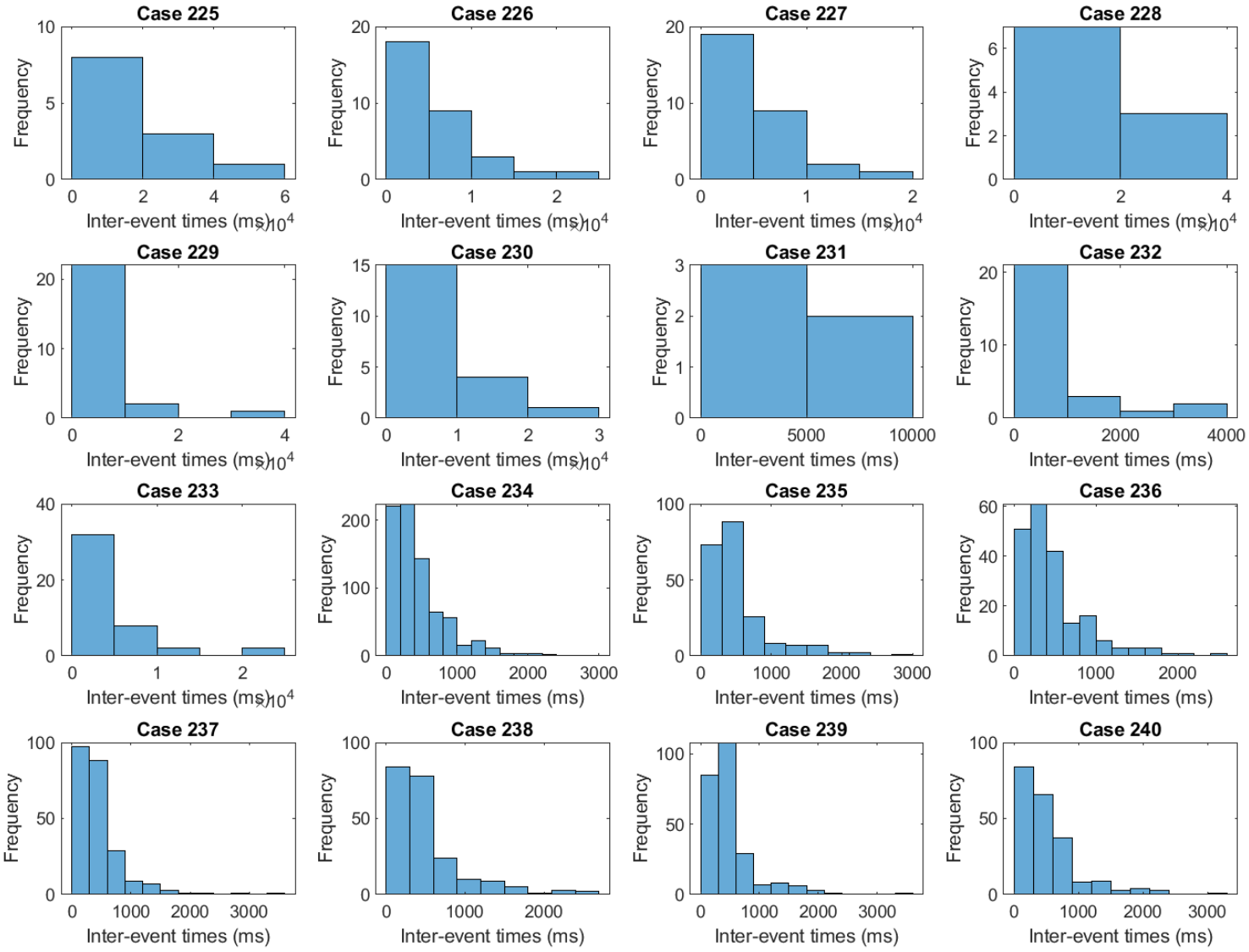
Case 225
Case 226
Case 227
Case 228
Case 229
Case 230
Case 231
Case 232
Case 233
Case 234
Case 235
Case 236
Case 237
Case 238
Case 239
Case 240
Frequency
Inter-event times (ms)
×10^4

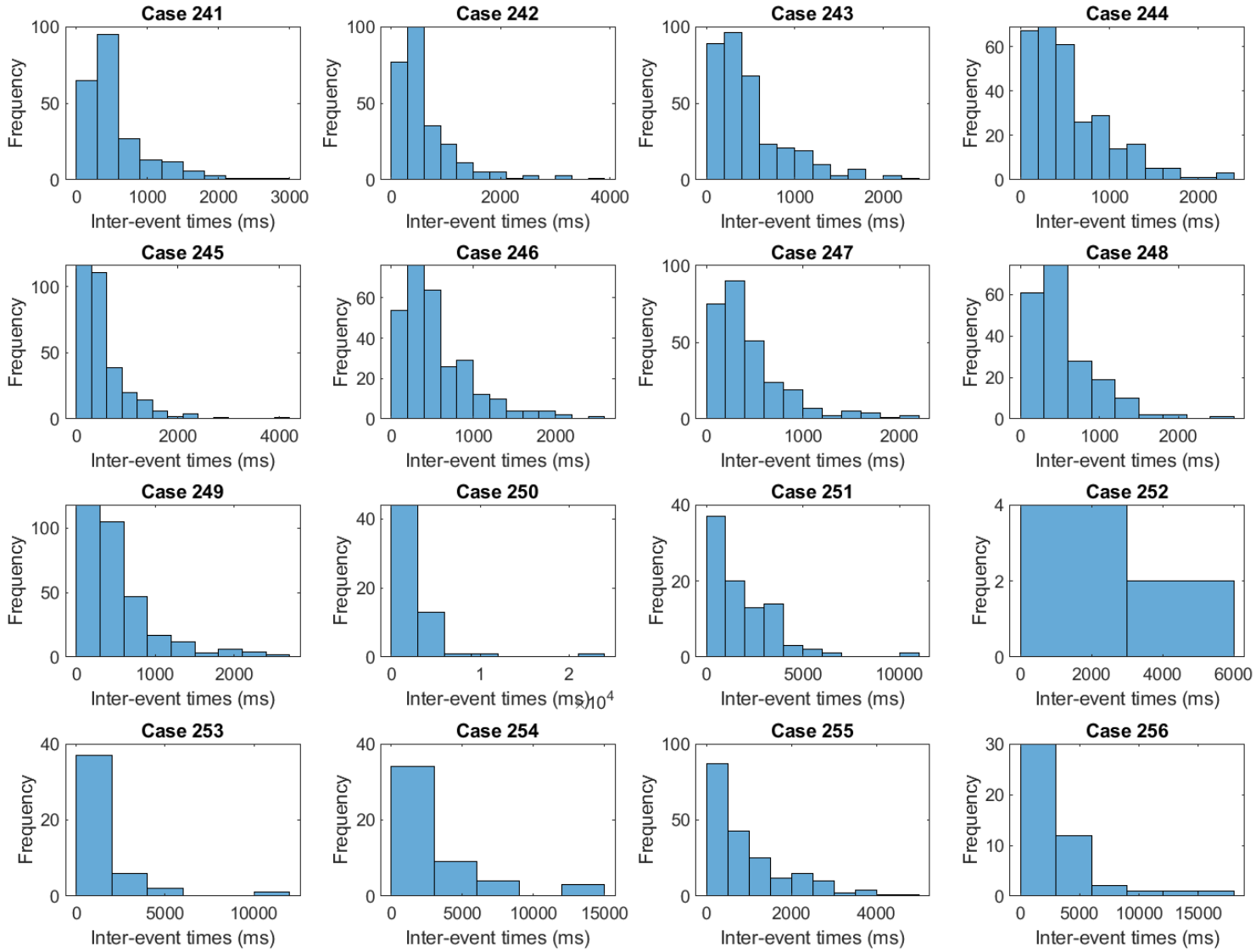
Case 241
Case 242
Case 243
Case 244
Case 245
Case 246
Case 247
Case 248
Case 249
Case 250
Case 251
Case 252
Case 253
Case 254
Case 255
Case 256
Frequency
Inter-event times (ms)
×10^4

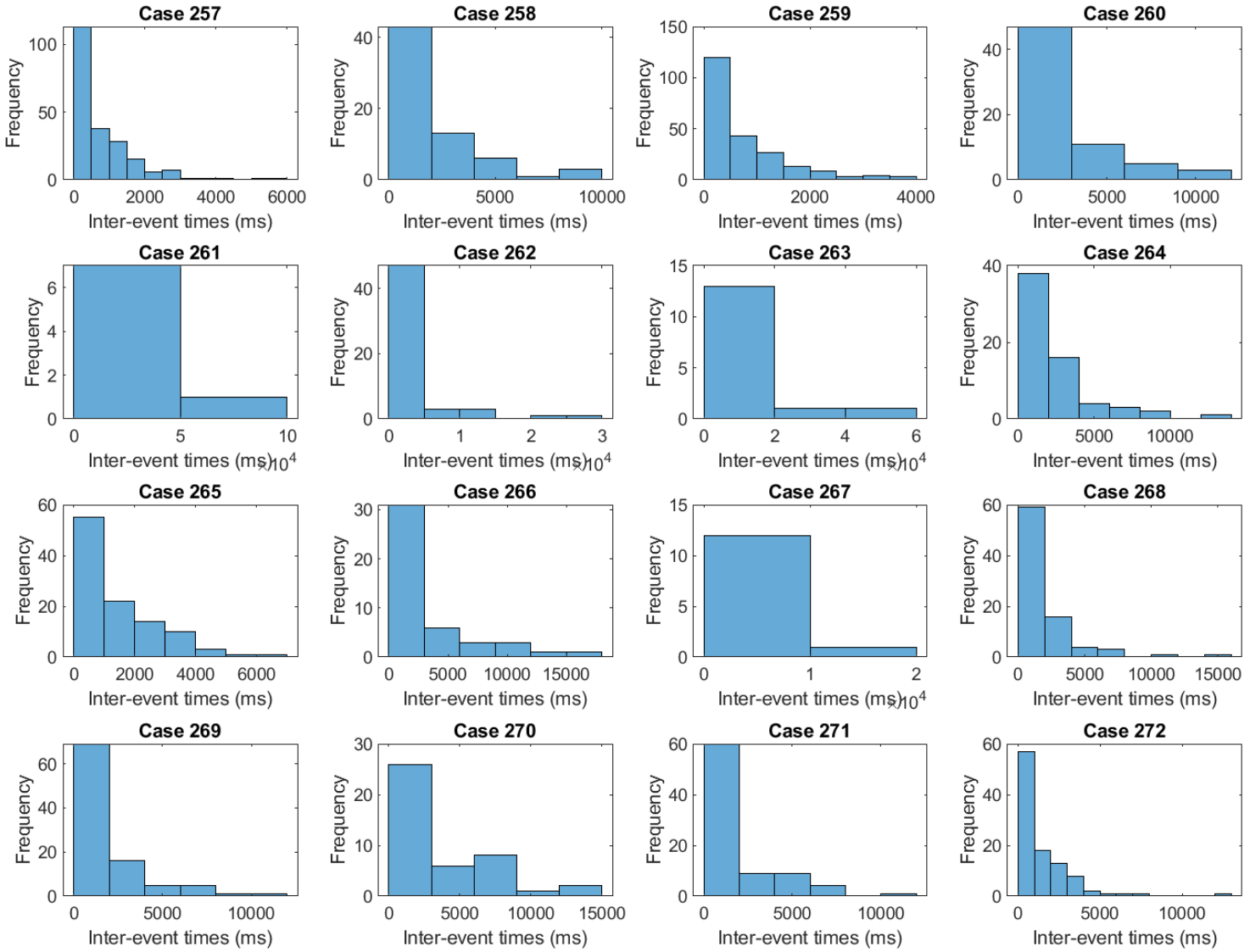
Case 257
Case 258
Case 259
Case 260
Case 261
Case 262
Case 263
Case 264
Case 265
Case 266
Case 267
Case 268
Case 269
Case 270
Case 271
Case 272
Frequency
Inter-event times (ms)
×10^4

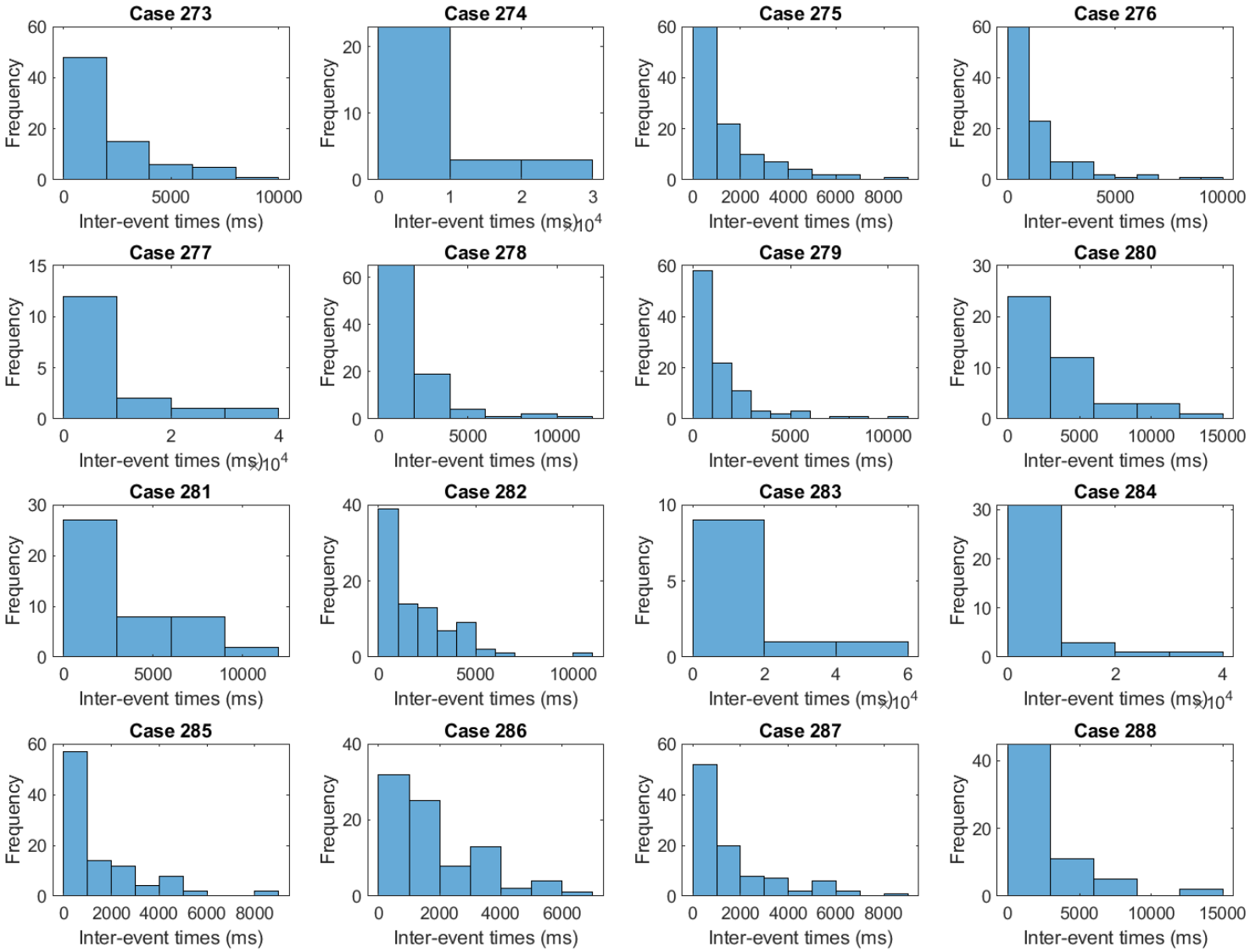
Case 273
Case 274
Case 275
Case 276
Case 277
Case 278
Case 279
Case 280
Case 281
Case 282
Case 283
Case 284
Case 285
Case 286
Case 287
Case 288
Frequency
Inter-event times (ms)
×10^4

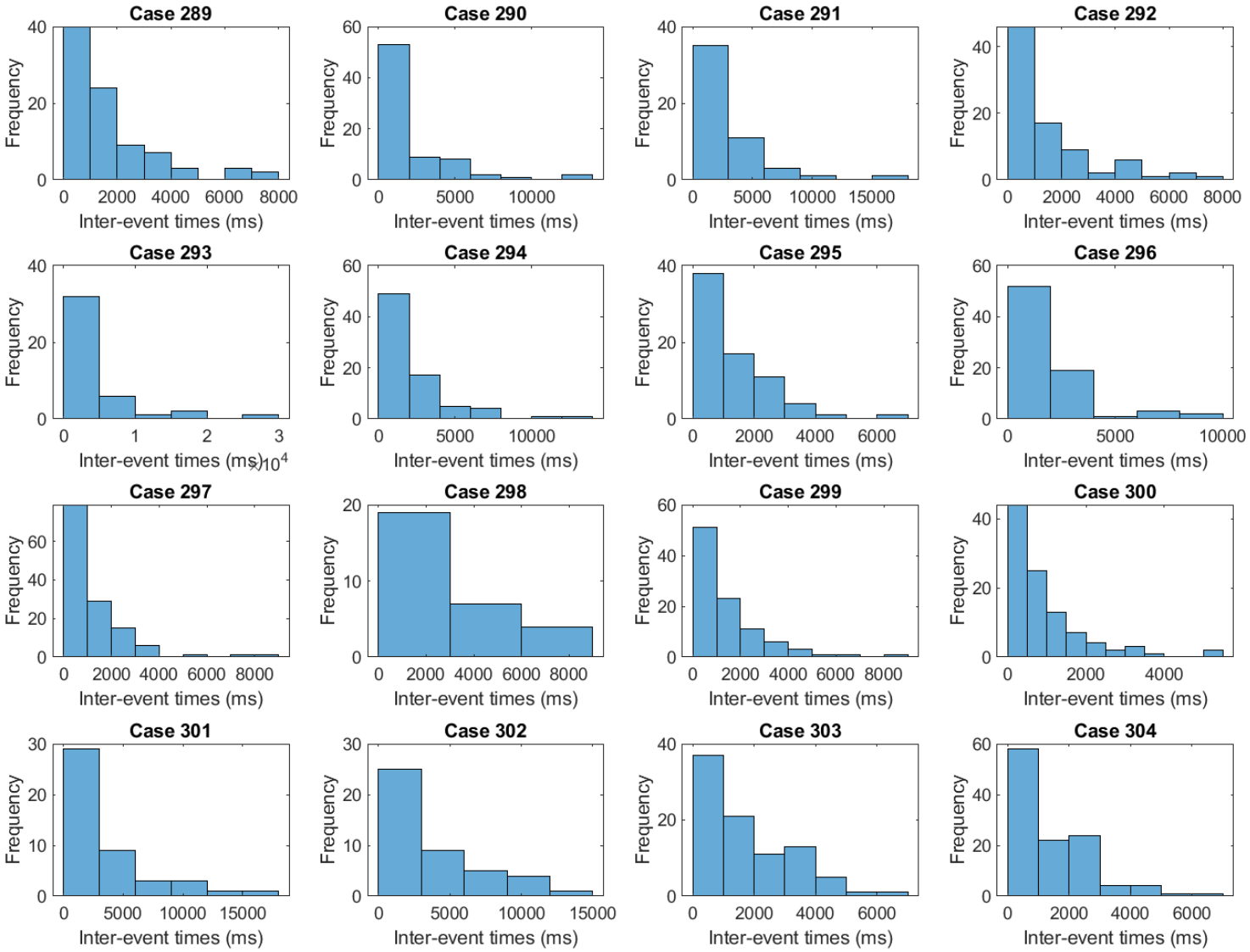
Case 289
Case 290
Case 291
Case 292
Case 293
Case 294
Case 295
Case 296
Case 297
Case 298
Case 299
Case 300
Case 301
Case 302
Case 303
Case 304
Frequency
Inter-event times (ms)
×10^4

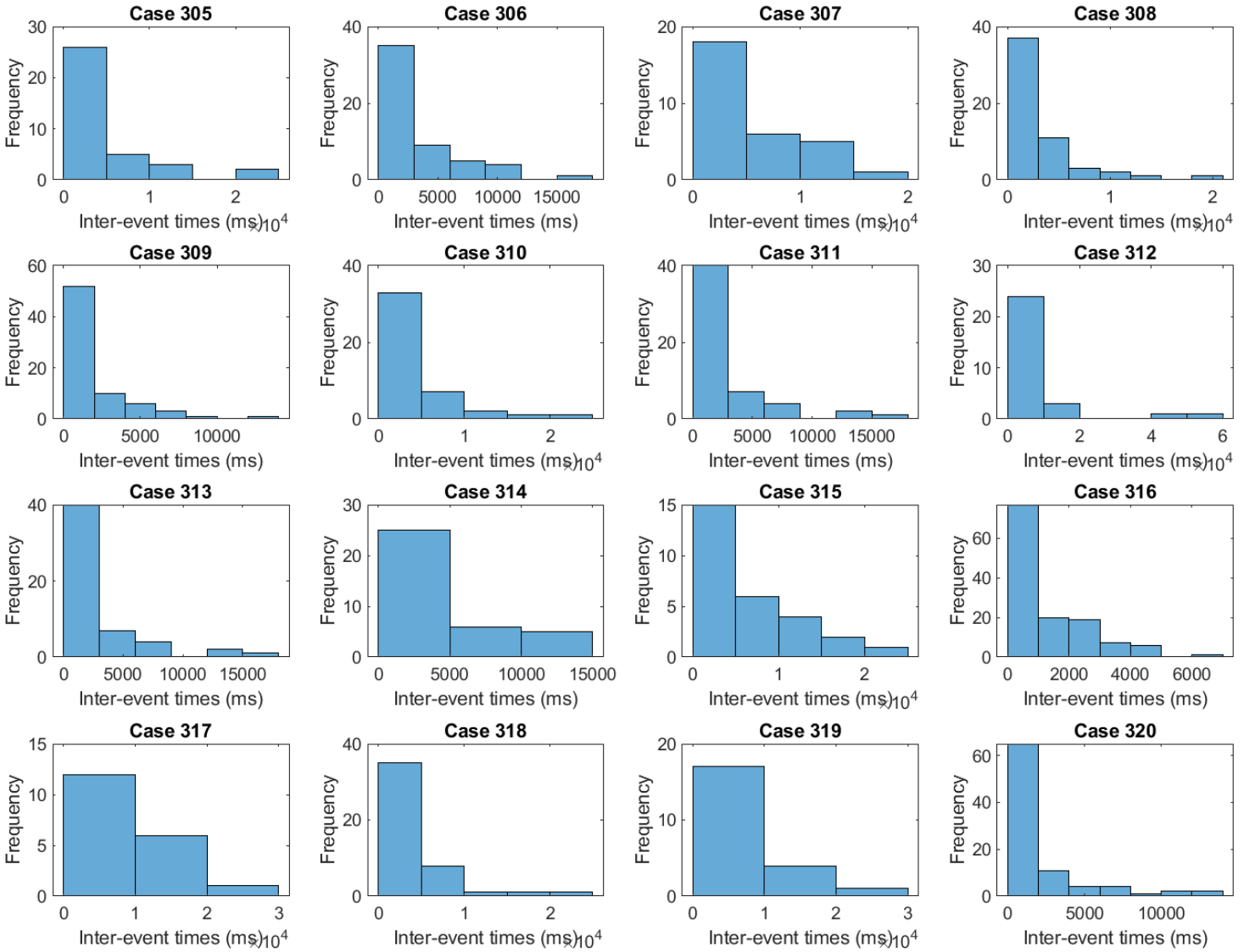
Case 305
Case 306
Case 307
Case 308
Case 309
Case 310
Case 311
Case 312
Case 313
Case 314
Case 315
Case 316
Case 317
Case 318
Case 319
Case 320
Frequency
Inter-event times (ms)
×10^4

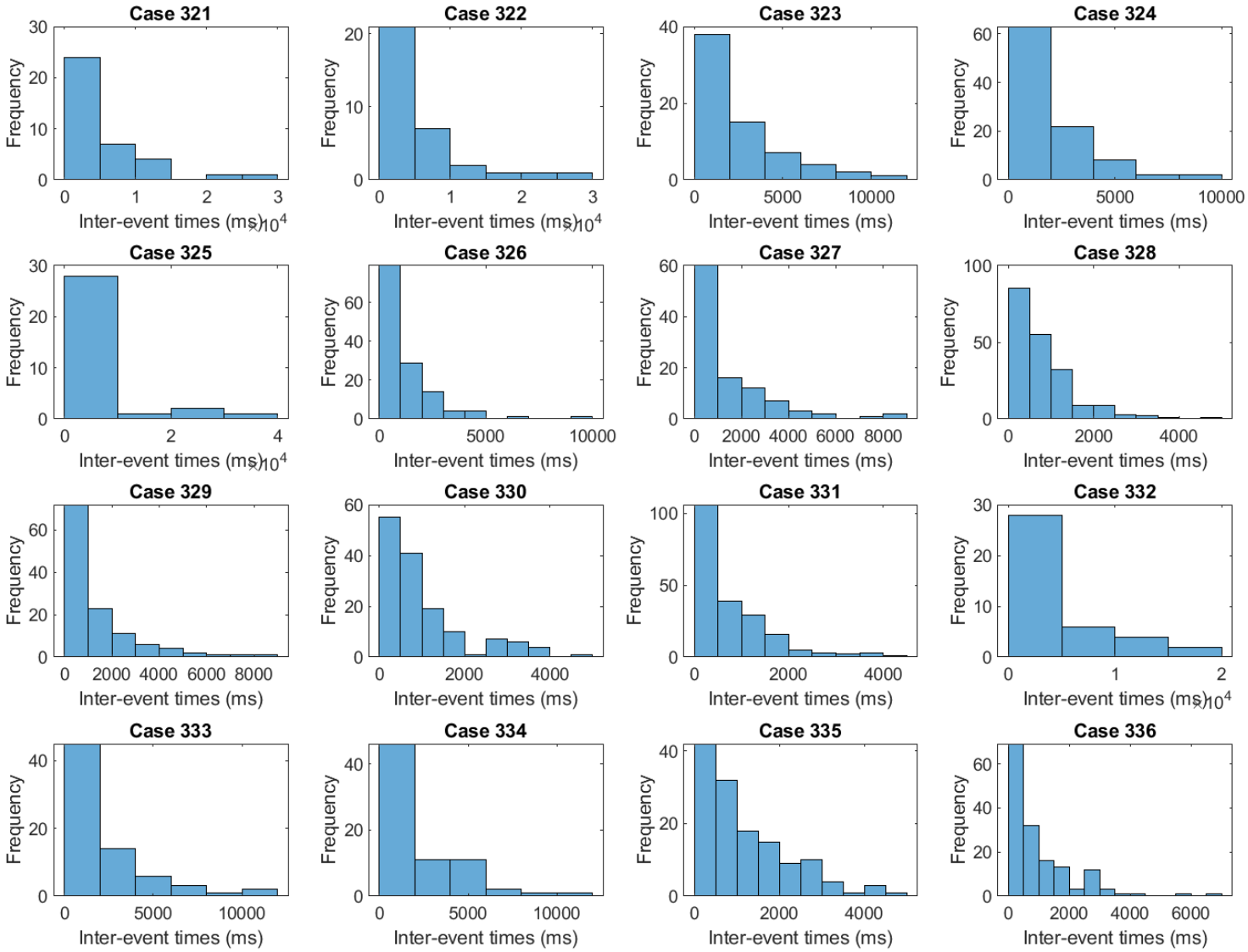
Case 321
Case 322
Case 323
Case 324
Case 325
Case 326
Case 327
Case 328
Case 329
Case 330
Case 331
Case 332
Case 333
Case 334
Case 335
Case 336
Frequency
Inter-event times (ms)
×10^4

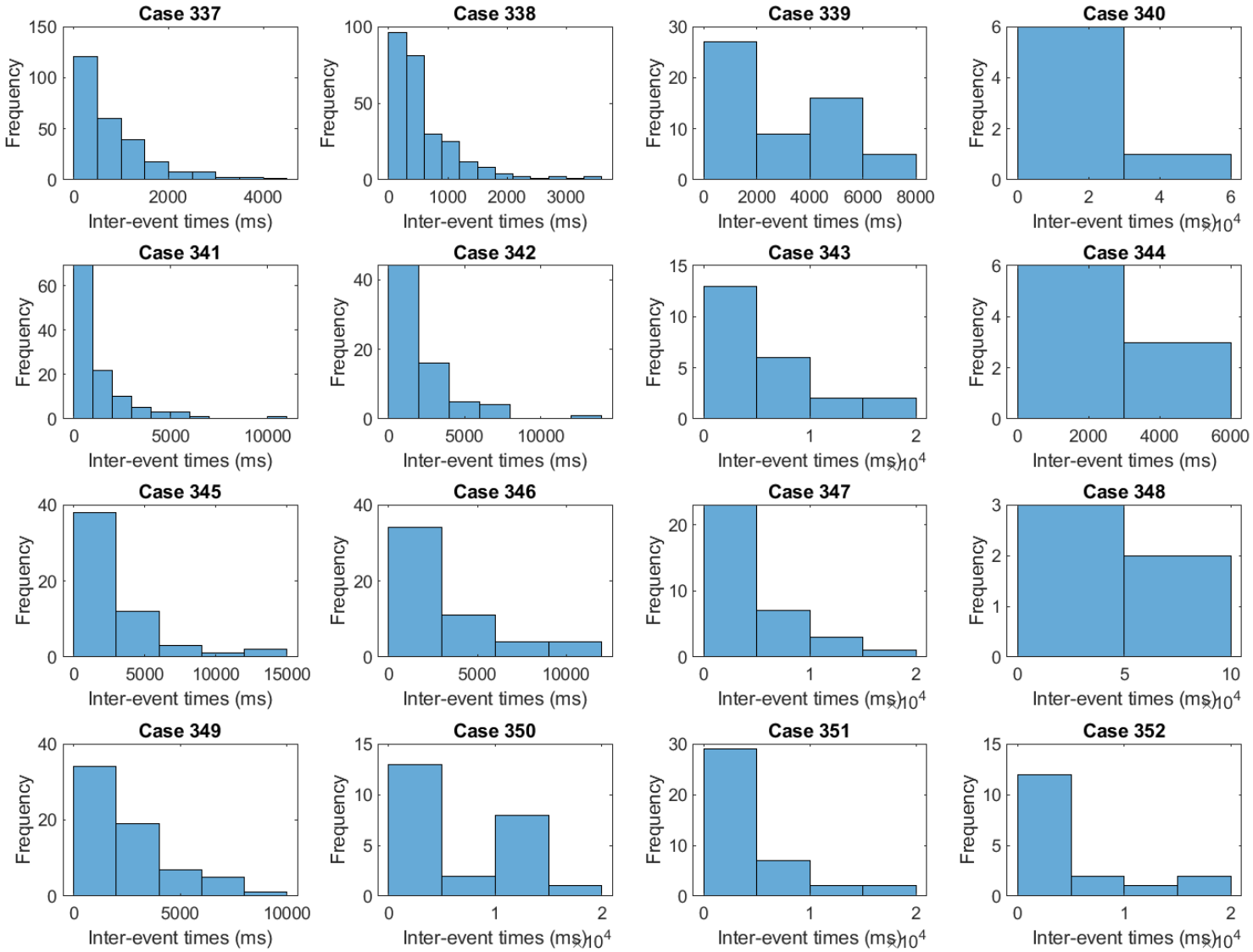
Case 337
Case 338
Case 339
Case 340
Case 341
Case 342
Case 343
Case 344
Case 345
Case 346
Case 347
Case 348
Case 349
Case 350
Case 351
Case 352
Frequency
Inter-event times (ms)
×10^4

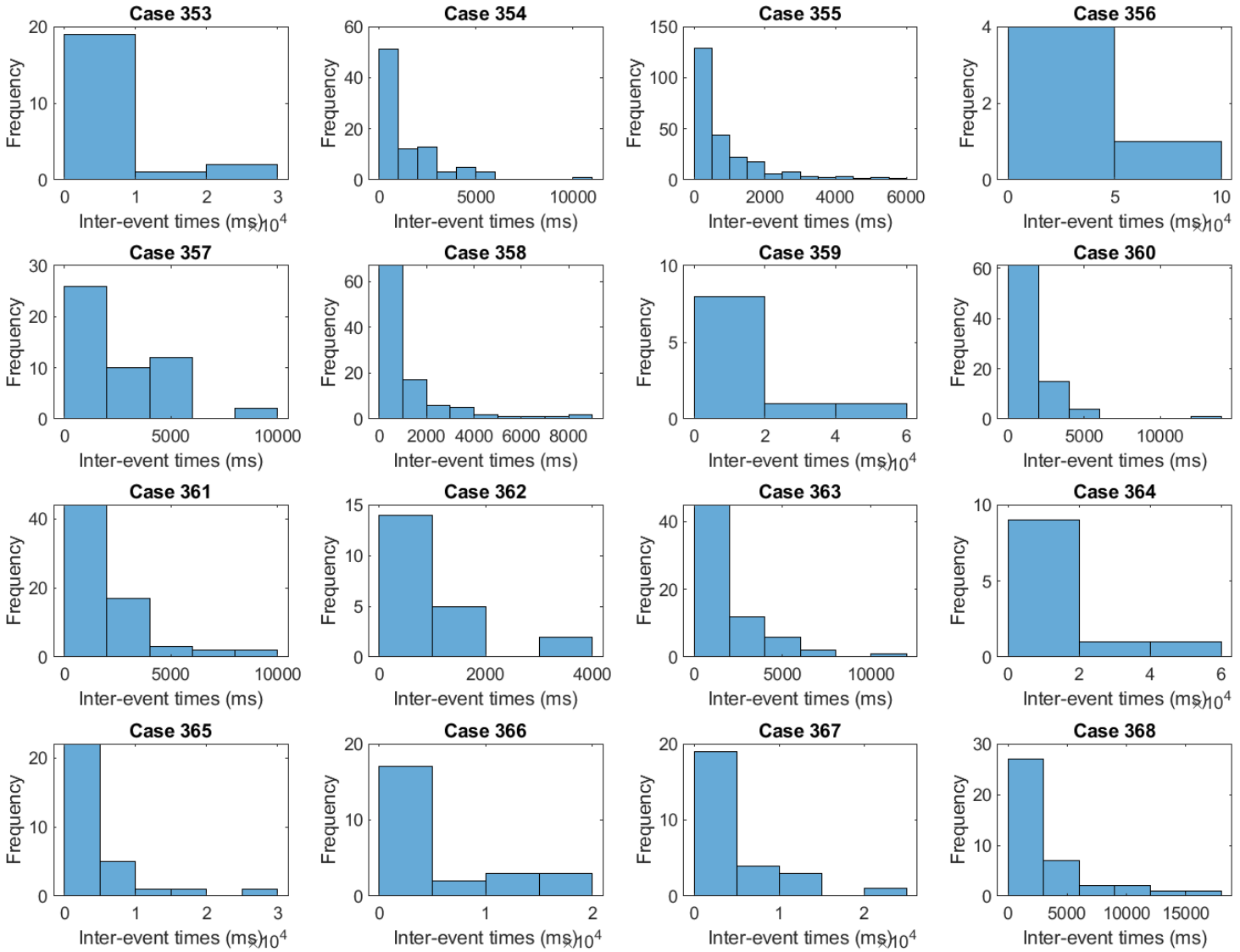
Case 353
Frequency
Inter-event times (ms)
×10^4
Case 354
Frequency
Inter-event times (ms)
Case 355
Frequency
Inter-event times (ms)
Case 356
Frequency
Inter-event times (ms)
×10^4
Case 357
Frequency
Inter-event times (ms)
Case 358
Frequency
Inter-event times (ms)
Case 359
Frequency
Inter-event times (ms)
×10^4
Case 360
Frequency
Inter-event times (ms)
Case 361
Frequency
Inter-event times (ms)
Case 362
Frequency
Inter-event times (ms)
Case 363
Frequency
Inter-event times (ms)
Case 364
Frequency
Inter-event times (ms)
×10^4
Case 365
Frequency
Inter-event times (ms)
×10^4
Case 366
Frequency
Inter-event times (ms)
×10^4
Case 367
Frequency
Inter-event times (ms)
×10^4
Case 368
Frequency
Inter-event times (ms)

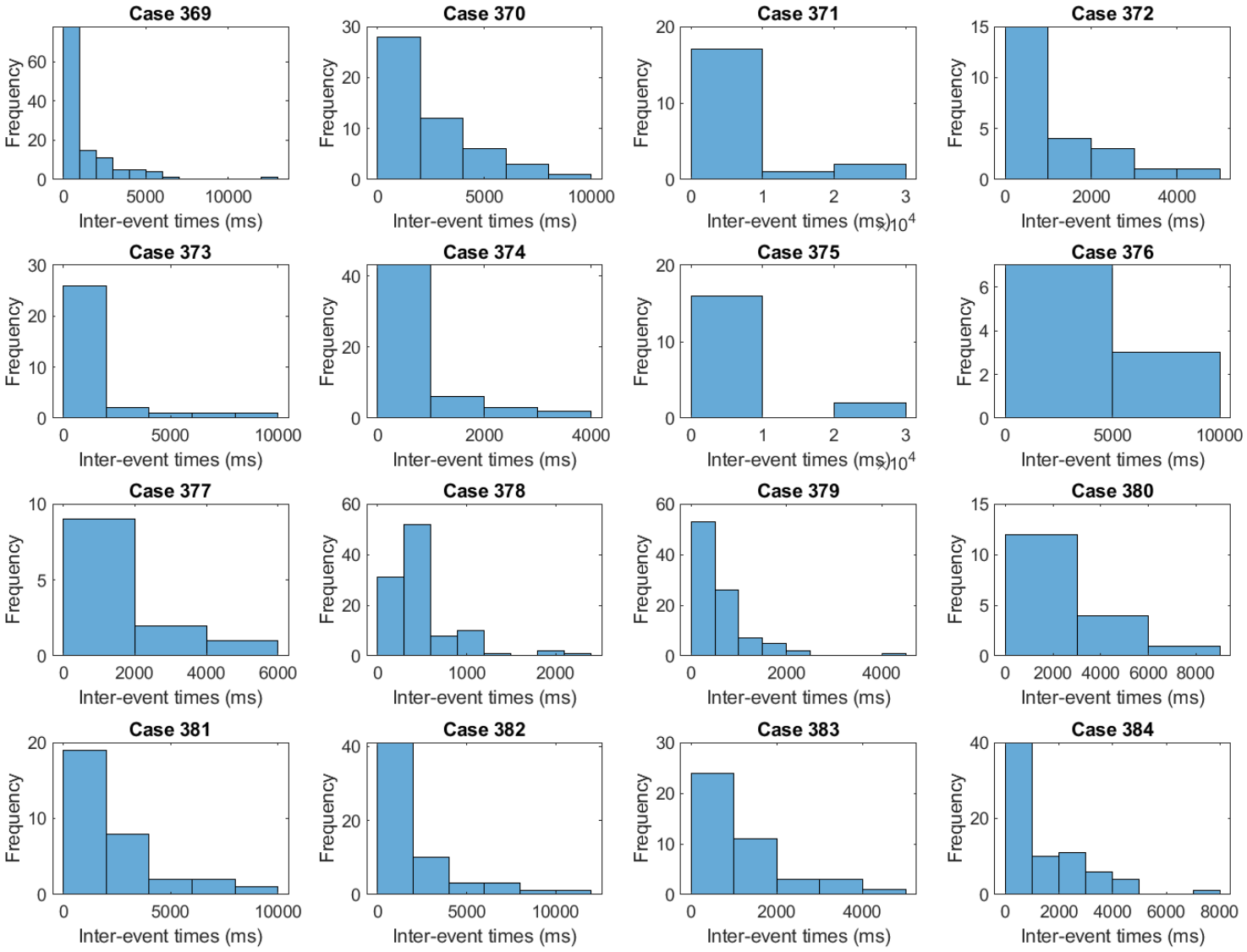
Case 369
Case 370
Case 371
Case 372
Case 373
Case 374
Case 375
Case 376
Case 377
Case 378
Case 379
Case 380
Case 381
Case 382
Case 383
Case 384
Frequency
Inter-event times (ms)
×10^4

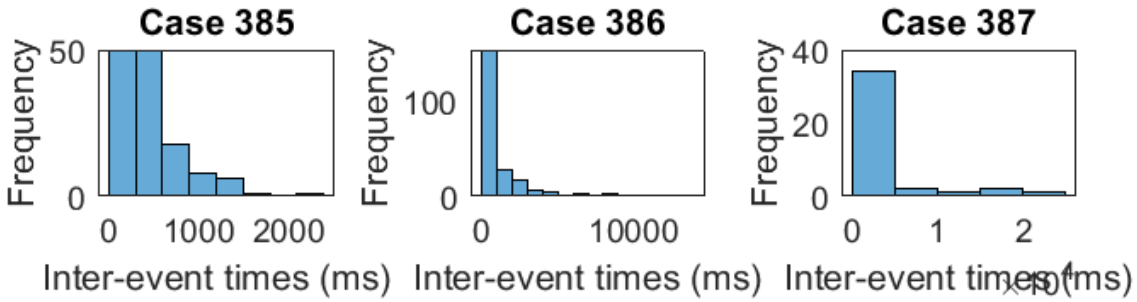
Case 385
Frequency
50
0
0
1000
2000
Inter-event times (ms)
Case 386
Frequency
100
0
0
10000
Inter-event times (ms)
Case 387
Frequency
40
20
0
0
1
2
Inter-event times (ms)